

XLPR MODELS SUBGROUP REPORT

CRACK STABILITY



PROBABILISTIC FRACTURE MECHANICS CODE

DISCLAIMER

THIS PUBLICATION WAS PREPARED AS AN ACCOUNT OF WORK JOINTLY SPONSORED BY THE ELECTRIC POWER RESEARCH INSTITUTE (EPRI) AND AN AGENCY OF THE U.S. GOVERNMENT. NEITHER EPRI NOR THE U.S. GOVERNMENT NOR ANY AGENCY THEREOF, NOR ANY EMPLOYEE OF ANY OF THE FOREGOING, MAKES ANY WARRANTY, EXPRESSED OR IMPLIED, OR ASSUMES ANY LEGAL LIABILITY OR RESPONSIBILITY FOR ANY THIRD PARTY'S USE, OR THE RESULTS OF SUCH USE, OF ANY INFORMATION, APPARATUS, PRODUCT, OR PROCESS DISCLOSED IN THIS PUBLICATION, OR REPRESENTS THAT ITS USE BY SUCH THIRD PARTY COMPLIES WITH APPLICABLE LAW.

THIS PUBLICATION DOES NOT CONTAIN OR IMPLY LEGALLY BINDING REQUIREMENTS. NOR DOES THIS PUBLICATION ESTABLISH OR MODIFY ANY REGULATORY GUIDANCE OR POSITIONS OF THE U.S. NUCLEAR REGULATORY COMMISSION AND IS NOT BINDING ON THE COMMISSION.

xLPR Models Subgroup Report

Crack Stability

xLPR-MSGR-Stability Version 1.0

Author Signature	Date
<i>Rick Olson</i> Rick Olson xLPR Crack Stability Subgroup Leader	06/20/16
Reviewer Signatures	Date
<i>Bruce Young</i> Bruce Young xLPR Crack Stability Subgroup Member	06/17/16
<i>Paul Scott</i> Paul Scott Crack Stability Subgroup Member	06/17/16
Approver Signatures	Date
<i>Marjorie Erickson</i> Marjorie Erickson, PEAI xLPR Models Group Lead	06/16/16
<i>Craig D. Harrington</i> Craig D. Harrington xLPR Code Development Lead	06/20/16

THE TECHNICAL CONTENTS OF THIS DOCUMENT WERE NOT PREPARED IN ACCORDANCE WITH THE XLPR SOFTWARE QUALITY ASSURANCE PLAN.

Revision History

Version Number	Description of Changes	Issue Date
1.0	Initial Issue	6/20/2016
	The U.S. Nuclear Regulatory Commission Office of Nuclear Regulatory Research's and the Electric Power Research Institute's xLPR Project Contacts approved an administrative update in 2021 to support public release of this document without incrementing the version number or issue date. The administrative updates included: (a) title changed from "Axial and Circumferential Crack Stability Module Development for xLPR Version 2.0" to "xLPR Models Subgroup Report—Crack Stability" throughout the document, (b) cover and title pages updated accordingly, (c) disclaimer statement added, (d) notice regarding official document version records storage location during code development removed as it is no longer needed, and (e) statement that the document was not prepared in accordance with the xLPR Software Quality Assurance Plan added.	

EXECUTIVE SUMMARY

Modules for assessing the stability of cracks in nuclear power plant piping systems have been developed as part of xLPR Version 2.0. These modules assess the stability of both axially-oriented and circumferentially-oriented surface cracks (SC) and through-wall cracks (TWC) in pipes.

The SC_fail module assesses the stability of multiple circumferentially-oriented surface cracks (SC) in a pipe subjected to combined tension and bending loading. This module is valid for cases when one or more cracks are present in the pipe. Based on input pipe/crack geometries, pipe material properties, and loads, the ultimate moment-carrying capacity of multiple surface cracks, as well as an individual surface crack, are compared with the current (applied) loading. A flag is returned that indicates the results of this comparison: Predicted failure, yes or no, along with the ratio of the current (applied) bending moment to the bending moment which would result in an instability of the surface crack or cracks. Three surface crack ultimate load carrying capacity prediction routines have been coded:

- Multiple surface cracks using the constant depth Net-Section-Collapse (NSC) analysis method,
- Multiple surface cracks using the NSC solution for the semi-elliptical crack profile, and
- Multiple surface cracks using the NSC solution for the parabolic crack profile.

At this time, the semi-elliptical and parabolic crack depth analyses are not used in the xLPR Framework, but the coding for these solutions has been done. Eventually, a local collapse surface crack solution and/or an elastic-plastic fracture mechanics (EPFM) surface crack solution may be included in xLPR. Accordingly, the inputs for SC_fail have been designed to accommodate these updates, so no revision to the calling routine will be required when these features are added.

The TWC_fail module assesses the stability of a circumferentially-oriented through-wall crack (TWC) in a pipe subjected to combined tension and bending loading. Based on input pipe/crack geometries, pipe material properties, and loads, the critical crack size of the through-wall crack (θ_{crit}) is compared with the current crack size. A flag is returned that indicates the results of this comparison: Predicted failure, yes or no, as well as the ratio of the current crack angle (θ) to the critical crack angle (θ_{crit}).

The TWC_fail module uses a main subroutine TWC_fail, for doing the through-wall crack assessment. Presently, two TWC critical crack size (θ_{crit}) prediction methodologies are implemented:

- Idealized through-wall crack NSC analysis method, and
- LBB.ENG2 elastic-plastic fracture mechanics (EPFM) through-wall crack J-estimation scheme.

Eventually, other through-wall crack solutions might be included in xLPR. Accordingly, the inputs for TWC_fail have been designed to accommodate these updates, so limited revisions to the calling routine will be required when these features are added.

In the current version of TWC_fail, both the idealized crack NSC and LBB.ENG2 elastic-plastic through-wall crack predictions are made. Upon return to the calling program, the solution that yields the smallest critical crack size is used for the pass/fail assessment and for calculating the ratio of the current crack size to the critical crack size.

The axial surface crack and axial through-wall crack stability modules are stand-alone modules called from within the xLPR Framework. The Axial_SC_fail Module employs a plastic collapse analysis to assess the stability of an internal axial surface crack, while the Axial_TWC_fail Module employs both limit load and elastic-plastic fracture mechanics (EPFM) analyses to assess the stability of an idealized axial TWC in a single pipe material. (Note that analysis of an axial crack in welds with two separate materials, namely a base-metal and a weld, is beyond the scope of the present design.)

The Axial_SC_fail subroutine performs the stability calculation for an axial surface crack using a plastic collapse method when called. The ratio of the input pressure to the critical pressure for the rupture of the pipe, p/p_{crit} , for the given input SC configuration is calculated and returned to the calling program. Based on the critical pressure calculated, the Axial_SC_fail subroutine returns a flag indicating if the input pressure is greater than or equal to the critical pressure (indicative of SC failure/rupture). If the input pressure is less than the critical pressure, the subroutine also returns the pressure margin by computing the ratio of the input pressure to the critical pressure (p/p_{crit}).

The Axial_TWC_fail subroutine calculates the critical axial through-wall crack length using both limit load and EPFM methods and compares the smaller of these two values to the current axial through-wall crack length. If the current crack length is greater than the critical crack length (i.e., the smaller of the two values obtained from the limit load and EPFM solutions), then the axial TWC fails. If not, then the TWC remains stable.

The verification of the SC_fail, TWC_fail, and axial crack stability models (Axial_SC_fail and Axial_TWC_fail) is documented in detail in the Software Test Results Reports (STRR) for each of these models. The testing activities described in the STRRs are intended to verify that the requirements specified in the applicable Software Requirements Documents (SRD) are met. To date, most of these requirements have been shown to have been met. However, some of the requirements in these SRDs are applicable to the xLPR Framework, and thus, verification of those requirements can only be accomplished when these modules are integrated into the Framework.

Validation of these models was accomplished by comparing the predictions from the various models with available experimental data from full-scale pipe experiments. In validating the SC_fail module, there were a total of 169 full-scale, single surface cracked pipe experiments to compare with the results from SC_fail. For these 169 experiments, the average value of the bending moment ratio (experimental bending moment to predicted bending moment) was 0.987 with a standard deviation of 0.268. This level of agreement between the experiments and the predictions easily meets the requirement for validation as specified in the SRD for this module. While the database of single surface crack experiments was extensive, the database of multiple surface crack experiments was quite limited. In total, only 3 multiple surface crack experiments were found in the literature. For these 3 experiments, the value of the bending moment ratio ranged from 1.03 to 1.05, which easily meets the requirement for validation, as specified in the SRD for this module.

In validating the TWC_fail module a total of 32 through-wall cracked pipe experiments were included in the validation matrix. These experiments considered a wide range of pipe sizes (2 to

42-inch nominal diameter), crack sizes (half crack angles of 0.35 to 1.4 radians), materials (carbon steel and stainless steels and their associated weldments), and loading conditions (simple four-point bending, combined pressure and four-point bending, and dynamic, cyclic pipe system experiments with internal pipe pressure). The results of this validation exercise were found to be highly dependent on the choice of pipe material toughness (J-R) curve used, i.e., J-R curves from C(T) specimens with and without side-grooves and J-R curves from fatigue pre-cracked CT specimens or C(T) specimens which were not fatigue pre-cracked, i.e., sharp machine notched specimens), and the formulation of J used in the analysis, i.e., deformation J (J-D) or modified J (J-M). It was found as part of this validation exercise that the TWC_fail module resulted in a better prediction of the critical crack size when using the modified formulation of J (J-M) than the deformation formulation of J (J-D). However, it was thought that it would not be possible to specify to the end user of xLPR what formulation of J to use or what geometry of fracture toughness specimen to use (side-grooved or not and fatigue pre-cracked or not), so an assessment of the validity of the TWC_fail module was made considering all possible combinations of fracture toughness specimen geometries using both J-D and J-M formations for J. The resultant average value of the ratio of the current crack angle (crack angle at maximum load from the pipe experiment) to the critical crack angle (smaller of the two crack angles from the NSC and ENG2 analysis methods) was 1.34 with a standard deviation of 0.53. This level of uncertainty was deemed to exceed the validity requirement in the SRD. As a result, additional analyses were undertaken in an attempt to isolate the cause of this uncertainty.

In assessing the results from the TWC_fail validation exercise discussed above, it was concluded that the overall uncertainty observed was the result of two separate but equally important factors. One, it was thought that there is a level of uncertainty due solely to the model (model uncertainty), and two, it was thought that there is a level of uncertainty due to the inputs (input uncertainty). With respect to the input uncertainty, one leading contributor is the uncertainty due to the choice of J-R curve to use in the analysis. In an attempt to separate the model uncertainty from the input uncertainty due to the choice of J-R curve, η -factor analyses were conducted in order to establish a J-R curve directly from pipe experimental load-displacement data. It was then thought that if one used these η -factor-derived J-R curves from the pipe experiments in the TWC_fail analyses, one could get an idea of the uncertainty due solely to the model, i.e., model uncertainty. In order to conduct these η -factor analyses, additional data were needed from the pipe experiments, e.g., details on the moment arm pipes and the compliance of the test frame used. For a number of the 32 experiments considered in the original validation efforts for TWC_fail, these data were unavailable. As a result, the validation matrix for these η -factor analyses only included 12 experiments. For these 12 experiments, the average value of the ratio of the current crack angle (crack angle at maximum moment from the pipe experiment) to the critical crack angle was 1.14 with a corresponding standard deviation of 0.17. It was felt that this level of agreement better represents the overall uncertainty of the model (model uncertainty), separate from the input uncertainty.

A total of seventeen axial SC pipe experiments were chosen for validation of the Axial_SC_fail module. The ratio of the experimental pressure to the critical pressure using the Ductile Fracture Handbook [20] plastic collapse method was the validation metric. For these Axial_SC_fail predictions, the computation of an effective half-crack length for a semi-elliptical surface crack was turned off because the axial surface cracks used in these experiments were constant depth surface cracks. Overall, the average value of $p_{\text{Expt}}/p_{\text{Crit}}$ for these 17 experiments was 1.070 with a standard deviation of 0.190, which indicates that the Axial_SC_fail model slightly underpredicts (slightly conservative) the experimental results.

A total of 26 axial TWC pipe experiments were chosen for validation of the Axial_TWC_fail limit load model. The ratio of the experimental half crack length to the critical half crack length predicted using the limit load solution was the validation metric. Overall, the average value of C_{Expt}/C_{Crit} for these 26 experiments was 0.850 with a standard deviation of 0.142, which indicates that the limit load solution in the Axial_SC_fail model over predicts (i.e., non-conservatively predicts) the critical crack size. Because the Ramberg-Osgood and J-resistance curve parameters were not available for these materials, it was necessary to estimate the required material properties (stress-strain and fracture toughness data) using available strength properties (yield and ultimate) and Charpy energy (upper shelf) data along with correlations available in the literature in order to validate the Axial_TWC_fail EPFM solution. A total of 12 experiments were used for this validation exercise. For these 12 experiments, the average ratio of C_{Expt}/C_{Crit} was 0.875 (again slightly non-conservative) with a standard deviation of 0.111.

Overall, some of the stability models exhibit conservatism while others do not, with respect to the experimental pipe fracture data available. In general, all of the models provide reasonably good estimates of rather complex behavior, considering that they are engineering estimates. When viewed with respect to the total suite of deterministic models in xLPR, the uncertainty of the crack stability modules is not likely to be a large contributor to overall model uncertainty because, in most cases, PWSCC crack growth is not so fast that inspection and leak detection will not identify problems before the cracks have grown large enough to become unstable.

Notwithstanding the fact that the stability modules do a pretty good job of replicating pipe fracture experiments, one cannot lose sight of the fact that neither the models nor the experiments represent the characteristics of PWSCC cracks of primary concern in xLPR. In the models and the experiments, the crack is planar with two distinctly parallel crack faces. PWSCC, on the other hand, has no single distinct crack. Rather, it has many smaller branching and interconnected cracks with ligaments remaining across the crack faces constraining crack opening. Accordingly, the current stability models can only be considered an approximation of PWSCC crack geometry, and, lacking any pipe fracture experiments performed on pipes with PWSCC, a direct assessment of conservatism, with respect to stability predictions, cannot be made, although heuristically, it would seem that the present models must overpredict the occurrence of ruptures because they ignore the “ligaments” of material across the crack.

TABLE OF CONTENTS

EXECUTIVE SUMMARY	IV
TABLE OF CONTENTS	VIII
TABLE OF FIGURES	X
TABLE OF TABLES.....	XI
NOMENCLATURE/LIST OF SYMBOLS	XII
ACRONYMS AND INITIALISMS	XV
1. INTRODUCTION.....	1
2. THE STABILITY MODELS	3
2.1 The SC_fail Model.....	3
2.2 The TWC_fail Model.....	5
2.2.1 Ideal Through-Wall Crack Net-Section Collapse Model.....	6
2.2.2 ENG2_mp Through-Wall Crack Model	7
2.2.3 Axial Force Calculation	12
2.3 The Axial Crack Stability Models	13
2.3.1 Axial_SC_fail Model	13
2.3.2 Axial_TWC_fail Model.....	14
3. MODULE DEVELOPMENT.....	17
3.1 SC_Fail Module.....	17
3.1.1 SC_fail Module Requirements.....	17
3.1.2 SC_fail Module Inputs and Outputs.....	18
3.1.3 SC_fail Structure.....	21
3.2 TWC_Fail Module.....	22
3.2.1 TWC_fail Requirements	23
3.2.2 TWC_fail Module Inputs and Outputs.....	23
3.2.3 TWC_fail Structure.....	23
3.3 Axial Crack Failure Modules.....	28
3.3.1 Axial Crack Failure Modules Requirements.....	28
3.3.2 Axial Crack Failure Modules Inputs and Outputs.....	30
3.3.3 Axial Crack Failure Modules Structure	36
3.4 Stability Module General Considerations.....	37
3.5 Module Verification.....	38
3.5.1 SC_fail Module Verification	38
3.5.2 TWC_fail Module Verification	39
3.5.3 Axial Crack Stability (AxCS) Module Verification	40
3.6 Module Validation.....	42
3.6.1 SC_fail Module Validation	42
3.6.2 TWC_fail Module Validation	50
3.6.3 Axial Crack Stability (AxCS) Module Validation	64
3.7 Limitations with the Crack Stability Modules.....	68
4. RECOMMENDATIONS FOR VERSION 3.0 MODIFICATIONS.....	72
5. LESSONS LEARNED.....	73

6. ASSUMPTIONS AND IMPLICATIONS	75
7. SUMMARY.....	79
8. REFERENCES.....	82

TABLE OF FIGURES

Figure 1.	Crack definition for surface crack Net-Section Collapse submodule.....	3
Figure 2.	Assumed flow stress conditions for Net-Section Collapse	4
Figure 3.	TWC_fail pipe geometry	6
Figure 4.	Crack definition for Net-Section Collapse submodule	6
Figure 5.	Reduced section analogy of the LBB.ENG2 J-estimation scheme	8
Figure 6.	BM ratio versus crack length for all single crack cases.....	49
Figure 7.	BM ratio versus crack depth for all single crack cases.....	49
Figure 8.	Net Section Collapse predictions, with and without considering induced bending, as a function of the ratio of the through-wall crack length to the pipe circumference	53
Figure 9.	Comparison of J-R curves for weld F49W between 0% and 20% side-grooves (F49W is weld material evaluated in Experiment 1.1.1.24)	62
Figure 10.	Plot of the ratio_theta values for the pipe experiments considered in this validation exercise as a function of the ratio of the crack size at maximum moment to the crack size at crack initiation	62
Figure 11.	Post-test photograph of Experiment 1.1.1.21 showing out of plane crack growth	63
Figure 12.	Distribution of θ/θ_{crit} results from Table 17 using J-M fracture toughness data.....	63
Figure 13.	Plot of the ratio of the failure stress to Net-Section-Collapse stress as a function of the Dimensionless Plastic Zone Parameter (DPZP).....	70
Figure 14.	Effect of specimen orientation on fracture toughness in terms of Charpy Energy	70

TABLE OF TABLES

Table 1.	SRD requirements for SC_fail module [1]	17
Table 2.	Description of circumferential surface crack stability module (SC_fail) input variables	18
Table 3.	Description of circumferential surface crack stability module (SC_fail) output variables	20
Table 4.	Errors and warnings for the SC_fail module	21
Table 5.	SRD requirements for TWC_fail module [2]	24
Table 6.	Description of circumferential through-wall crack stability module (TWC_fail) input variables	25
Table 7.	Description of circumferential through-wall crack stability module (TWC_fail) output variables	26
Table 8.	TWC_fail module error code (i_err_code) values	26
Table 9.	SRD requirements for axial surface crack and axial through-wall crack modules [11]	29
Table 10.	Description of Axial TWC and SC stability input variables	30
Table 11.	Description of Axial TWC and SC stability output variables	31
Table 11.	Description of Axial TWC and SC stability output variables (Cont)	32
Table 12.	AxCS error code description and module guidance to xLPR framework.....	34
Table 13.	Inputs and output BM Ratio for SC_fail single crack validation cases.....	45
Table 14.	Inputs and output BM Ratio for SC_fail single crack validation cases (cont)	46
Table 15.	Comparison of old SC_fail module, new SC_fail module, and pipe experiments for multiple crack cases	50
Table 16.	Validation matrix for TWC_fail module.....	54
Table 17.	Results of TWC_fail validation analysis using J-M fracture toughness data	58
Table 18.	Results of TWC_fail validation analysis using J-D fracture toughness data.	59
Table 19.	Comparison of η -factor extrapolated J-R curve coefficients and CT or 3-point bend specimen extrapolated J-R curve coefficients.....	60
Table 20.	Comparison of results of TWC_fail analyses between when using η -factor derived J-R curves and CT or 3-point bend specimen J-R curves	61
Table 21.	Input and output from validation limit load solutions in of Axial_SC_fail module	64
Table 22.	Input and output from validation of limit load solutions within Axial_TWC_fail module	65
Table 23.	Pipe dimensions and material properties from twelve AEC tests used in EPFM analysis [53]	67
Table 24.	Comparison of Axial_TWC_ratio obtained from limit load and EPFM analysis	68
Table 25.	List of assumptions and implications of those assumptions made during the SC_fail, TWC_fail and AxCS development processes.....	75

NOMENCLATURE/LIST OF SYMBOLS

Symbols

a	Half the circumferential crack length or surface crack depth
a_0	Crack depth of constant depth surface crack
a_{0j}	Crack depth of constant depth surface crack from an ensemble of surface cracks
BM	Bending moment
BM_{max}	Critical bending moment
C	Coefficient in extrapolated J-R curve expression
C(T)	Compact tension specimen
c	Half the axial crack length
c_{eff}	Effective half the axial crack length
c_{crit}	Half the axial critical crack length
c_{Expt}	Effective half axial crack length
c_1, c_2, c_3	Various different crack lengths
d	Crack depth of an axial surface crack
e	Through-wall crack axial force eccentricity
D_m	Mean pipe diameter
E	Elastic modulus
F	Shape factor for axial TWC solution stress intensity factor
F_{ax}	Applied axial force, exclusive of pressure effects
F_b	Stress intensity shape factor for bending
F_t	Stress intensity shape factor for tension
H_b	Plastic J bending influence function
H_t	Plastic J tension influence function
h_1	Fully plastic influence function for the GE/EPRI method
I_b	Bending compliance function
I_t	Tension compliance function
J	Elastic plastic fracture toughness
$J_{applied}$	Applied J
J-D	Deformation theory J
J_e	Elastic component of J
J_i	J at crack initiation
$J_{material}$	Material J
J-M	Modified J
J_p	Plastic component of J
J-R	J-Resistance of the material
J_R	J-Resistance
J_1, J_2, J_3	J at various different crack sizes
K	Stress intensity factor
K_I	Mode I (crack opening) stress intensity factor

\hat{K}	Bending integration function for bending equivalent thickness
L'_b	Elastic-to-plastic influence function for bending
L'_t	Elastic-to-plastic influence function for tension
m	Extrapolated J-R curve exponent
M	Bending moment
M_1	Folias bulging factor for axial through-wall crack
M_2	Folias bulging factor for axial surface crack
M_{eff}	Effective moment
M_{NSC}	Net-Section Collapse moment
n	Strain hardening exponent
p	Pipe pressure
p_{eff}	Effective pressure
p_L	Limit pressure
P_{crit}	Critical pressure from axially cracked pipe experiment
P_{expt}	Pressure from axially cracked pipe experiment
P_{pred}	Predicted pressure from axially cracked analysis
p_{SESC}	Critical pressure for axial surface crack solution
p_0	Axial surface crack normalized pressure
r_y	Plastic zone correction radius
R_i	Inside pipe radius
R_m	Mean pipe radius
R_o	Outside pipe radius
t	Pipe wall thickness
t_e	Equivalent pipe wall thickness
T	Tension force
T_{mat}	Tearing modulus
α	Coefficient in Ramberg-Osgood relationship
α	Half crack angle between the tips of two adjacent circumferential surface cracks
β	Complement of the angle from crack centerline to the neutral axis
β_N	Complement of the angle from crack centerline to the neutral axis for an ensemble of surface cracks
Γ	Mathematical gamma function
γ_j	Angular location from top of crack to the center of a surface crack in an ensemble of surface cracks
Δa	Crack growth
δ^c	Axial displacement due to a crack
δ_e^c	Elastic axial displacement due to a crack
δ_p^c	Plastic axial displacement due to a crack
ε	Strain
ε_0	Ramberg-Osgood reference strain
η	Geometric factor used in calculation of J-R curve from pipe experiment

θ_j	Half angular size of a surface crack in an ensemble of surface cracks
θ	Half the current crack angle
θ_{crit}	Half the critical crack angle
λ	Axial surface crack normalized crack length
ξ	Angular integration variable
σ	Stress
σ_b	Bending stress
σ_f	Flow stress
σ_u	Ultimate strength
σ_t	Tension stress
σ_y	Yield strength
σ_0	Ramberg-Osgood reference stress
σ_∞	Remote stress
ϕ	Plastic zone correction factor
ϕ^c	Rotation due to a crack
ϕ_e^c	Elastic rotation due to a crack
ϕ_p^c	Plastic rotation due to a crack

ACRONYMS AND INITIALISMS

BINP	Battelle Integrity of Nuclear Piping
COD	Crack Opening Displacement
CS	Carbon Steel
CT	Compact Tension
DLL	Dynamic Link Library
DMW	Dissimilar Metal Weld
DPZP	Dimensionless Plastic Zone Parameter
DP3-II	Degraded Piping Program – Phase II
EDF	Electricité de France
Emc ²	Engineering Mechanics Corporation of Columbus
ENG2	EPFM solution in TWC_fail
EPFM	Elastic Plastic Fracture Mechanics
EPRI	Electric Power Research Institute
GE	General Electric
ID	Inside Diameter
IPIRG	International Piping Integrity Research Group
JAERI	Japanese Atomic Energy Research Institute
MPA	Staatliche Materialprüfungsanstalt (Germany)
MVR	Module Validation Report
NRC	Nuclear Regulatory Commission
NSC	Net-Section-Collapse
NUPEC	Nuclear Power Engineering Test Center (Japan)
OD	Outside Diameter
PRCI	Pipeline Research Council International
PWSCC	Primary Water Stress Corrosion Cracking
QA	Quality Assurance
RTM	Requirements Traceability Matrix
SC	Surface Crack
SDD	Software Design Description
SI	Système International d’Unités
SRD	Software Requirements Document
SQA	Software Quality Assurance
SS	Stainless Steel
STP	Software Test Plan
STRR	Software Test Results Report
TG	Tokyo Gas
TWC	Through-Wall Crack
V&V	Verification and Validation
xLPR	eXtremely Low Probability of Rupture

1. INTRODUCTION

The Crack Stability Subgroup within the xLPR Models Group was charged with developing a number of new crack stability models for both axially and circumferentially oriented cracks. Stability models were developed for both surface cracks and through-wall cracks for both flaw orientations. The different models developed were:

- SC_fail – crack stability model for circumferentially oriented surface cracks (SC)
- TWC_fail – crack stability model for circumferentially oriented through-wall cracks (TWC)
- Axial_SC_fail – crack stability model for axially oriented SCs
- Axial_TWC_fail – crack stability model for axially oriented TWCs.

Each of these types of potential flawed pipe “failure” were coded into modules to be implemented as part of the xLPR Version 2 Code to assess probability of pipe rupture due to the presence of primary water stress corrosion cracks (PWSCC) and fatigue cracks in dissimilar metal (DM) piping welds. From a documentation perspective, separate Software Requirements Documents (SRDs) [1,2], Software Design Descriptions (SDDs) [3,4], Software Test Plans (STPs) [5,6], Software Test Results Reports (STRRs) [7,8], and Module Validation Reports (MVRs) [9,10] were developed for the SC_fail and TWC_fail stability modules. For the axial crack case, a single SRD [11], SDD [12], STP [13], STRR [14], and MVR [15] was developed for both the Axial_SC_fail and Axial_TWC_fail modules, e.g., a single SRD, so-called AxCS SRD, was written that addressed the requirements for both the axial surface crack and axial through-wall crack stability modules.

The SC_fail module assesses the ultimate moment-carrying capacity of either multiple surface cracks or an individual surface crack and compares those values with the current (applied) moments based on input pipe/crack geometries, pipe material properties, and loads using the method documented in Reference [16]. A flag is returned that indicates the results of this comparison: Predicted failure, yes or no, along with the ratio of the current (applied) bending moment to the bending moment that would result in surface crack instability.

The TWC_fail module assesses the stability of a through-wall crack (TWC) in a pipe subjected to combined tension and bending loading. Based on input pipe/crack geometries, pipe material properties, and loads, the critical crack size of the through-wall crack (θ_{crit}) is compared with the current crack size. A flag is returned that indicates the results of this comparison: Predicted failure, yes or no, as well as the ratio of the current crack angle (θ) to the critical crack angle (θ_{crit}). TWC_fail calculates the critical crack size using both the Net-Section-Collapse limit load analysis [17,18] and an elastic plastic fracture mechanics (EPFM) analysis based on the LBB.ENG2 [19] method, and uses the smaller of these two crack sizes as the critical crack size to compare with the current crack size to assess the stability of the through-wall crack.

The axial surface crack and through-wall crack stability modules are separate modules called from within the xLPR Framework, even though they share some common QA documentation. The Axial_SC_fail module employs a plastic collapse analysis to assess the stability of an internal axial surface crack [20], while the Axial_TWC_fail module employs both limit load [20] and EPFM analyses [21] to assess the stability of an idealized axial TWC. Axial_SC_fail calculates the critical pressure and compares this to the user input pressure. Axial_TWC_fail calculates the critical axial through-wall crack length using both limit load and EPFM methods and compares the smaller of these two values to the current axial through-wall crack length

Within each of these subroutines (SC_fail, TWC_fail, Axial_SC_fail, and Axial_TWC_fail), limited checking of input data is performed and appropriate error flags are generated and passed back to the xLPR Framework.

2. THE STABILITY MODELS

In this section of this report a brief description of the technical basis of each of the stability models is presented. Further details of the technical basis of these models can be found in their respective Software Design Descriptions [3,4,12].

2.1 The SC_fail Model

The SC_fail module considers a generalized method for Net-Section Collapse (NSC) analysis of surface cracked pipes with multiple arbitrary crack shapes. This method can be used to calculate the maximum load of a circumferentially cracked pipe containing multiple internal cracks subjected to combined bending and tension (pressure induced) loads. Hoop stress is not considered.

The formulation for the idealized multiple surface crack NSC analysis is based on the analysis presented in Reference [16]. As presented in Reference [16], the NSC equations are developed for the most generalized multiple crack NSC case, a collection of arbitrary depth, internal surface cracks. At one extreme, the surface cracks can be constant depth surface cracks, and at the other extreme, the surface cracks can be completely arbitrarily-shaped surface cracks. Figure 1 shows the basic geometry and two extremes of crack shape.

Consider the generalized multiple surface crack NSC development. For some collection of constant depth cracks, $a_i(\xi) = a_i$, half crack lengths described with the angle, θ_i , with crack centers located at some orientation, γ_i as shown in Figure 1, the cracked section's neutral axis is located at the angle β_N . Depending on the flaw lengths and locations, the cracks may be entirely in the tension zone, in both the tension and compression zones, or solely in the compression zone.

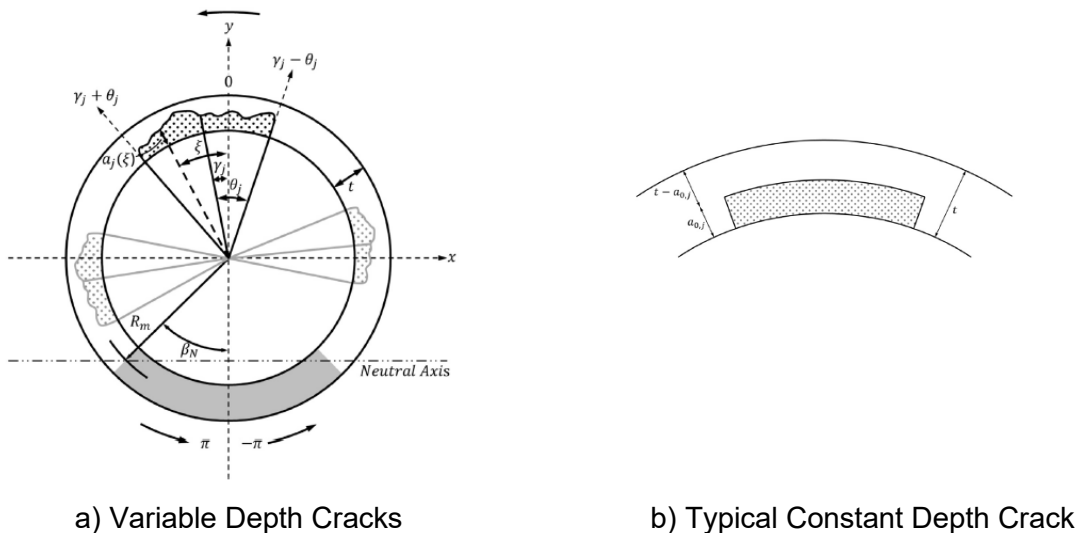


Figure 1. Crack definition for surface crack Net-Section Collapse submodule

Assuming that the stress goes to \pm flow stress, as shown in Figure 2, and that thin shell behavior applies, by applying moment and force equilibrium, the collapse moment can be calculated for cracks located in the tension zone as

$$M = 2\sigma_f R_m^2 t \left[2 \sin \beta_N - \sum_{j=1}^N \frac{a_{0j}}{t} \cos \gamma_j \sin \theta_j \right] \quad (\text{Eqn. 1})$$

where

$$\beta_N = \pi - \frac{\pi R_i^2 p_{eff}}{2\sigma_f R_m t} - \sum_{j=1}^N \frac{a_{0j}}{t} \theta_j \quad (\text{Eqn. 2})$$

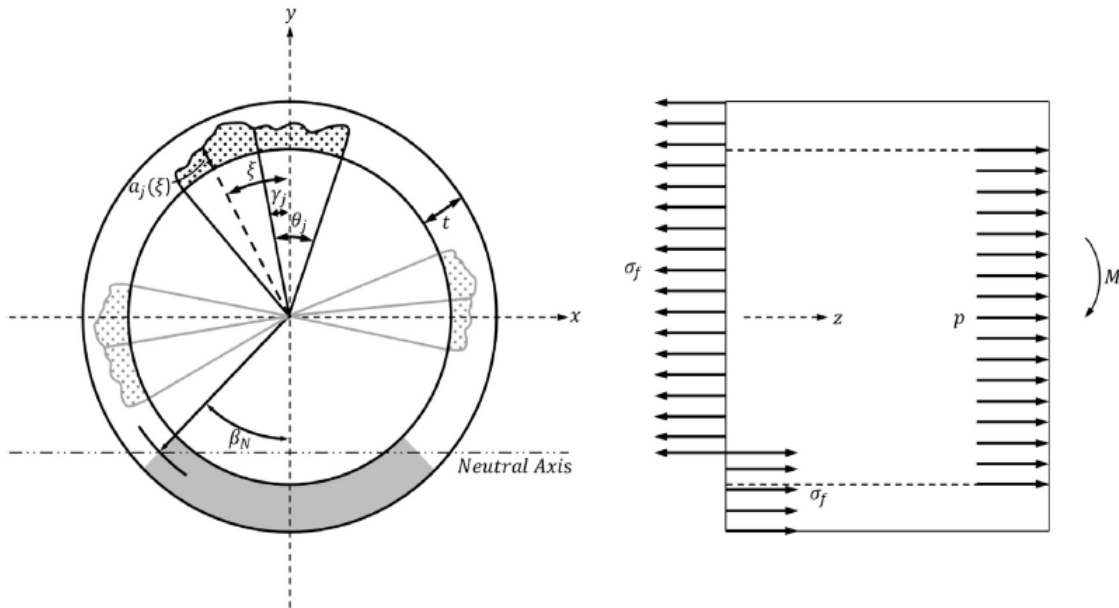


Figure 2. Assumed flow stress conditions for Net-Section Collapse

Various adjustments and exclusions are applied to (Eqn. 1) and (Eqn. 2) to take care of asymmetric cracks, cracks that extend either partially or fully into the compression zone, and crack closure effects when portions of crack go into compression. In any event, the basic forms of (Eqn. 1) and (Eqn. 2) apply with various exclusions to accommodate the different possible configurations.

The formulation for the NSC analysis for multiple surface cracks with constant depths is based on an analysis methodology initially presented in Reference [22]. Note that some errors have been found in the paper by Li, et al., notably the denominator in Equation (23) of Reference [22] has some missing terms. These errors have been fixed and reported in Reference [16]. The full formulation is presented in Reference [16].

2.1.1 Axial Force Calculation

The equations used to predict failure of surface cracks are traditionally expressed in terms of pressure as the sole contributor to the axial load. Indeed, this is not the usual case in most piping systems where there are also axial loads resulting from deadweight, thermal expansion, and dynamic excitation. In order to leave the underlying surface crack analysis equations in a form best suitable for QA, the contribution of axial loads, exclusive of pressure, are accounted for by use of an effective pressure. That is, when the surface crack analysis is performed, the pressure sent to subroutines, including the effect of applied axial loads other than pressure, is derived from the axial stress equation, see (Eqn. 3).

$$\sigma_{ax} = \frac{\pi R_i^2 p + F_{ax}}{2\pi R_m t} = \frac{\pi R_i^2 p_{eff}}{2\pi R_m t} \quad (\text{Eqn. 3})$$

where

- σ_{ax} = total axial stress
- R_i = pipe inner radius
- p = pipe internal pressure
- F_{ax} = applied axial force (excluding pressure contribution)
- R_m = pipe mean radius
- t = pipe wall thickness
- p_{eff} = effective pipe internal pressure.

Thus,

$$p_{eff} = \frac{\pi R_i^2 P + F_{ax}}{\pi R_i^2} \quad (\text{Eqn. 4})$$

2.2 The TWC_fail Model

The TWC_fail module uses two models to evaluate the stability of circumferential through-wall cracks subjected to combined bending and tension loads. The first model, idealized through-wall crack Net-Section Collapse (NSC) [17,18], considers the crack to have radially directed crack faces symmetric about the principle axis of bending, with the crack plane loaded by stresses that equilibrate fully plastic tension and compression stresses at a value of flow stress, i.e., the average of the yield and ultimate strengths. The second model, the LBB.ENG2 elastic-plastic fracture mechanics (EPFM) through-wall crack J-estimation scheme [19], considers the same crack geometry but in this case, the crack is assumed to grow by ductile tearing subjected to a remotely applied bending moment and tension. The model with the lowest failure condition is assumed to govern the overall behavior. A summary of the models and relevant solution strategy is given below.

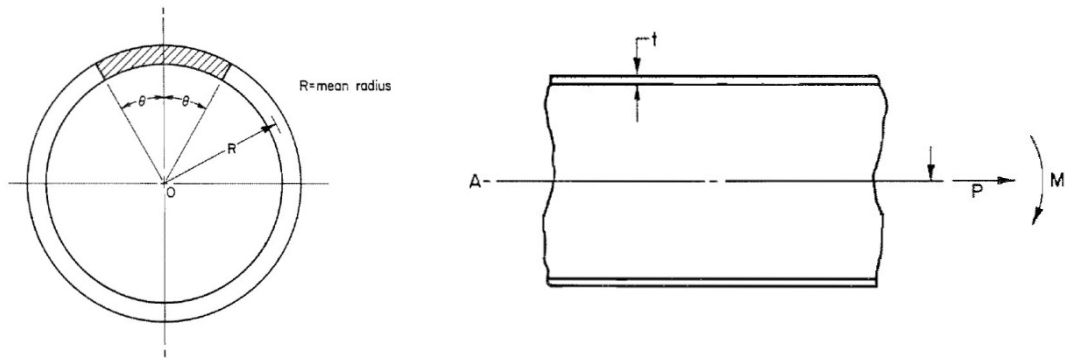


Figure 3. TWC_fail pipe geometry

2.2.1 Ideal Through-Wall Crack Net-Section Collapse Model

The formulation for the idealized through-wall crack Net-Section Collapse (NSC) analysis is based on the analysis presented in References [17] and [18].

As presented in Reference [18], the NSC equations are developed for the most generalized NSC case, an internal surface crack. In the limit, the surface crack can be a constant depth surface crack, and at the extreme, the surface crack will be an idealized through-wall crack.

Consider then, the generalized NSC development. For a given constant crack depth, $a(\xi) = a_0$ and a half crack length described with the angle, θ , as shown in Figure 4, the cracked section's neutral axis is located at the angle β . For an ideal through-wall crack, the crack depth, a_0 , is equal to the pipe wall thickness. Depending on the flaw length, the crack area may be entirely in the tension zone or in both the tension and compression zones. In addition, the solution is slightly modified if the crack face is assumed to take compressive loads.

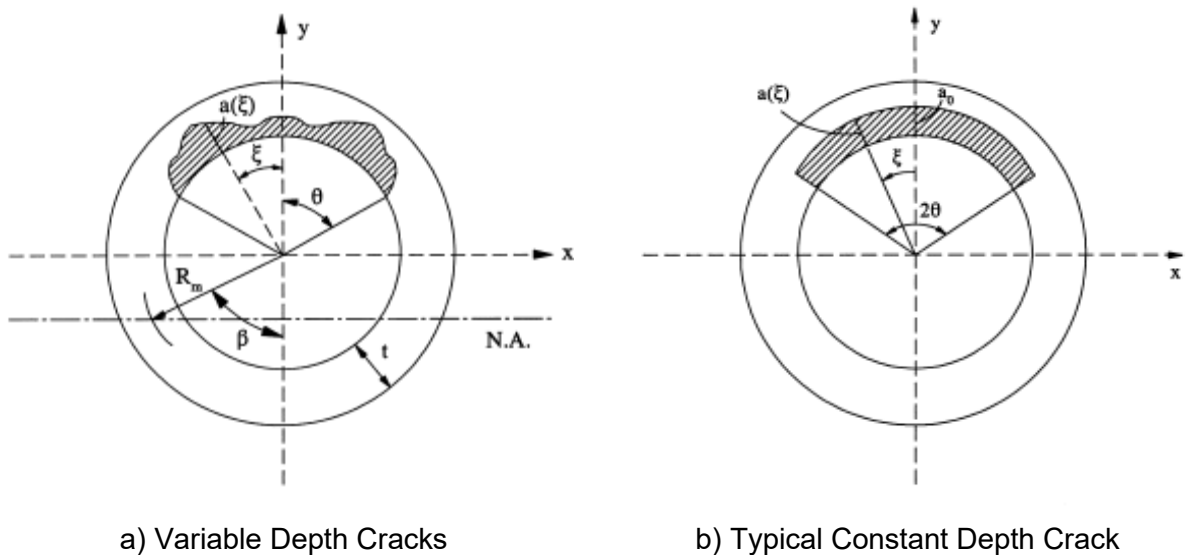


Figure 4. Crack definition for Net-Section Collapse submodule

Assuming that the stress goes to \pm flow stress in the uncracked ligament and thin shell behavior applies, just as was done for the SC_fail model, and applying moment and force equilibrium, the collapse moment can be calculated for cracks located in the tension zone ($\theta \leq \pi - \beta$) as

$$M_{NSC} = 2\sigma_f R_m^2 t \left[2 \sin \beta - \frac{a_0}{t} \sin \theta \right], \theta \leq \pi - \beta \quad (\text{Eqn. 5})$$

where

$$\beta = \frac{\pi - \frac{a_0}{t} \theta}{2} - \frac{\pi R_i^2 p_{eff}}{4\sigma_f R_m t} \quad (\text{Eqn. 6})$$

and

- M_{NSC} = collapse moment
- σ_f = flow stress = $\frac{1}{2}(\sigma_y + \sigma_u)$
- σ_y = yield strength
- σ_u = ultimate strength
- R_m = pipe mean radius
- t = pipe wall thickness
- a_0 = crack depth = t for a through-wall crack
- R_i = pipe inner radius
- p_{eff} = pipe effective internal pressure, as defined above
- θ = half of the included crack angle
- β = complement of the angle from crack centerline to the neutral axis.

For an ideal through-wall crack, it is not physically possible for the crack tips to be below the neutral axis, so there is no need to even consider this possibility in the solution.

The term a_0/t is unity for a through-wall crack, so the equations above simplify to:

$$M_{NSC} = 2\sigma_f R_m^2 t [2 \sin \beta - \sin \theta], \theta \leq \pi - \beta \quad (\text{Eqn. 7})$$

where

$$\beta = \frac{\pi - \theta}{2} - \frac{\pi R_i^2 p_{eff}}{4\sigma_f R_m t} \quad (\text{Eqn. 8})$$

2.2.2 ENG2_mp Through-Wall Crack Model

The ENG2_mp module calculates the critical crack size for an ideal through-wall crack in a pipe subjected to combined tension and bending loading using a J-estimation scheme technique. The theoretical development is from Brust and Gilles [19].

Using the geometry of the pipe and crack as shown in Figure 5, and a Ramberg-Osgood description of the elastic-plastic behavior of the material at the crack, Brust/Gilles calculate the elastic and plastic contributions to the applied J-integral for tension and bending loading of the crack.

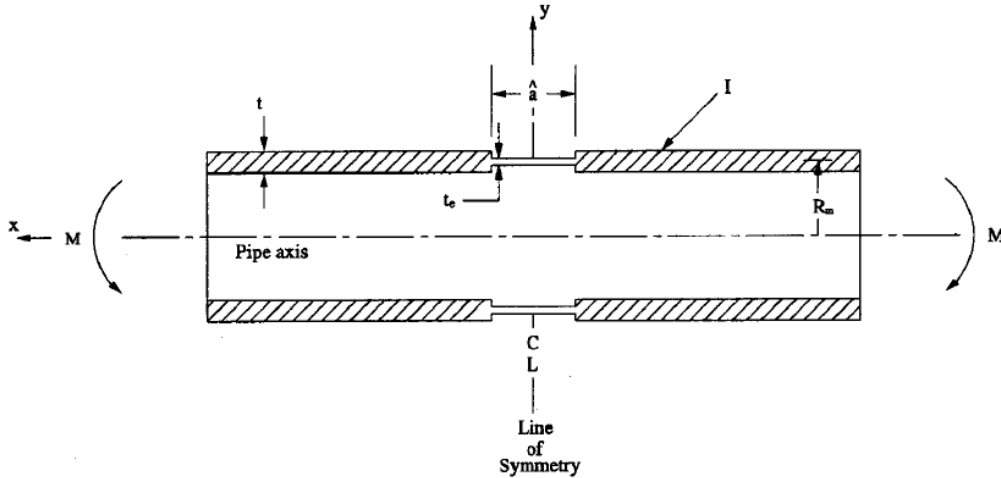


Figure 5. Reduced section analogy of the LBB.ENG2 J-estimation scheme

The LBB.ENG2 J-integral estimation method is developed based on the assumption of deformation plasticity and thin-shell behavior. It is assumed that the J-integral is obtained by the sum of an elastic part (J_e) and the plastic part (J_p).

$$J = J_e + J_p \quad (\text{Eqn. 9})$$

The subscripts e and p refer to elastic and plastic components, respectively. Similarly, the total rotation (ϕ^c) and axial displacement (δ^c) due to the crack are written as

$$\phi^c = \phi_e^c + \phi_p^c \quad (\text{Eqn. 10})$$

$$\delta^c = \delta_e^c + \delta_p^c \quad (\text{Eqn. 11})$$

where the superscript c refers to the crack.

The stress-strain constitutive relation is represented by the Ramberg-Osgood equation,

$$\frac{\varepsilon}{\varepsilon_o} = \frac{\sigma}{\sigma_o} + \alpha \left(\frac{\sigma}{\sigma_o} \right)^n \quad (\text{Eqn. 12})$$

where σ_o is a reference stress that is usually assumed to be yield stress; $\varepsilon_o = \sigma_o/E$ is the associated strain with elastic modulus E ; and α and n are the model parameters that fit experimental data.

2.2.2.1 ELASTIC SOLUTION

The elastic component of the J-integral can be obtained as

$$J_e = \frac{K_I^2}{E} \quad (\text{Eqn. 13})$$

where K_I is the mode I stress intensity factor. The K_I solution is given as

$$K_I = (F_t \sigma_t + F_b \sigma_b) \sqrt{\pi R_m \theta} \quad (\text{Eqn. 14})$$

where σ_t and σ_b are applied stresses due to axial tension (T) and global bending (M), respectively. F_t and F_b are the corresponding shape factors that are a function of pipe geometry and crack size (θ/π). The shape factors are provided in Reference [19].

The elastic components of the rotation and axial displacement are given as,

$$\phi_e^c = \frac{M}{\pi R_m^2 t E} I_b(\theta) \quad (\text{Eqn. 15})$$

$$\delta_e^c = \frac{T}{4\pi t E} I_t(\theta) \quad (\text{Eqn. 16})$$

where I_b and I_t are defined as,

$$I_b(\theta) = 4 \int_0^\theta \xi F_b^2(\xi) d\xi \quad (\text{Eqn. 17})$$

$$I_t(\theta) = 4 \int_0^\theta \xi F_t^2(\xi) d\xi \quad (\text{Eqn. 18})$$

and the subscripts b and t refer to bending moment and axial tension, respectively. Details for the derivations of (Eqn. 15) and (Eqn. 16) can be found in Reference [19].

2.2.2.2 PLASTIC SOLUTION

The plastic part of the J-integral is defined below, again, separated into bending and tension components as,

$$J_p^b = - \int_0^{\phi_p^c} \left. \frac{\partial M}{\partial A} \right|_{\phi_p^c} d\phi_p^c \quad (\text{Eqn. 19})$$

$$J_p^t = - \int_0^{\delta_p^c} \left. \frac{\partial T}{\partial A} \right|_{\delta_p^c} d\delta_p^c \quad (\text{Eqn. 20})$$

where A is the exposed crack area.

In order to obtain J_p , the relationship between M and ϕ_p^c or T and δ_p^c needs to be estimated, depending on the type of applied loads.

When the plastic part of (Eqn. 12) applies, it is assumed that,

$$\phi_p^c = L'_b \alpha \left(\frac{\sigma_b}{\sigma_o} \right)^{n-1} \phi_e^c \quad (\text{Eqn. 21})$$

$$\delta_p^c = L'_t \alpha \left(\frac{\sigma_t}{\sigma_o} \right)^{n-1} \delta_e^c \quad (\text{Eqn. 22})$$

utilizing (Eqn. 15) and (Eqn. 16).

Using an analogy between the cracked pipe and a reduced thickness pipe, Figure 5, wherein the competent, but reduced thickness section that responds in the same way as the cracked pipe, L'_b and L'_t in (Eqn. 21) and (Eqn. 22) can be determined by applying classical beam theory with appropriate boundary conditions, compatibility conditions, and equations for the elastic and plastic parts of the rotation and axial displacement due to the respective sections. The equivalent reduced thickness, t_e , can then be determined by forcing the limit load of the reduced pipe section to be equivalent to the limit load of the cracked pipe section.

For a circumferential TWC in a single-material pipe subjected to bending load, L'_b and L'_t can be shown to be, after some manipulation,

$$L'_b = \left(\frac{t}{t_e} \right)^{n-1} \left(\frac{\pi}{4\hat{K}} \right)^n \quad (\text{Eqn. 23})$$

$$L'_t = \left(\frac{t}{t_e} \right)^{n-1} \quad (\text{Eqn. 24})$$

where

$$\hat{K} \approx \frac{\sqrt{\pi}}{2} \frac{\Gamma\left(1+\frac{1}{2n}\right)}{\Gamma\left(\frac{3}{2}+\frac{1}{2n}\right)} \quad (\text{Eqn. 25})$$

and $\Gamma(x)$ is the gamma function. Note: For a single material pipe, which is always assumed in xLPR (the effect of a dissimilar metal weld is approximated by using “smeared” material properties), the solution for J at the crack is independent of the reduced thickness section length, \hat{a} .

After determining the M - ϕ_p^c and T - δ_e^c relationships from (Eqn. 21) and (Eqn. 22), (Eqn. 19) and (Eqn. 20) can be integrated to evaluate J_p in closed-form as

$$J_p^b = \frac{\pi R_m}{2} \left(\frac{\alpha}{E \sigma_o^{n-1}} \right) \left(\frac{1}{n+1} \right) H_b L'_b I_b \left(\frac{M}{\pi R_m^2 t} \right)^{n+1} \quad (\text{Eqn. 26})$$

$$J_p^t = \frac{\pi R_m}{2} \left(\frac{\alpha}{E \sigma_0^{n-1}} \right) \left(\frac{1}{n+1} \right) H_t L'_t I_t \left(\frac{T}{2\pi R_m t} \right)^{n+1} \quad (\text{Eqn. 27})$$

where

$$H_b = \frac{1}{I_b} \frac{\partial I_b}{\partial \theta} + \frac{1}{L'_b} \frac{\partial L'_b}{\partial \theta} \quad (\text{Eqn. 28})$$

and

$$H_t = \frac{1}{I_t} \frac{\partial I_t}{\partial \theta} + \frac{1}{L'_t} \frac{\partial L'_t}{\partial \theta} \quad (\text{Eqn. 29})$$

For combined tension and bending moment conditions, J_p is estimated as

$$J_p = J_p^b + J_p^t \quad (\text{Eqn. 30})$$

Because the tension load is assumed to be applied at the neutral axis of the pipe, the moment M in Eq. (17) must be replaced with an effective moment M_{eff} ,

$$M_{eff} = M + T e \quad (\text{Eqn. 31})$$

where

$$e = R_m \sin \left(\frac{\theta}{2} \right) \quad (\text{Eqn. 32})$$

The derivatives of the I -functions (I_b , I_t) and L -functions (L'_b , L'_t) can be explicitly derived in closed form for efficient solution.

Consistent with typical fracture mechanics treatment, crack “size” is always assumed to be a length. Accordingly, in the LBB.ENG2 solution, a simple linear transformation from the angular specification of the crack size in radians, θ , is replaced by the arc length of the crack at the mean radius in length units as

$$a = R_m \theta \quad (\text{Eqn. 33})$$

Assuming that the applied tension load and bending moment are constant, two conditions must be satisfied at crack instability (i.e., current crack size = critical crack size). Those two conditions are:

$$J(a_0, a^*)_{applied} = J(a_0, a^*)_{material} \quad (\text{Eqn. 34})$$

$$\frac{dJ(a_0, a^*)}{da}_{applied} = \frac{dJ(a_0, a^*)}{da}_{material} \quad (\text{Eqn. 35})$$

where a_0 is an unknown initial crack length and a^* is the critical crack length at instability. Note: the critical crack length at instability, a^* , is always larger than the initial crack size, a_0 .

Given a model for the pipe material's J-resistance, given by

$$J_{material} = J_i + C(\Delta a)^m \quad (\text{Eqn. 36})$$

where

- J_i = fracture initiation toughness
- C = fitting coefficient for extrapolated J-R curve
- Δa = crack growth
- m = J-R curve hardening exponent,

the ENG2_mp subroutines find the initial crack length and critical crack length that satisfy the two conditions listed above.

Further details regarding the technical basis behind the TWC_fail model and its implementation can be found in the appendices of the SDD for TWC_fail [4].

2.2.3 Axial Force Calculation

The through-wall crack equations are traditionally expressed in terms of pressure as the sole contributor to the axial load. Indeed, this is not the usual case in most piping systems where there are axial loads from deadweight, thermal expansion, and dynamic excitation. As was the case for SC_fail, in order to leave the underlying through-wall crack analysis equations in a form best suited for QA, the contribution of axial loads, inclusive of pressure, is accounted for by use of an effective pressure term.

$$\sigma_{ax} = \frac{\pi R_i^2 p + F_{ax}}{2\pi R_m t} = \frac{\pi R_i^2 p_{eff}}{2\pi R_m t} \quad (\text{Eqn. 37})$$

where

- σ_{ax} = total axial stress
- R_i = pipe inner radius
- p = pipe internal pressure
- F_{ax} = applied axial force due to deadweight, thermal expansion, and dynamic excitation (excluding pressure contribution)
- R_m = pipe mean radius
- t = pipe wall thickness
- p_{eff} = effective pipe internal pressure.

Thus,

$$p_{eff} = \frac{\pi R_i^2 P + F_{ax}}{\pi R_i^2} \quad (\text{Eqn. 38})$$

2.3 The Axial Crack Stability Models

The axial surface crack and axial through-wall crack stability modules are stand-alone modules called from within the xLPR Framework. The Axial_SC_fail module employs a plastic collapse model to assess the stability of an internal axial surface crack, while the Axial_TWC_fail module employs both limit load and elastic-plastic fracture mechanics (EPFM) models to assess the stability of an idealized axial TWC in a single pipe material. Neither of the axial crack stability models, presently, include the effects of weld residual stresses. It is also to be noted that cracks in welds with two separate materials, namely a base-metal and a weld metal, are beyond the scope of the present module design.

2.3.1 Axial_SC_fail Model

The Axial_SC_fail module performs the stability calculation for an axial SC using a plastic collapse method. By using the constant depth surface crack plastic collapse solution from the Ductile Fracture handbook [20], the model finds the critical pressure for the input SC configuration. For the case of a semi-elliptical SC, the area of the semi-elliptical surface crack is equated to the area of a constant depth surface crack to arrive at the effective half-crack length (c_{eff}), where the area is divided by the maximum depth of the semi-elliptical crack.

The following (Eqn. 39) is used within this subroutine to calculate the critical pressure, pSESC for the axial half-crack length.

$$p_{SESC} = p_o [(1-d/t)/(1-d/t/(tM_2))] \quad (\text{Eqn. 39})$$

where

- $p_o = (t \sigma_f)/R_o$
- $M_2 = [1 + 1.61 \lambda^2]^{0.5}$, a so called bulging factor for an axial crack that accounts for the fact axially cracked pipes “bulge” when pressurized.
- $\lambda = c/(R_m t)^{0.5}$
- σ_y = yield stress
- σ_u = ultimate stress
- σ_f is the flow stress calculated as, $\sigma_f = 0.5(\sigma_y + \sigma_u)$
- R_o = outer radius of the pipe,
- R_m = mean radius of the pipe,
- d = crack depth,
- t = pipe wall thickness, and
- c = axial half-crack length of the constant depth surface crack.

2.3.2 Axial_TWC_fail Model

The Axial_TWC_fail module uses two models to calculate the critical axial through-wall crack length. The first model, a limit load solution, uses only crack geometry, yield and ultimate strengths to estimate the critical crack size. The second model uses an EPFM method to perform a J-tearing analysis to estimate the critical crack size.

2.3.2.1 Axial Through-wall Crack Limit Load Model

The axial through-wall crack limit load model uses a model in the Ductile Fracture Handbook [20] to calculate the critical axial half-crack length using the Net-Section Collapse (NSC) equations. The initial guess for the half-crack length is obtained from the first two terms of the Folias/bulging factor (M_1) for an axial through-wall crack in a pipe [20].

(Eqn. 40) is used to calculate the axial critical half-crack length for the through-wall crack for limit load conditions as,

$$p = (t \sigma_f) / (R_m M_1) \quad (\text{Eqn. 40})$$

where

$$M_1 = [1 + 1.2987\lambda^2 - 0.026905\lambda^4 + 5.3549 \times 10^{-4} \lambda^6]^{0.5} \quad (\text{Eqn. 41})$$

$$\lambda = c / (R_m t)^{0.5} \quad (\text{Eqn. 42})$$

and,

- p = applied pressure,
- R_m = mean radius of pipe,
- t = pipe wall thickness,
- c = the current axial half-crack length,
- σ_f = flow stress, and
- M_1 = the Folias/bulging factor for an axial through-wall crack.

The model employs an iterative numerical procedure while solving for the critical half-crack length until the difference in pressure and the difference in half-crack length between successive iterations, termed “[perror]” and “[cerror]”, respectively, are both within 0.1% of the pressure and half-crack length calculated in the previous iteration. The numerical method employed is similar to a gradient-descent method allowing for rapid convergence. The solution is applicable within the range of $0 < \lambda \leq 5$.

2.3.2.2 Axial Through-wall Crack EPFM Model

The axial crack EPFM analysis uses the model described in the paper by Kim, et al. [21] to obtain the critical axial half-crack length using an EPFM solution for the input pressure specified.

Derivatives of the J values (applied crack-driving force) at the current iteration crack length (c) are found numerically using three values, J_1 , J_2 , and J_3 at small increments of crack growth as shown in (Eqn. 43) and (Eqn. 44),

$$dJ/da = (J_3 - J_1)/(c_3 - c_1) \quad (\text{Eqn. 43})$$

$$d^2J/da^2 = (J_3 - 2J_2 + J_1)/(0.001c)^2 \quad (\text{Eqn. 44})$$

Similarly, the J_{material} (fracture toughness denoting the material resistance) values and the derivatives of J_{material} with respect to the crack length are computed using the user input fracture toughness parameter values, J_i , C , and m , using (Eqn. 45) through (Eqn. 47),

$$J_{\text{material}} = J_i + C(\Delta a)^m \quad (\text{Eqn. 45})$$

$$dJ_{\text{material}}/da = m C(\Delta a)^{(m-1)} \quad (\text{Eqn. 46})$$

$$d^2J_{\text{material}}/da^2 = m(m-1) C(\Delta a)^{(m-2)} \quad (\text{Eqn. 47})$$

where

- J_i = the initiation fracture toughness,
- C = the coefficient for the J - R curve,
- m = the exponent for the J - R curve, and
- Δa = crack growth, i.e. difference in the crack length between the initial and current crack length.

The axial TWC EPFM model uses the non-dimensional crack length parameter, $\lambda = c/(R_m t)^{0.5}$, and influence functions to obtain the parametric coefficients for calculating the plastic part of the crack-driving force, J_p . During the solution process, the half the hoop stress (see (Eqn. 48)), the elastic part of the crack-driving force, J_e (see (Eqn. 49)), the plastic limit pressure p_L (see (Eqn. 50)), and the plastic part of the crack-driving force, J_p (see (Eqn. 51)) are used to obtain the total crack-driving force, $J = J_e + J_p$, for an applied pressure, p , and crack length, c . As in the GE/EPRI EPFM cracked pipe analysis method, a plastic zone correction (Δr_y) is added to the half-crack length (c) to obtain the effective half-crack length ($c_e = c + \Delta r_y$) in the estimation of J_e , where the terms Δr_y and Δr_y are defined in (Eqn. 52).

$$\sigma^\infty = (p R_i)/(2t) \quad (\text{Eqn. 48})$$

$$J_e = (1/E) \{ (\sigma^\infty (\pi c)^{0.5} F)^2 \} \quad (\text{Eqn. 49})$$

$$p_L = (2/3^{0.5}) \sigma_y (t/R_m) (1 / \{ 1 + 0.34\lambda + 1.34\lambda^2 \}^{0.5}) \quad (\text{Eqn. 50})$$

$$J_p = \alpha \sigma_y \varepsilon_0 c h_1(n) (\rho/\rho_L)^{n+1} \quad (\text{Eqn. 51})$$

$$\phi = 1/\{1 + (\rho/\rho_L)^2\}, r_y = \{1/(2\pi)\}\{(n-1)/(n+1)\}\{(K/\sigma_y)^2\} \quad (\text{Eqn. 52})$$

and

$$K = (J_e E)^{0.5} \quad (\text{Eqn. 53})$$

where

- p = applied pressure
- R_i = pipe inner radius
- R_m = mean pipe radius
- t = pipe wall thickness
- E = elastic modulus of the material
- c = current axial half crack length
- ρ = non-dimensional crack length $\rho = c/(R_m t)^{0.5}$
- F = a shape factor
- α = coefficient of Ramberg-Osgood model
- σ_y = yield strength
- σ[∞] = half the value of the hoop stress
- ε₀ = reference strain, e.g., strain at yielding
- h₁ = fully plastic influence function for the GE/EPRI method
- n = hardening exponent in the Ramberg-Osgood model
- ρ_L = plastic limit pressure, assuming a yield strength of σ_y
- J_e = calculated value of the elastic part of the J-integral
- J_p = calculated value of the plastic part of the J-integral
- K = stress intensity factor.

Values of the influence functions h_1 , and F for values of R_m/t , ρ , and n are found using look-up tables provided in Kim, et al. [21] and linear interpolation within the look-up table values. The parameter values are limited to the ranges of: $5.0 < R_m/t < 20$, $1.0 < n < 7.0$, and $0.5 < \rho < 3.0$. For cases that exceed (smaller or larger) these limits, the bounding values of the influence functions are used in the calculated J values.

3. MODULE DEVELOPMENT

3.1 SC_Fail Module

The SC_fail module assesses the stability of multiple circumferentially-oriented surface cracks (SC) in a pipe subjected to combined tension and bending loading. This module is valid for cases when one or more cracks are present in the pipe. Based on input pipe/crack geometries, pipe material properties, and loads, the ultimate moment-carrying capacity of multiple surface cracks, or in the limit an individual surface crack, are compared with the current (applied) loading. A flag is returned that indicates the results of this comparison: Predicted failure, yes or no, along with the ratio of the current (applied) bending moment to the bending moment that would result in an instability.

3.1.1 SC_fail Module Requirements

The specific requirements for the SC_fail module were generated as part of the development process for the SRD for the SC_fail [1] module. These requirements are provided in tabular form in Table 1. The requirement appended with an asterisk at the end (i.e., SCF-4*) is a Framework interface or integration requirement. This kind of requirement relates to the interfacing of the SC_fail module with the overhead DLL wrapper, the xLPR Computational Framework, the Inputs Database, or other Models Group modules, such as the Crack Growth or Leak Rate modules.

Table 1. SRD requirements for SC_fail module [1]

Requirement	Short Description of Requirement
SCF-1	Develop a software application that will determine if a circumferential surface crack instability has occurred and provide a ratio of current (applied) bending moment to bending moment which would result in an instability.
SCF-2	The application must be designed in such a way that the design attributes of adaptability, modularity, maintainability, portability, and extensibility can be realized successfully by future developers who were not necessarily involved in the original task of creating the software. The module will minimize the need for computational resources.
SCF-3	The application must comply with all xLPR Project Software Quality Assurance (SQA) requirements as specified in References [23] and [24], including evaluations for correctness, consistency, completeness, accuracy, readability, and testability, and be prepared to successfully meet the criteria of all SQA audits.
SCF-4*	Develop the SC_fail Module to be implemented as an external DLL element where the actor is the GoldSim xLPR application.
SCF-5	The required inputs and outputs are presented in Tables 1 and 2 of the SRD [1].
SCF-6	Inputs will be required in the SI system of units (see Table 1 from the SC_fail SRD [1]) for xLPR, but the module will actually only need a consistent set of units. Additionally, the physical models will be implemented using the SI system of units.
SCF-7	Develop a suite of tests that exercise all significant elements of the module. The agreement between the maximum moment values for a series of surface crack pipe experiments and the corresponding predicted maximum moments from the SC_fail module are to be within 10%, on average.

Requirement	Short Description of Requirement
SCF-8	Implement validity checks for all inputs and report invalid inputs to the user by returning a termination code flag.
SCF-9	Identify those conditions where the implemented models are beyond the bounds of the known solutions and report these cases to the user by returning a warning code flag. Calculations will be implemented at the bounds and those values (along with the warning flag) will be returned.

3.1.2 SC_fail Module Inputs and Outputs

The specific input and output variables used by the SC_fail Module are described in Table 2 and Table 3. Table 4 specifies a list of errors (code execution should terminate) and warnings (a log of the warning messages should be maintained for subsequent user interpretation). The module relies on the xLPR Framework to sample any random variables and pass them to the module as input arguments.

Table 2. Description of circumferential surface crack stability module (SC_fail) input variables

Input Variable Name	Type	Description	Units	Value	Limits / Comments
R_o	Real	Pipe outer radius	mm	Defined in Inputs Database	Ro > thick
Thick	Real	Pipe wall thickness	mm	Defined in Inputs Database	Thick > 0
Step_size	Real	Step size for crack discretization	mm	Calculated in the Framework	Step_size>0
Ncracks	Integer	Number of cracks	Unitless	Provided by the Framework	N>=0
Depth(N)▪	Real	Crack depth array	mm	Defined in Crack Growth Database	depth < thick
Theta(N)▪	Real	Half crack length array	radians	Defined in Crack Growth Database	0 < Theta < π
Gamma(N)▪	Real	Crack location array	radians	Defined in Crack Growth Database	- π < Gamma < π
Sigy	Real	Pipe yield stress	MPa	Sampled by the Framework	sigy > 0
Sigu	Real	Pipe ultimate stress	MPa	Sampled by the Framework	sigu >= sigy
RO_alpha	Real	Ramberg-Osgood coefficient	Unitless	Sampled by the Framework	RO_alpha > 0
RO_sigo	Real	Ramberg-Osgood reference stress	MPa	Sampled by the Framework	RO_sigo > 0
RO_epso	Real	Ramberg-Osgood reference strain	Unitless	Sampled by the Framework	RO_epso > 0

Input Variable Name	Type	Description	Units	Value	Limits / Comments
RO_n	Real	Ramberg-Osgood exponent	Unitless	Sampled by the Framework	RO_n > 0
Resist_Jic	Real	Pipe material initiation J-resistance	N/mm	Sampled by the Framework	Resist_Jic > 0
Resist_C	Real	Pipe material J-resistance coefficient	N/mm ^(Resist_m+1)	Sampled by the Framework	Resist_C > 0
Resist_m	Real	Pipe material initiation J-resistance exponent	Unitless	Sampled by the Framework	Resist_m > 0
Step_phi♦	Integer	Number of steps for discretization of phi over [-π,π]	Unitless	Not currently used in Framework	Step_phi>=0
Uncert_Flag♦	Integer	Uncertainty flag	Unitless	Not currently used in Framework	Uncert_Flag>=0
usample♦	Integer	Sample size for uncertainty	Unitless	Not currently used in Framework	Usample>=0
Uampli♦	Real	Amplitude of uncertainty	Unitless	Not currently used in Framework	Uampli>=0
Rseed♦	Integer	Random seed used for uncertainty	Unitless	Not currently used in Framework	Rseed>=0
BM	Real	Applied bending moment	N-mm	Defined in Loads Database	BM>=0
pressure	Real	Pipe internal pressure	MPa	Defined in Loads Database	Pressure>=0
F_ax	Real	Applied axial force (excluding pressure effect) [force], N	N	Defined in Loads Database	F_ax >=0
DMW_ratio	Real	Mixture Fraction for DMW analyses	Unitless	Constant value passed by Framework from Inputs Database	0<=DMW_ratio<=1
DMW_flag	Integer	Flag to indicate that a DMW analysis is being done	Unitless	Constant value passed by Framework from Inputs Database	=0, not DMW analysis =1,DMW analysis
crack_morph	Integer	SC analysis method = 1, constant depth surface crack NSC = 2, parabolic surface crack NSC♦ = 3, semi-elliptical surface crack NSC♦	Unitless	User Defined	crack_morph = 1 crack_morph = 2 crack_morph = 3
i_write	Integer	Solution write flag = 0, do not write = 1, write solution values to file "SC_Fail.out"	Unitless	User Defined, not currently used in Framework	i_write = 0 i_write = 1
Loopopt♦	Integer	Looping options	Unitless	User Defined, not currently used in Framework	

♦ Variables used in the implementation of the work found in [16] that provide additional flexibility to handle crack profile uncertainty and possible future enhancements for later versions

▪ Depth, theta, and gamma may be passed as a matrix to the source code

Table 3. Description of circumferential surface crack stability module (SC_fail) output variables

Output Variable Name	Type	Description	Units	Value	Limits / Comments
if_flag	Integer	Solution return code [integer], unitless = 0, the SC does not fail = 1, the SC will fail under the applied loads = -1, no solution due to an error	Unitless	Set in Module	
i_error	Integer	Solution return code [integer], unitless = 101, Crack depth greater than or equal to thickness for any crack = 102, Outer radius less than or equal to 2*thick = 103, Crack half-length less than or equal to 0 or greater than or equal to π for any crack = 104, Crack location less than $-\pi$ or greater than π = 105, Overlapping cracks = 106, Yield stress less than or equal to 0 or ultimate stress less than or equal to zero or yield stress greater than ultimate stress = 107, Any of the four Ramberg-Osgood parameters (Ro_alpha, RO_sigo, RO_epso, RO_n) less than 0 = 108, And of three J-R curve constants (resist_Jic, resist_C, resist_m) less than zero = 109, Applied internal pressure less than 0 or applied bending moment less than 0 = 110, Loading and/or crack size put neutral axis out of range	Unitless	Set in Module	
ratio_BM	Real	Bending moment ratio [real], unitless ≥ 0.0 , BM/BM_max = -1.0, if_flag <0	Unitless	Calculated in Module	

Table 4. Errors and warnings for the SC_fail module

If_flag value	Error / Warning	Description
0	N / A	Valid Solution - SC does not fail
1	N / A	Valid Solution – single SC fails under the applied loads
-1	Error	No Solution
i_error value	Error / Warning	Description
101	I/O Error	Crack depth greater than or equal to thickness for any crack
102	I/O Error	Outer radius less than or equal to 2*thick
103	I/O Error	Crack half-length less than or equal to 0 or greater than or equal to π for any crack
104	I/O Error	Crack location less than $-\pi$ or greater than π
105	I/O Error	Overlapping cracks
106	I/O Error	Yield stress less than or equal to 0 or ultimate stress less than or equal to zero or yield stress greater than ultimate stress
107	I/O Error	Any of the four Ramberg-Osgood parameters (Ro_alpha, RO_sigo, RO_epso, RO_n) less than 0
108	I/O Error	And of three J-R curve constants (resist_Jic, resist_C, resist_m) less than zero
109	I/O Error	Applied internal pressure less than 0 or applied bending moment less than 0
110	I/O Error	Loading and/or crack size put neutral axis out of range

3.1.3 SC_fail Structure

The SC_fail module uses a wrapper, Subroutine SC_fail, for doing the surface crack assessment and providing the user the option to select any of a number of surface crack analyses by an input flag. Presently, three surface crack ultimate load carrying capacity prediction routines have been developed:

- Multiple surface cracks with constant depth Net-Section-Collapse (NSC) analysis method [16],
- Multiple surface cracks using a NSC solution with a semi-elliptical crack profile [16], and
- Multiple surface cracks using a NSC solution with a parabolic crack profile [16].

At this time, the semi-elliptical and parabolic crack depth analyses are not used in the Framework. Eventually, a local collapse surface crack solution and/or an elastic-plastic fracture mechanics (EPFM) surface crack solution may be included in xLPR. Accordingly, the inputs for SC_fail have been designed to accommodate these updates, so no revision to the calling routine will be required when these features are added.

The basic flow of the SC_fail wrapper is as follows:

- Perform some simple input validity checks.
- Prepare data for calling the appropriate SC analysis.
- Perform the SC stability assessment based on the method selected by an input flag.
- Compare the predicted surface crack load-carrying capacity with the applied loads.
- Return the result of the SC assessment: the ratio of the bending moments (applied/critical) and a flag: 0, if no failure; 1, if failure is predicted for a single crack; and 2, if failure is predicted for the multiple crack case.

The SC_fail wrapper has been designed to run in any consistent set of units. A recommended set of basic units is as follows:

- Length: mm
- Force: Newtons (N)
- Angles: radians

Accordingly, derived consistent units are as follows:

- Moment: N-mm
- Stress: $\text{N/mm}^2 = \text{MPa}$
- Strain: mm/mm (unitless)
- Pressure: $\text{N/mm}^2 = \text{MPa}$
- Initiation toughness (J_{ic}): $\text{N/mm} = \text{kJ/m}^2$
- Fracture resistance constant (C): $\text{N/mm}^{(m+1)}$
- Ramberg-Osgood parameter (α), unitless
- Exponents for Ramberg-Osgood strain hardening (n) and fracture resistance (m) (unitless).

3.2 TWC_Fail Module

The TWC_fail module assesses the stability of a circumferentially-oriented through-wall crack (TWC) in a pipe subjected to combined tension and bending loading. Based on input pipe/crack geometries, pipe material properties, and loads, the critical crack size of the through-wall crack (θ_{crit}) is compared with the current crack size. A flag is returned that indicates the results of this comparison: Predicted failure, yes (if_flag = 1) or no (if_flag = 0), as well as the ratio of the current crack angle (θ) to the critical crack angle (θ_{crit}).

3.2.1 TWC_fail Requirements

The specific requirements for the TWC_fail module were generated as part of the development process for the SRD for the TWC_fail [2] module. These requirements are provided in tabular form in Table 5. Those requirements appended with an asterisk at the end (i.e., TWCF-10* thru TWCF-15*) are Framework interface or integration requirements. These requirements relate to the interfacing of the TWC_fail modules with the overhead DLL wrapper, the xLPR Computational Framework, the Inputs Database, or other Models Group modules, such as the Crack Growth or Leak Rate modules.

3.2.2 TWC_fail Module Inputs and Outputs

The specific input and output variables used by the TWC_fail Module are described in Table 6 and Table 7. Table 8 specifies a list of errors (code execution should terminate) and warnings (a log of the warning messages should be maintained for subsequent user interpretation). The module relies on the xLPR Framework to sample any random variables and pass them to the module as input arguments.

3.2.3 TWC_fail Structure

The TWC_fail module uses a main subroutine, TWC_fail, for doing the through-wall crack assessment. Presently, two TWC critical crack size (θ_{crit}) prediction methodologies are implemented:

- Idealized through-wall crack Net-Section Collapse (NSC) analysis method [17,18], and
- LBB.ENG2 elastic-plastic fracture mechanics (EPFM) through-wall crack J-estimation scheme [19].

Eventually, other through-wall crack solutions may be included in xLPR. Accordingly, the inputs for TWC_fail have been designed to accommodate these updates, so limited revisions to the calling routine will be required when these features are added.

In the current version of TWC_fail, both the idealized crack NSC and LBB.ENG2 elastic-plastic through-wall crack predictions are made. Upon return to the calling program, the solution that yields the smallest critical crack is used for the pass/fail assessment and for calculating the ratio of the current crack size to the critical crack size.

The basic flow of the TWC_fail main subroutine is as follows:

- Perform some simple input validity checks,
- Prepare data for calling the appropriate TWC analysis,
- Perform the TWC stability assessment using the Net-Section Collapse method,
- Perform the TWC stability assessment using the LBB.ENG2 EPFM method,
- Using the minimum critical crack size from the two methods (NSC and ENG2), compare the current crack size to the critical crack size, and
- Return the results of the TWC assessment: a flag: 0, if no failure or 1, if failure is predicted; the crack size ratio (current/critical); and some flags providing information about the solution.

Table 5. SRD requirements for TWC_fail module [2]

Requirement	Short Description of Requirement
TWCF-1	Develop a software application that will determine if a through-wall crack instability has occurred and provide a ratio of current crack angle (θ) to the critical crack angle (θ_{crit}) which would result in instability.
TWCF-2	The application must be designed in such a way that the design attributes of adaptability, modularity, maintainability, portability, and extensibility can be realized successfully by future developers who were not necessarily involved in the original task of creating the software. The module will minimize the need for computational resources.
TWCF-3	The application must comply with all xLPR Project Software Quality Assurance (SQA) requirements as specified in References [23] and [24], including evaluations for correctness, consistency, completeness, accuracy, readability, and testability, and be prepared to successfully meet the criteria of all SQA audits.
TWCF-4	Develop the TWC_fail Module to be implemented as an external DLL element where the actor is the GoldSim xLPR application
TWCF-5	The required inputs and outputs are presented in Tables 1 and 2 of the TWC_fail SRD [2].
TWCF-6	Inputs will be required in the SI system of units (see Table 1 of the TWC_fail SRD) for xLPR, but the module will actually only need a consistent set of units. Additionally, the physical models will be implemented using the SI system of units
TWCF-7	Develop a suite of tests that exercise all significant elements of the module. The agreement between the through-wall crack sizes for a series of through-wall crack pipe experiments and the predicted critical crack sizes from TWC_fail are to be within 10%, on average.
TWCF-8	Implement validity checks for all inputs and report invalid inputs to the user by returning a termination code flag.
TWCF-9	Identify those conditions where the implemented models are beyond the bounds of the known solutions and report these cases to the user by returning an error code. Calculations will be implemented at the bounds and those values (along with the warning flag) will be returned.
TWCF-10*	The xLPR Framework shall call the TWC_fail module when any of the following conditions are met: <ul style="list-style-type: none"> • The first time a TWC or a transitioning crack appears • Any time the applied loads change • Any time the material properties change, such as when mitigation is applied • After a TWC exists and when the crack size has grown by PWSCC, fatigue, etc. to 95% or more of θ_{crit} calculated when TWC_fail is first called.
TWCF-11*	The xLPR framework shall pass input geometry to the module
TWCF-12*	The xLPR framework shall pass the appropriate sampled material properties to the module. If a DM weld is being analyzed, the appropriate mixture percentage shall be applied to the sampled material properties before passing them to the module.
TWCF-13*	If a crack is transitioning from a surface crack to an idealized through-wall crack, the framework must calculate an equivalent idealized through wall crack length/angle by averaging the transitioning cracks ID and OD crack lengths/angles.
TWCF-14*	The framework shall pass the appropriate moments and forces to the module per the stress requirement document
TWCF-15*	The Framework shall terminate either the realization or the simulation if the if_flag is negative. For all other flags, the framework shall note the message and continue.

Table 6. Description of circumferential through-wall crack stability module (TWC_fail) input variables

Input Variable Name	Type	Description	Units	Value	Limits/ Comments
Ro	Real*8	Pipe outer radius	mm	Defined in Inputs Database	Ro > thick
Thick	Real*8	Pipe wall thickness	mm	Defined in Inputs Database	Thick > 0
Theta	Real*8	Half crack length	Radians	Defined in Crack Growth Database	0 < Theta < pi
sigy	Real*8	Pipe yield stress	MPa	Sampled by the Framework	sigy > 0
sigu	Real*8	Pipe ultimate stress	MPa	Sampled by the Framework	sigu >= sigy
RO_alpha	Real*8	Ramberg-Osgood coefficient	Unitless	Sampled by the Framework	RO_alpha > 0
RO_sigo	Real*8	Ramberg-Osgood reference stress	MPa	Sampled by the Framework	RO_sigo > 0
RO_epso	Real*8	Ramberg-Osgood reference strain	Unitless	Sampled by the Framework	RO_epso > 0
RO_n	Real*8	Ramberg-Osgood exponent	Unitless	Sampled by the Framework	RO_n > 0
Resist_Jic	Real*8	Pipe material initiation J-resistance	N/mm (or KJ/m ²)	Sampled by the Framework	Resist_Jic > 0
Resist_C	Real*8	Pipe material J-resistance coefficient	N/mm ^(Resist_m+1)	Sampled by the Framework	Resist_C > 0
Resist_m	Real*8	Pipe material initiation J-resistance exponent	Unitless	Sampled by the Framework	Resist_m > 0
pressure	Real*8	Pipe internal pressure	MPa	Defined in Loads Database	pressure >= 0
BM	Real*8	Applied bending moment	N-mm	Defined in Loads Database	BM >= 0
F_ax	Real*8	Applied axial force (excluding pressure effect)	N	Defined in Loads Database	F_ax >=0
i_write	Integer	Solution debug write flag =0, do not save =1, save analysis results for NSC and ENG2 calculations to file TWC_fail.out	Unitless	User Defined	i_write = 0 i_write = 1

Table 7. Description of circumferential through-wall crack stability module (TWC_fail) output variables

Output Variable Name	Type	Description	Units	Value	Limits/ Comments
if_flag	Integer	Solution return code =-1, no solution has been found = 0, the TWC does not fail = 1, the TWC will fail under the applied loads	unitless	Set in Module	
ratio_theta	Real*8	Crack size ratio, normally ≥ 0.0 , θ/θ_{max} =-1.0, no valid solution, see if_flag and i_err_code values < 300	unitless	Calculated in Module	
i_err_code	Integer	See Table 3 of TWC_fail SDD [4]	unitless	Set in Module	

Table 8. TWC_fail module error code (i_err_code) values

i_err_code	Condition	if_flag	ratio_theta
100	$R_o \leq 2 \cdot \text{thick}$	-1	-1.0
101	$\theta \leq 0$ OR $\theta > \pi$	-1	-1.0
102	$\text{sigy} \leq 0$ OR $\text{sigu} \leq 0$ OR $\text{sigy} > \text{sigu}$	-1	-1.0
103	$RO_alpha < 0$ OR $RO_sigo < 0$ OR $RO_epso < 0$ OR $RO_n < 0$	-1	-1.0
104	$RO_alpha = 0$ AND $RO_sigo = 0$ AND $RO_epso = 0$ AND $RO_n = 0$	-1	-1.0
105	$\text{Resist_Jic} < 0$ OR $\text{Resist_C} < 0$ OR $\text{Resist_m} < 0$	-1	-1.0
106	$\text{Resist_Jic} = 0$ AND $\text{Resist_C} = 0$ AND $\text{Resist_m} = 0$	-1	-1.0
107	$\text{pressure} < 0$ OR $\text{BM} < 0$	-1	-1.0
200	NSC solution produced a negative infinity result	-1	-1.0
201	NSC solution produced a positive infinity result	-1	-1.0
202	NSC solution produced a not-a-number result	-1	-1.0
203	ENG2 solution produced a negative infinity result	-1	-1.0
204	ENG2 solution produced a positive infinity result	-1	-1.0
205	ENG2 solution produced a not-a-number result	-1	-1.0
206	NSC and ENG2 solutions produced a negative infinity result	-1	-1.0
207	NSC and ENG2 solutions produced a positive infinity result	-1	-1.0
208	NSC and ENG2 solutions produced a not-a-number result	-1	-1.0
209	NSC iteration limit (5000) exceeded	-1	-1.0
210	NSC solution not in range of $0.0 < \theta < \pi$	-1	-1.0
211	ENG2 initial crack size starting guess could not be found in 5000 iterations	-1	-1.0
212	ENG2 solution not in range of $0.0 < \theta < \pi$	-1	-1.0

i_err_code	Condition	if_flag	ratio_theta
213	ENG2 Newton's Method iteration limit exceeded and stress is intermediate but could not find a solution for minimum error of J and dJ_da equations	-1	-1.0
300	no failure with limit defined by NSC	0	0<=value<1
301	no failure with limit defined by ENG2	0	0<=value<1
302	failure by NSC	1	value>=1
303	failure by ENG2	1	value>=1
304	no failure with limit defined by NSC. ENG2 critical crack size has stress on remaining ligament>sigu.	0	0<=value<1
305	no failure with limit defined by ENG2. ENG2 critical crack size stress on remaining ligament>sigu.	0	0<=value<1
306	failure by NSC. ENG2 critical crack size stress on remaining ligament>sigu.	1	value>=1
307	failure by ENG2. ENG2 critical crack size stress on remaining ligament>sigu.	1	value>=1
308	no failure with limit defined by NSC. ENG2 reached a Newton's Method iteration limit and stress is intermediate: ENG2 theta solution is a minimum of error of J and dJ_da equations.	0	0<=value<1
309	no failure with limit defined by ENG2. ENG2 reached a Newton's Method iteration limit and stress is intermediate: ENG2 theta solution is a minimum of error of J and dJ_da equations.	0	0<=value<1
310	failure by NSC. ENG 2 reached a Newton's Method iteration limit and stress is intermediate: ENG2 theta solution is a minimum of error of J and dJ_da equations.	1	value>=1
311	failure by ENG2. ENG2 reached a Newton's Method iteration limit and stress is intermediate: ENG2 theta solution is a minimum of error of J and dJ_da equations.	1	value>=1
312	no failure with limit defined by NSC. ENG2 reached a Newton's Method iteration limit and stress is high: ENG2 theta solution is assumed to be theta_max=0.0.	0	0<=value<1
313	no failure with limit defined by ENG2. ENG2 reached a Newton's Method iteration limit and stress is high: ENG2 theta solution is assumed to be theta_max=0.0.	0	0<=value<1
314	failure by NSC. ENG2 reached a Newton's Method iteration limit and stress is high: ENG2 theta solution is assumed to be theta_max=0.0.	1	value>=1
315	failure by ENG2. ENG2 reached a Newton's Method iteration limit and stress is high: ENG2 theta solution is assumed to be theta_max=0.0.	1	value>=1
316	no failure with limit defined by NSC. ENG2 reached a Newton's Method iteration limit and stress is low: ENG2 theta solution is assumed to be theta_max=π.	0	0<=value<1
317	no failure with limit defined by ENG2. ENG2 reached a Newton's Method iteration limit and stress is low: ENG2 theta solution is assumed to be theta_max=π.	0	0<=value<1
318	failure by NSC. ENG2 reached a Newton's Method iteration limit and stress is low: ENG2 theta solution is assumed to be theta_max=π.	1	value>=1
319	failure by ENG2. ENG2 reached a Newton's Method iteration limit and stress is low: ENG2 theta solution is assumed to be theta_max=π.	1	value>=1

The TWC_fail main subroutine has been designed to run in any consistent set of units. A recommended set of basic units is as follows:

- Length: mm
- Force: Newtons
- Crack size or crack angle: radians

Accordingly, derived consistent units are as follows:

- Moment: N-mm
- Stress: N/mm² = MPa
- Strain: mm/mm (unitless)
- Pressure: N/mm² = MPa
- Initiation toughness (J_{ic}): N/mm = kJ/m²
- Fracture resistance constant (C): N/mm(m+1)
- Ramberg-Osgood coefficient (α), unitless
- Exponent for J-R curve fracture resistance relationship (m), unitless
- Exponent for Ramberg-Osgood curve (n), unitless.

3.3 Axial Crack Failure Modules

The axial surface crack and axial through-wall crack stability modules are separate modules called from within the xLPR Framework, even though they share some common Q/A documentation. The Axial_SC_fail module employs a plastic collapse analysis to assess the stability of an internal axial surface crack, while the Axial_TWC_fail Module employs both limit load and elastic-plastic fracture mechanics (EPFM) analyses to assess the stability of an idealized axial TWC in a single pipe material. These modules use input variables for the pipe and axial crack dimensions and pipe material properties obtained from the xLPR Framework. The modules are implemented in two Fortran subroutines, one for the stability of an axial SC and one for an axial TWC, with each of them containing several subroutines and functions that can be compiled within a Dynamic-link library (DLL) executable that would be called by the xLPR Framework. Once the axial crack type (axial SC or axial TWC) has been identified by the xLPR Framework, the Framework calculates and passes the half-crack length and other necessary input parameters to the Axial_SC_fail or Axial_TWC_fail modules. Axial_SC_fail and Axial_TWC_fail do some limited checking of input data and appropriate error flags are generated and passed back to the xLPR Framework to make further decisions. Neither of the axial crack stability modules presently includes the effects of weld residual stresses. It is also to be noted that cracks in welds with two separate materials, namely a base-metal and a weld metal, are beyond the scope of the present module design.

3.3.1 Axial Crack Failure Modules Requirements

The specific requirements for the Axial_SC_fail and Axial_TWC_fail modules were generated as part of the development process for the SRDs for the Axial Crack Stability [11] modules. These requirements are provided in tabular form in Table 9. Those requirements appended with an asterisk at the end (i.e., RACS-1*, RACS-2*, RACS-4*, RACS-5* and RACS-7* through RACS-10*) are Framework interface or integration requirements. These requirements relate to the interfacing of the Axial Crack Stability modules with the overhead DLL wrapper, the xLPR Computational Framework, the Inputs Database, or other Models Group modules, such as the Crack Growth or Leak Rate modules.

Table 9. SRD requirements for axial surface crack and axial through-wall crack modules [11]

Requirement	Short Description of Requirement
RACS-1*	The xLPR Framework shall call the Axial TWC Stability Module when any of the following conditions are met: <ul style="list-style-type: none"> • Any active axial through-wall crack is initiated • When a through-wall crack is found and the ratio $c/ccrit > 0.9$ • The xLPR Framework shall call the Axial SC when any active axial surface crack is found •
RACS-2*	The xLPR Framework shall calculate/confirm the following before passing to the respective Axial SC or TWC Module: <ul style="list-style-type: none"> • Half-crack length, [c] of the axial SC or TWC Note: For transitioning TWC, average the ID and OD crack lengths before calculating the half-crack length (c) <ul style="list-style-type: none"> • Determine the crack type, [i_ctype] before passing to the corresponding SC or TWC module DLL wrapper code.
RACS-3	Tables 1 and 2 of the SRD [11] provide the inputs and outputs to the Axial SC and TWC Stability modules.
RACS-4*	The xLPR Framework shall call the Axial SC or TWC Stability modules with a set of inputs that are in conformance with the required units, data types, and within the valid range, as specified in Table 1 of the SRD [11].
RACS-5*	The xLPR Framework shall accept the outputs in conformance with the required units, data types, and within the valid range, as specified in Table 2 of the SRD [11].
RACS-6	Figure 1 of the SRD [11] provides a schematic of the Axial SC and TWC Stability modules.
RACS-7*	If the Axial SC or TWC Stability module is called by the DLL wrapper, the inputs and outputs shall be communicated with explicit passing of variables as shown in Figure 1 of the SRD [11].
RACS-8*	The xLPR Framework shall be able to accept the following output if the incoming crack type, [i_ctype] is SC: <ul style="list-style-type: none"> • Number: [Axial_SC_Ratio] • Flag: [i_sc_pc] • Flag: [if_flag_sc] • Error Code: [i_err_code] If the incoming crack type [i_ctype] is TWC, then the xLPR Framework should be able to accept the following outputs: <ul style="list-style-type: none"> • Number: [Axial_TWC_Ratio] • Flag: [i_twc_ll] • Flag: [i_twc_epfm] • Flag: [if_flag_twc] • Error Code: [i_err_code]
RACS-9*	If the pressure is greater than or equal to the critical pressure [$p/pcrit \geq 1$], [Axial_SC_fail]=1 is to be passed to xLPR Framework, and the xLPR Framework will be required to set [i_ctype]=1, because the axial SC has now become an axial TWC, and [c_over_ccrit] is set equal to its initial value of 1. The xLPR Framework also has to set the initial TWC crack length to be equal to the SC crack length before SC plastic collapse failure.
RACS-10*	The $c/ccrit$ is calculated and passed to the xLPR Framework as [Axial_TWC_ratio], the first time the Axial TWC module is called. Once this is passed to the xLPR Framework, the Axial TWC module is only called when the TWC crack length becomes such that $c/ccrit \geq 0.9$. The xLPR Framework is to check the variable [c_over_ccrit] and call the Axial TWC Module again, only when [c_over_ccrit] ≥ 0.9 .
RACS-11	Coding follows guidelines established in Recommended Programming Practices for the xLPR Pilot Project (2010)
RACS-12	The Axial SC and TWC Stability modules must be developed such that the resulting DLL to be integrated into the GoldSim Probabilistic SW Program can be replaced easily by another similar functioning DLL module.
RACS-13	The shape factors and influence coefficients as described in Reference [21] shall be used for the EPFM solution.
RACS-14	The User Manual shall contain minimum requirements.

3.3.2 Axial Crack Failure Modules Inputs and Outputs

The specific input and output variables used by the Axial Crack Stability modules are described in Table 10 and Table 11. Table 12 specifies a list of errors (code execution should terminate) and warnings (a log of the warning messages should be maintained for subsequent user interpretation). The module relies on the xLPR Framework to sample any random variables and pass them to the modules as input arguments.

Table 10. Description of Axial TWC and SC stability input variables

Input Variable Name	Type	Description	Units	Value	Limits / Comments
R_o	Real(8)	Pipe outer radius	mm	Defined in Inputs Database	R_o > 0
thick	Real(8)	Pipe wall thickness	mm	Defined in Inputs Database	0 < thick < R_o
depth	Real(8)	Surface crack depth	mm	Defined in Inputs Database	0 < depth < thick
axial_c	Real(8)	Half axial crack length	mm	Defined in Inputs Database	axial_c > 0
sigy	Real(8)	Pipe yield stress	MPa	Defined in Inputs Database	sigy > 0
sigu	Real(8)	Pipe ultimate stress	MPa	Defined in Inputs Database	sigu > 0
RO_alpha	Real(8)	Ramberg-Osgood coefficient	unitless	Defined in Inputs Database	RO_alpha > 0
RO_sigo	Real(8)	Ramberg-Osgood reference stress	MPa	Defined in Inputs Database	RO_sigo > 0
RO_epso	Real(8)	Ramberg-Osgood reference strain	unitless	Defined in Inputs Database	RO_epso > 0
RO_n	Real(8)	Ramberg-Osgood exponent	unitless	Defined in Inputs Database	RO_n > 1
Resist_Jic	Real(8)	Pipe material initiation J-resistance	N/mm	Defined in Inputs Database	Resist_Jic > 0
Resist_C	Real(8)	Pipe material J-resistance coefficient	N/mm ^(Resist_m+1)	Defined in Inputs Database	Resist_C > 0
Resist_m	Real(8)	Pipe material initiation J-resistance exponent	unitless	Defined in Inputs Database	Resist_m > 0
pressure	Real(8)	Pipe internal pressure	MPa	Defined in Loads Database	pressure >= 0

Table 11. Description of Axial TWC and SC stability output variables

Output Variable Name	Type	Description	Units	Value	Limits / Comments
Axial_TWC_fail	Integer	Predicted failure of TWC	-	0 or 1	0, TWC does not fail 1, TWC will fail under the applied pressure
Axial_TWC_ratio	Real(8)	Ratio of the current crack size to the critical crack size	-	Calculated in Axial TWC Module	c/c_{crit}
Axial_SC_fail	Integer	Predicted failure of SC	-	0 or 1	0, SC does not fail 1, SC will fail under the applied pressure
Axial_SC_ratio	Real(8)	Ratio of the current pressure to the critical pressure	-	Calculated in Axial SC Module	p/p_{crit}
i_err_code	Integer	Input error code returned to framework	-	101 to 109	101, pipe outer radius, $[R_o]$ is less than 0 102, $2x[thick]$, wall thickness exceeds pipe diameter 103, crack length, c is less than 0.0 or greater than $100 \times R_{mean}$ 104, yield strength, $[sigy]$ is less than 0, or ultimate strength $[sigu]$ is less than 0, or $[sigy] \geq [sigu]$ 105, one or more of Ramberg-Osgood parameters is/are less than 0 106, one or more of material fracture resistance, J-R curve parameters is/are less than 0 107, applied internal pressure, $[pressure]$ is less than 0.0 108, pipe wall thickness $[thick]$ is less than 0 109, Depth of surface crack, $[depth]$ is less than 0
if_flag_twc	Integer	Failure indication flag for TWC	-	-2 to 2	0, Axial TWC does not fail 1, Axial TWC fails under applied loads by limit load 2, Axial TWC fails under applied loads by EPFM -1, no solution from limit load or EPFM and $[i_err_code] = 204$ is returned to framework -2, Input error has occurred and corresponding $[i_err_code]$ in the range from 101 – 109 is returned to the xLPR Framework

Table 11. Description of Axial TWC and SC stability output variables (Cont)

Output Variable Name	Type	Description	Units	Value	Limits / Comments
if_flag_sc	Integer	Failure indication flag for SC	-	-3 to 1	<p>0, Axial SC does not fail</p> <p>1, Axial SC fails under the applied loads</p> <p>-1, not a surface crack, since [depth] ≥ [thick], and [i_err_code]=201 is returned to the xLPR Framework to set [i_ctype] = 1</p> <p>-2, Input error has occurred and corresponding [i_err_code] in the range from 101 – 109 is returned to the xLPR Framework</p> <p>-3, loading and/or crack such that no solution found for the pressure, and [i_err_code] = 202 is returned to the xLPR Framework</p>
i_twc_ll	Integer	Limit load solution status flag for TWC	-	-3 to 0	<p>0, unqualified good solution and [i_err_code] = 302 is returned to the xLPR Framework</p> <p>-1, solution not attempted because of bad input data, and the corresponding [i_err_code] = 101 – 109 is returned to the xLPR Framework</p> <p>-2, iteration limit of 5000 is exceeded, and [i_err_code] = 205 is returned to xLPR Framework</p> <p>-3, solution for the maximum crack length outside the range. [c_max] is less than 0.0 or greater than 100xmean radius, R_mean, and the [i_err_code] = 303 is returned to the xLPR Framework</p>

Table 11. Description of Axial TWC and SC stability output variables (Cont)

Output Variable Name	Type	Description	Units	Value	Limits / Comments
i_twc_epfm	Integer	EPFM solution status flag for TWC	-	-4 to 4	<p>0, unqualified good solution, and the [i_err_code] = 304 is returned to the xLPR Framework. [i_err_code] = 309 is returned when one or more of the R_m/t, ρ, n, is beyond the range for which influence coefficients (h_1, F) are available [21]</p> <p>1, good solution, but stress in ligament at maximum crack length, [c_max] exceeds ultimate strength, [sigu], and [i_err_code] = 305 is returned to xLPR Framework</p> <p>2, solution found, but iteration limit exceeded and [c_max] solution is minimum of error of J and dJ/da equations, and [i_err_code] = 306 is returned to xLPR Framework</p> <p>3, Numerical solution method iteration limit exceeded and stress is high, then [c_max] = 0.0 is assumed, and [i_err_code] = 307 is returned to xLPR Framework</p> <p>4, Numerical solution method's iteration limit exceeded and stress is low, [c_max] = 100x R_{mean}, mean radius is assumed, and [i_err_code] = 308 is returned to xLPR Framework</p> <p>-1, solution not attempted due to faulty input data, and the corresponding [i_err_code] in the range from 101 – 108 is returned to xLPR Framework</p> <p>-2, initial crack size starting guess could not be found in 5000 iterations, , and [i_err_code] = 206 is returned to xLPR Framework</p> <p>-3, initial crack size starting estimate not within the bounds of 0.0 and 100xmean radius, R_{mean}, , and [i_err_code] = 207 is returned to xLPR Framework</p> <p>-4, numerical solution iteration limit exceeded and could not find solution for minimum error of J and dJ/da equations, , and [i_err_code] = 310 is returned to xLPR Framework</p>

Table 11. Description of Axial TWC and SC stability output variables (Cont)

Output Variable Name	Type	Description	Units	Value	Limits / Comments
i_sc_pc	Integer	Plastic Collapse solution status flag for SC	-	-2 to 0	0, unqualified good solution, and [i_err_code] = 301 is returned to xLPR Framework -1, solution not attempted because of bad input data, and the corresponding [i_err_code] = 101 – 109 is returned to xLPR Framework -2, solution for the maximum pressure, [p_max] outside the range. [p_max] is less than 0.0 or greater than 1000xapplied pressure, [pressure], and [i_err_code] = 203 is returned to the xLPR Framework

Table 12. AxCS error code description and module guidance to xLPR framework

Error Code	Description	Module Guidance to xLPR Framework
101	Pipe Outer Radius is less than 0	Move to next case while specifying Input Error for this case in the Output file
102	2xWall Thickness Exceeds Pipe Diameter	Move to next case while specifying Input Error for this case in the Output File
103	Axial half-crack length is less than 0 or greater than 100×R _m	Write Input error message in the Output file, and Call the Axial Crack Stability Module when change in crack length occurs
104	One or more of the material yield, ultimate stress is less than 0, Or yield stress is greater than ultimate stress	Move to next case while specifying Input Error for this case in the Output File
105	One or more of the Ramberg-Osgood parameters is less than 0	Move to next case while specifying Input Error for this case in the Output File
106	One or more of the material fracture resistance, J–R curve is less than 0	Move to next case while specifying Input Error for this case in the Output File
107	Applied internal pressure is less than 0	Write Input error message in the Output file, and Call the Axial Crack Stability Module when change in pressure occurs
108	Pipe wall thickness is less than 0	Move to next case while specifying Input Error for this case in the Output File
109	Surface crack depth is less than 0	Write Input error message in the Output file, and Call the Axial Crack Stability Module when change in surface crack depth occurs
201	Crack is not a surface crack since crack depth is greater than pipe wall thickness	Write logical error message and Call the Axial Through-wall Crack Stability module
202	Loading and/or crack such that no solution is found for axial SC stability	Write logical error message and Call the Axial Crack Stability Module when crack and/or loading change occurs

Error Code	Description	Module Guidance to xLPR Framework
203	Solution for maximum pressure is outside the range of [0, 1000×applied pressure]	Write logical error message and Call the Axial Crack Stability Module when crack and/or loading change occurs
204	Solution not found for axial TWC stability from limit load or EPFM methods	Write logical error message and Call the Axial Crack Stability Module when crack and/or loading change occurs
205	Iteration limit of 5000 exceeded but no limit load solution found for axial TWC stability	Write logical error message and Call the Axial Crack Stability Module when crack and/or loading change occurs
206	Initial crack size starting estimate for axial TWC stability from EPFM solution could not be found in 5000 iterations	Write logical error message and Call the Axial Crack Stability Module when crack and/or loading change occurs
207	Initial crack size starting estimate for axial TWC stability not within bounds, [0, 100×R _m]	Write logical error message and Call the Axial Crack Stability Module when crack and/or loading change occurs
301	Unqualified good solution or trivial case solution found for the axial SC stability	Write informational message to output file and move to next case
302	Unqualified good solution or trivial case solution found for the axial TWC stability using limit load Calculations	Write informational message to output file and move to next case
303	Axial TWC limit load solution not in the range, [0,100×R _m]	Write informational message to output file and move to next case
304	Unqualified good solution or trivial case solution found for the axial TWC stability from EPFM calculations	Write informational message to output file and move to next case
305	Solution found for axial TWC stability using EPFM, but stress in ligament at c _{max} (maximum crack length for failure) exceeds ultimate stress	Write informational message to output file and move to next case
306	Solution found for axial TWC stability using EPFM, but numerical method's iteration limit has been exceeded and stress is intermediate, c _{max} solution is from minimum error of J and dJ/da equations	Write informational message to output file and move to next case
307	Numerical solution method's iteration limit exceeded when performing axial TWC stability using EPFM calculations, and stress is high, c _{max} = 0 is assumed	Write informational message to output file and move to next case
308	Numerical solution method's iteration limit exceeded when performing axial TWC stability using EPFM calculations, and stress is low. Hence c _{max} = 100×R _m is assumed	Write informational message to output file and move to next case
309	One or more of R _m /t, rho, Ramberg-Osgood hardening exponent n, is beyond the range for which influence coefficients (h ₁ ,F) are available [21]	Write informational message to output file and move to next case
310	Numerical iteration limit exceeded for axial TWC stability from EPFM solution, and stress is intermediate, but solution for minimum error of J and dJ/da equations could not be found	Write logical error message and Call the Axial Crack Stability Module when crack and/or loading change occurs

3.3.3 Axial Crack Failure Modules Structure

The SC_Axial_Fail module uses a main subroutine SC_Axial_Fail, for performing the SC stability assessment. The Plastic Collapse of the ligament (or Net-Section Collapse) methodology is employed for the SC stability assessment calculations.

The basic flow of the SC_Axial_Fail main subroutine is as follows:

- Perform some simple input validity checks,
- Compute an effective axial crack length,
- Calculate the critical pressure (P_{crit}) for a semi-elliptical surface crack
- Compare the current pressure to the critical pressure,
- Return the results of the axial SC assessment: a flag: 0, if no failure or 1, if failure is predicted; the crack size ratio (current/critical); and some flags providing information about the solution.

The TWC_Axial_Fail module uses a main subroutine, TWC_Axial_Fail, for conducting the through-wall crack stability assessment. Presently, two different TWC critical half-crack size (c_{crit}) prediction methodologies are implemented in the assessment routine:

- A Limit Load or Net-Section Collapse (NSC) analysis method per Section 8.3-1 of the DFH [20], and
- An Elastic Plastic Fracture Mechanics (EPFM) solution, which employs a J-integral fracture mechanics parameter approach using GE/EPRI-type J estimation equations [21].

The basic flow of the TWC_Axial_Fail main subroutine is as follows:

- Perform some simple input validity checks,
- Prepare data for calling the appropriate TWC analysis,
- Perform the TWC stability assessment using the Net-Section Collapse method,
- Perform the TWC stability assessment using the EPFM method,
- Using the minimum critical crack size from the two methods (NSC and EPFM), compare the current crack size to the critical crack size, and
- Return the results of the TWC assessment: a flag: 0, if no failure or 1, if failure is predicted; the crack size ratio (current/critical); and some flags providing information about the solution.

The axial crack failure modules have been designed to run in any consistent set of units. A recommended set of basic units is as follows:

- Length: mm
- Force: Newtons

Accordingly, derived consistent units are as follows:

- Moment: N-mm
- Stress: N/mm² = MPa
- Strain: mm/mm (unitless)
- Pressure: N/mm² = MPa
- Initiation toughness (J_{ic}): N/mm = kJ/m²
- Fracture resistance constant (C): N/mm(m+1)
- Ramberg-Osgood coefficient (α), unitless
- Exponent for J-R curve fracture resistance relationship (m), unitless
- Exponent for Ramberg-Osgood curve (n), unitless.

3.4 Stability Module General Considerations

The SC_fail, TWC_fail, and Axial Crack Stability modules all use the following interfaces:

- They receive information on pipe geometry from the Framework
- They receive material property information from the Framework
- They receive information on current crack geometry from the Framework
- They receive information on applied loads from the Framework
- They output the results from the crack stability analyses back to the Framework
 - The SC_fail module outputs a flag to indicate whether a circumferential surface crack instability has occurred and provides a ratio of current (applied) bending moment to bending moment that would result in an instability.
 - The TWC_fail module outputs a flag to indicate whether a through-wall crack instability has occurred and provides a ratio of current crack angle (θ) to the critical crack angle (θ_{crit}) that would result in instability.
 - The Axial_SC_fail subroutine returns a flag to indicate whether the input pressure is greater than or equal to the critical pressure (indicative of SC failure/rupture), as well as the pressure margin to rupture by computing the ratio of the input pressure to the critical pressure (p/p_{crit}).
 - The Axial_TWC_fail subroutine returns a flag to indicate whether the pressure load is great enough to cause the TWC to fail and the crack size margin by computing the ratio of the current crack size to the critical crack size (c/c_{crit}).
- The Framework performs actions based on error or warning flags provided by the modules
 - Errors should terminate the code
 - Warnings should be logged for user interpretation.

3.5 Module Verification

This section summarizes the results from the verification exercises carried out on the SC_fail, TWC_fail, Axial_SC_fail, and Axial_TWC_fail modules. Further details of the verification activities can be found in the Software Test Plans (STP) [5,6,13] and Software Test Results Reports (STRR) [7, 8,14] for the SC_fail, TWC_fail, and the Axial Crack Stability modules, respectively.

3.5.1 SC_fail Module Verification

The verification of the SC_fail module is documented in detail in the STRR for the SC_fail module [7]. The testing activity described in the STRR was intended to verify that the requirements specified in the SC_fail Software Requirements Document (SRD) were met [1]. The STRR covers 4 static and 30 dynamic test cases referred to in the SC_fail Software Test Plan (STP) [5], plus one additional static and 10 additional dynamic test cases created by the tester. Testing consisted of both manual inspection of the source code for the static test cases and execution testing of the source code for the dynamic test cases. One of the requirements in the SRD [1] is applicable to the Framework (SCF-4) and thus, verification of this requirement has been deferred until integration of the SC_fail module into the xLPR Framework. Below are summaries of the testing activities that were conducted.

Manual inspection of source code for requirements – TCSCF_S_001 to TCSCF_S_004:

Manual inspection of the SC_fail source code was performed per the requirements in the SRD [1] in which the verification of the design and source code logic is required as part of the acceptance criteria. Test outcomes are reported in Table 3.1 in Section 3.1 of the SC_fail STRR [7]. During manual inspection, one anomaly was found and reported under JIRA issue number XLPR-447. The details of this JIRA issue are that the subroutine inputs do not match the tables specifying the inputs in the SRD and SDD, i.e., Table 1 in both the SRD and SDD. The input “step_size” is not included in the input tables in the SRD and SDD, but it is clearly an input into the subroutine. The input vectors depth, theta, and gamma are lumped together in the matrix “cracks”. Minor revisions were made to the SRD and SDD to make the inputs match the subroutine by adding “step_size” to Table 1 of the SRD and SDD adding a footnote to these tables to indicate that the parameters depth, theta, and gamma could be passed to the source code in an array. This action resolved this JIRA issue.

Manual inspection of code for recommended programming practices – TCSCF_S_005:

Manual inspection of the final source code against the recommended programming practices [25] was performed. As recommended by Reference [25], built in MS Visual Studio diagnostics were used to check the source code. The text output (or “Build Log”) from the compiler diagnostics is included in Section 5.1 of the STRR. The results of TCSCF_S_005 are reported in Table 3.1 in Section 3.1 of the STRR. For this test, no anomalies were found that warranted the creation of JIRA issues.

Dynamic test cases for requirements – TCSCF_D_001 to TCSCF_D_040: An alternative calculation, in the form of an Excel spreadsheet, was created by the code developer and provided to the tester. This alternative calculation was reviewed by the tester and found to be adequate. A Fortran driver was written to execute the dynamic test cases, record the SC_fail module output, and the time of execution. The SC_fail STP [5] describes specific acceptance criteria for each test case. The test cases required a comparison of the alternative calculation to the module output or a comparison of the output error code against the SRD [1] requirements. Test cases TCSCF_D_031 through TCSCF_D_040 were added by the tester. For each dynamic test case, the relevant test outcomes (i.e., verification that the acceptance criteria were met) were reported

in Table 3.1 in Section 3.1 of the STRR. During dynamic testing, one anomaly was found and reported under JIRA issue XLPR-446. The details of this JIRA issue are that the error flag 105, for overlapping cracks was not triggered and the code crashed during the tester created test case TCSCF_D_031. A correction was made to the source code and a new version of the source code was released and retested successfully, thus resolving this JIRA issue. The alternative calculation spreadsheets, the Fortran driver and input files, and text file output from the dynamic test cases were published to an xLPR QA document repository.

Further detailed results from the independent verification of the SC_fail module are documented in the STRR for SC_fail [7].

3.5.2 TWC_fail Module Verification

The verification of the TWC_fail module is documented in detail in the STRR for the TWC_fail module [8]. The testing activity described in the STRR was intended to verify that the requirements specified in the TWC_fail Software Requirements Document (SRD) were met [2]. The STRR covers 62 dynamic test cases referred to in the TWC_fail Software Test Plan (STP) [6], plus additional dynamic and static tests created by the tester. Some of the requirements in the SRD [2] are applicable to the Framework and thus, verification of those requirements has been deferred until integration of the TWC_fail module into the xLPR Framework.

The results from the independent verification of the TWC_fail module, as documented in the STRR for TWC_fail [8], are summarized next:

Performance of TWC_fail STP test cases – Cases 1 to 46: These test cases were created by the code developer, along with expected results. The tester compiled the Fortran code *twc_fail_v2.0r01* using both 32- and 64-bit Intel compilers. Prior to actually running the test cases, the input files for all 46 test cases were compared with the input data specified in Table 6 of the STP [6]. The only discrepancies discovered were the internal pipe pressures for Test Cases 17 and 25. Table 6 of the STP specified that the pipe pressure for both cases was zero, while the input files specified that that the pipe pressure was 10 MPa for Test Case 17 and 15.5 MPa for Test Case 25. JIRA issue xLPR-439 was opened to document the need to resolve this issue. The 46 test cases were run by the tester using both the 32- and 64-bit compiled versions of the module. The output results for both versions were then compared with the results obtained by the developer using the file comparison utility *Beyond Compare 3* [26]. The tester found no anomalies during this testing phase. The only differences found between the two sets of output files were for Test Cases 45 and 46. For the results generated using the 32-bit version of TWC_fail, for both test cases (45 and 46), the values of θ_{max} were different, but in both cases the resultant answer was a constant raised to the e^{-299} power (essentially zero). In addition, for Case 45, the value of θ_o was different, but again the difference was in the constant raised to the e^{-307} power (again, essentially zero). For the results generated using the 64-bit version of TWC_fail, for both test cases, the values of θ_{max} were different, but for the case where the developer had obtained the solutions, the resultant answer was a constant raised to the e^{-299} power (essentially zero), whereas for the case where the tester obtained the solutions, the resultant answer was zero. A similar difference was observed for Case 45 for both the 32- and the 64-bit versions of TWC_fail for the value of θ_o .

Performance of STP test cases – Cases 47 to 62: These test cases were created by the code developer, along with expected results. The difference between the two sets of test cases is that the first set (Cases 1 to 46) were developed to demonstrate that the module properly implements the required validity checks for all inputs and properly determines if a through-wall crack instability

has occurred by calculating the ratio of the current crack angle (θ) to the critical crack angle (θ_{crit}). The second set of test cases (Cases 47 to 62) were developed to verify the module through a suite of test cases that correspond to existing experimental data. Prior to actually running the test cases, the input files for all 16 test cases were compared with the input data specified in Table 7 of the STP [6]. No discrepancies were found. The 16 test cases were run by the tester using both the 32- and 64-bit compiled versions of the module. The output results for both versions were then compared with the results obtained by the developer using file comparison utility *Beyond Compare 3* [26]. The tester found no anomalies during this testing phase.

Additional static testing: The tester examined the software requirements listed in the SRD to ensure that all requirements were tested and to determine appropriate static testing to be performed. The static testing involved examination of the code and associated documentation to verify that the listed requirements were met. Some of the elements of the verification process do not involve running the TWC_fail module to verify that it meets requirements. Rather, these cases involve issues such as: Is the code portable? Can it be turned into a DLL?, Are there any nonstandard input units considerations?, etc. Most of these cases were handled simply by inspection of the code. To formalize the traceability of requirements to the Requirements Traceability Matrix (RTM), five “static” test cases were developed in the TWC_fail STP [6], see Table 1 of the STP. Verification that TWC_fail meets these requirements simply required looking at the source code.

In addition, as an additional independent check, the tester developed an Excel spreadsheet to iteratively calculate the ratio of θ/θ_{max} for a set of input conditions which would result in a Net-Section-Collapse failure using the equations from Section 3.1.3 of the TWC_fail SDD [4]. The tester then ran TWC_fail using this set of input conditions and compared the Excel spreadsheet results with the results from TWC_fail and the agreement was exact.

Finally, the tester performed a comparison of output data from TWC_fail and an Excel spreadsheet (ENG2_mp_TWC_Fail Check.xlsx) for test cases where the failures are governed by EPFM (ENG2). The Excel spreadsheet calculates the difference between the applied J and the material J ($J_{applied} - J_{material}$) and the difference in the dJ/da values ($dJ/da_{applied} - dJ/da_{material}$), which should be the critical point reported by TWC_fail. For the test cases in the STP for which the TWC will fail under the applied loads ($if_flag = 1$) and for which the failure was predicted to be governed by the ENG2 method ($i_err_code = 303$ or 307), the values for θ_0 and θ_{max} from the TWC_fail output files, along with the other inputs from the STP, were entered in the Excel spreadsheet, and it was found that in each case, the differences between the applied J and the material J and the differences between the applied dJ/da values and the material dJ/da values were effectively zero, which is the governing constraint for a ENG2 solution. This comparison verifies that:

- The derivatives in the FORTRAN code are properly coded, and
- The ENG2 part of TWC_fail is actually finding the critical theta condition.

3.5.3 Axial Crack Stability (AxCS) Module Verification

The verification of the axial crack stability (AxCS) module is documented in detail in its STRR [14]. The testing activity described in the STRR was intended to verify that the requirements specified in the AxCS Software Requirements Document (SRD) were met [11]. This testing involves verification of both the surface crack and through-wall modules included in the AxCS suite. Separate documentation is provided in the STRR for both. The STRR covers the 48 test cases described in the AxCS Software Test Plan (STP) [13], 15 test cases to test the axial surface crack

model and 33 test cases to test the axial through-wall crack model, plus a set of static tests generated by the code developer as part of the STP. Some of the requirements in the SRD [11] are applicable to the xLPR Framework, and thus, verification of those requirements is deferred until integration of the AxCS module into the Framework.

Inputs for the 48 test cases created by the code developer were published as an Excel spreadsheet file in an xLPR Q/A document repository and provided to the tester by the code developer. Separate worksheets were provided in this file for the surface crack cases and the through-wall crack cases. Running these test cases independently confirms that the code can be successfully compiled and produces the expected results, as specified by the code developer. The tester compiled both the axial surface crack and axial through-wall crack codes using both 32-bit and 64-bit compilers. In addition, a Microsoft Excel spreadsheet was created to verify that the code produced the same results as the SDD [12] equations when programmed into Excel. Within round-off error, the results from running the axial crack stability code for the STP [13] test cases agreed with the Excel spreadsheet equations for the limit load solutions for both the axial through-wall crack cases and the axial surface crack cases as well as for the EPFM solution for the axial through-wall crack cases.

Below are summaries of the testing activities performed. Each summary includes a description of any issues uncovered and their resolution, as a result of these activities.

Performance of STP dynamic test cases – Test Cases TACS-D-1 thru TACS-D-33: These axial through-wall crack test cases were created by the code developer, along with expected results, to test the Axial_TWC_Fail module within the AxCS suite. The tester compiled the Fortran code Axial_TWC_Fail using both 32- and 64-bit Intel compilers. Prior to actually running the test cases, the input files for all 33 axial through-wall crack test cases were compared with the input data specified in the STP [13]. No discrepancies were uncovered. The 33 test cases were then run by the tester using both the 32- and 64-bit compiled versions of the module. The tester found no anomalies during this testing phase. Per the STP [13], these test cases verified Requirements RACS-3 and RACS-6 of the SRD [11]. RACS-3 specified that the module should accept input parameter values as outlined in Table 1 of the SRD and pass back to the xLPR Framework output parameter values as outlined in Table 2 of the SRD. RACS-6 specified that the modules should be developed as shown in Figure 1 of the SRD.

Performance of STP dynamic test cases – Test Cases TACS-D-50 thru TACS-D-64: These axial surface crack test cases were created by the code developer, along with expected results, to test the Axial_SC_Fail module within the AxCS suite. The tester compiled the Fortran code Axial_SC_Fail using both 32- and 64-bit Intel compilers. Prior to actually running the test cases, the input files for all 15 axial surface crack test cases were compared with the input data specified in the STP [13]. No discrepancies were found. The 15 test cases were then run by the tester using both the 32- and 64-bit compiled versions of the module. The tester found no anomalies during this testing phase. Per the STP [13], these test cases verified Requirements RACS-3 and RACS-6 of the SRD [11]. RACS-3 specified that the module should accept input parameter values as outlined in Table 1 of the SRD and pass back to the xLPR Framework output parameter values as outlined in Table 2 of the SRD. RACS-6 specified that the modules should be developed as shown in Figure 1 of the SRD.

Additional static testing: In addition to the 48 dynamic test cases discussed above, the code developer also created 8 static test cases which involved manually examining the source code to verify a number of the other requirements specified in the SRD. The static testing involved

examination of the code and associated documentation to verify that the listed requirements were met. In each case the specified requirement was met.

3.6 Module Validation

Each of the four crack stability modules, SC_fail, TWC_fail, Axial_SC_fail, and Axial_TWC_fail underwent module validation. This section summarizes the results from the validation exercises carried out on the modules. Further details of the validation activities can be found in the Module Validation Reports (MVR) [9,10,15] for the SC_fail, TWC_fail, and the Axial Crack Stability modules, respectively.

3.6.1 SC_fail Module Validation

The validation of the SC_fail module is documented in detail in the MVR for the SC_fail module [9]. The MVR documents the validation activities that characterize the predictive capability of the SC_fail module over a prescribed range of applicability, relative to available full-scale pipe test experimental data. The module was validated through comparison of the module outputs with an extensive database of single surface crack pipe fracture experiments and with a single set of multiple surface crack pipe fracture experiments.

The SC_fail module assesses the stability of surface cracks (SC) in a pipe subjected to combined tension, bending, and internal pressure loading. Based on input pipe/crack geometry, pipe material properties and loads, the critical bending moment (BM_{max}) for failure is compared with the current applied bending moment (BM). A flag is returned that indicates the result of this comparison: Predicted failure, yes (if_flag = 1) or no (if_flag = 0), as well as the ratio of the current applied bending moment (BM) to the critical bending moment (BM_{max}).

3.6.1.1 Comparisons with Single Crack Surface Crack Pipe Experiments

The first method of validation is comparing the outputs of the module with existing single crack full-scale pipe fracture experimental data (References [27] thru [50]). Over the years, a number of research programs have conducted full-scale pipe tests. Battelle has maintained a database of applicable full-scale surface crack pipe fracture data [27]. While there are a large number of experimental pipe fracture data in the Battelle database, not all of these tests were used for this validation effort because some of these tests were either missing necessary inputs to run the SC_fail module, or there were discrepancies between the test described and the results given (e.g., different references gave different values for the same tests).

The applicable and trustworthy experimental tests from the Battelle database were used in this validation. These tests can be classified into the following types of tests based on the loading conditions:

- Four Point Bending without Internal Pressure – these test cases (70 total) are for four point bending tests without internal pressure.
- Four Point Bending with Internal Pressure – these test cases (85 total) are for four point bending tests with internal pressure.
- Inertially Loaded Test Specimens – these test cases (4 total) are for pipes loaded through dynamic inertia. Bending is induced and internal pressure loading is included.

- Pipe System Experiments – these test cases (10 total) are for pipe system fracture tests. These tests include dynamic, cyclic bending and internal pressure loading.

This totals 169 full-scale single surface crack pipe experiments for validating the SC_fail module. For the validation of SC_fail, the code outputs the ratio of the applied bending moment to the calculated critical bending moment for a given test case. In these test cases, the applied bending moment used was the maximum bending moment from the pipe experiments. Ideally, the bending moment ratio output from SC_fail should be 1.0.

This data set of 169 pipe experiments chosen for validation of SC_fail should be sufficiently representative of field behavior because these experiments included the full spectrum of pipe materials (including weldments) and pipe sizes one might encounter in a commercial nuclear power plant. These 169 pipe experiments also represent the range of loading conditions that nuclear power plant piping systems may experience.

The required inputs for the SC_fail module include two types of input: inputs that change from case to case and inputs that do not change from case to case because these features either are not used and are merely placeholders for future expansion (e.g. crack toughness parameters) or inputs that are set by the Framework and the user has no control over them (e.g. looping options).

Inputs that change for each validation case

- Pipe outside radius, mm
- Pipe wall thickness, mm
- Yield strength, MPa
- Ultimate strength, MPa
- Depth of each crack, mm
- Half crack length of each crack, radians
- Maximum moment from the experiment, N-mm
- Pipe internal pressure, MPa

Inputs that do not change for each validation case

- Crack discretization step size, mm (always set to $\pi \cdot OD / 10000$)
- Number of cracks, unitless (always one for the single crack cases)
- Axial force, N (zero for all single crack cases)
- Crack center location of each crack, radians (zero, i.e. top dead center (i.e., maximum bending stress location), for all single crack cases)
- Crack morphology flag, unitless (always set to 1 for a constant depth surface crack)
- I_write flag, unitless (always set to zero to not write)
- Loopopt flag, unitless (always set to 1)
- Number of steps for discretization of phi, unitless (always set to 1000)
- Uncertainty flag, unitless (always set to 0; crack profile uncertainty is not used)
- Uncertainty sample size, unitless (always set to 100)
- Uncertainty amplitude, unitless (always set to 0.1)
- Random seed, unitless (always set to 15)
- Dissimilar metal weld mixture percentage, unitless (always set to 0.0)
- Dissimilar metal weld flag, unitless (always set to zero)
- Ramberg-Osgood alpha parameter, unitless (always set to zero)
- Ramberg-Osgood reference stress, MPa (always set to zero)

- Ramberg-Osgood reference strain, unitless (always set to zero)
- Ramberg-Osgood strain hardening exponent (n), unitless (always set to zero)
- Pipe material initiation toughness (J_{ic}), N/mm (always set to zero)
- Pipe material J-resistance coefficient (C), N/mm^(m+1) (always set to zero)
- Pipe material initiation J-resistance exponent (m), unitless (always set to zero).

The results of the validation analysis for the SC_fail module are provided in the far right column of Table 13 for the single crack cases. This column shows the value of BM ratio for each of the single crack pipe experiments analyzed (ratio of the current bending moment to the critical bending moment, where for this validation exercise, the current bending moment is the maximum bending moment from the pipe experiment). A value of 1.0 for BM ratio would indicate that there was perfect agreement between the SC_fail prediction and the experiment. Deviations from this value of 1.0 represent uncertainty in either the analysis methodology or the input data. The average value for the BM ratio was 0.987 with a standard deviation of 0.268. This level of uncertainty meets the requirement (SCF-7) specified in the SC_fail SRD [1] that:

Develop a suite of tests that exercise all significant elements of the module. The agreement between the maximum moment values for a series of surface crack pipe experiments and the corresponding predicted maximum moments from the SC_fail module are to be within 10%, on average. - **Requirement SCF-7**

The BM ratio values shown in **red font** in Table 13 are those values of BM ratio where the SC_fail predicted bending moment ratio was more than two standard deviations away from the mean of all of the single crack cases (BM ratio > 1.523 or BM ratio < 0.451). As can be seen from Table 13, there are 2 experiments (both from Schulze [28] 4-point bending + internal pressure tests) for which the BM ratio value was greater than the mean plus two standard deviations (1.523). The sixteen (16) 4-point bending + internal pressure experiments performed by Schulze only vary in the initial crack length. The radius, wall thickness, initial crack depth, material properties, and internal pressure (with the exception of one case) are all constant. The two cracks with the largest initial crack lengths (45.8% and 59.4% of pipe circumference) are these two cases where the BM ratio value was outside the mean plus two standard deviations range. This may be an indication that the SC_fail module performs poorly for larger crack lengths. However, there are many other test cases, (see Figure 6), with similar and larger crack lengths, where the SC_fail module performs much better. Consequently, it is possible that there is something anomalous about these two experiments in particular. Table 13 also shows that there are 6 experiments (all from Julisch [29] 4-point bending + internal pressure tests) for which the BM ratio value was less than the mean minus two standard deviations (0.451). Again, out of the twenty-four (24) 4-point bending + internal pressure experiments that Julisch performed, these particular test cases have the largest crack depths (90% of the pipe wall thickness). This may be an artifact of the fact that the SC_fail module performs poorly for very large crack depths. However, there are two other cases (see Kurihara results in Figure 7) with greater depths that perform better.

The single crack case validation results are also presented in Figure 6, which shows the BM ratio versus the crack length. Figure 7 shows the same results as a plot of BM ratio versus crack depth. Also presented in these figures are the mean value (solid black line) and the mean \pm one standard deviation values (dashed black lines).

Table 13. Inputs and output BM Ratio for SC_fail single crack validation cases

Experiment Number	Program	Yield Strength (MPa)	Ultimate Strength (MPa)	Maximum Experimental Moment (N-mm)	Pipe Internal Pressure (MPa)	Output BM Ratio	
Single Crack Four Point Bending Tests without Internal Pressure							
4112-1	Degraded Piping Program [30]	166.9	470.2	2.30E+08	0.0	0.88	
4112-2		146.9	448.8	2.95E+07	0.0	0.98	
4112-3		138.6	449.5	5.96E+07	0.0	1.17	
4112-4		151.0	477.1	1.01E+08	0.0	1.16	
4112-5		212.4	467.5	3.80E+07	0.0	1.02	
4112-6		319.9	620.5	8.01E+07	0.0	0.95	
4112-7		258.6	570.2	1.17E+08	0.0	1.11	
4112-8		237.2	610.2	7.48E+08	0.0	0.91	
4112-9		262.0	611.6	3.66E+08	0.0	0.82	
4115-1		239.2	527.4	2.21E+08	0.0	0.98	
4115-2		239.2	527.4	2.34E+08	0.0	1.02	
4115-4		138.6	449.5	7.14E+07	0.0	1.02	
4115-5		138.6	449.5	6.50E+07	0.0	0.99	
4115-7		138.6	449.5	6.52E+07	0.0	1.36	
4115-8		138.6	449.5	6.03E+07	0.0	1.19	
4115-9		138.6	449.5	6.35E+07	0.0	1.33	
4131-6		138.6	449.5	5.53E+07	0.0	1.28	
4131-8		239.2	527.4	1.95E+08	0.0	0.97	
EPRI-13S	EPRI-NP-2347 Vol 2 [31]	299.2	739.1	1.26E+09	0.0	1.05	
EPRI-2S		246.8	629.5	4.11E+07	0.0	1.24	
EPRI-3S		246.8	629.5	3.30E+07	0.0	1.26	
EPRI-5S		246.8	629.5	3.77E+07	0.0	1.06	
EPRI-6S		246.8	629.5	3.36E+07	0.0	1.03	
EPRI-8S		246.8	629.5	3.75E+07	0.0	1.20	
EPRI-9S		246.8	629.5	3.03E+07	0.0	1.46	
EPRI-10S		246.8	629.5	3.23E+07	0.0	1.18	
1.2.1.21	Short Cracks in Piping [27]	151.0	477.1	1.54E+08	0.0	1.34	
1.2.1.22		146.9	448.8	4.43E+07	0.0	1.01	
	Schulze [28]	335.1	490.2	8.70E+06	0.0	1.22	
4C3II035	Milella, CISE (Italy) tests [32]	284.1	426.1	4.03E+07	0.0	1.23	
4B4II050		284.1	426.1	3.07E+07	0.0	1.13	
4C1II07		284.1	426.1	1.92E+07	0.0	1.06	
4C2II07		284.1	426.1	1.92E+07	0.0	1.06	
4B1II025		284.1	426.1	3.64E+07	0.0	1.02	
4B3II050		284.1	426.1	3.07E+07	0.0	1.13	
4B2II025		284.1	426.1	3.07E+07	0.0	0.86	
6D1II050		303.0	466.1	9.03E+07	0.0	1.11	
6D2II050		303.0	466.1	8.71E+07	0.0	1.07	
6C2II025		303.0	466.1	1.16E+08	0.0	1.09	
6C1II025		303.0	466.1	1.15E+08	0.0	1.08	
6F3II05		303.0	466.1	1.15E+08	0.0	1.08	
L64II		171.0	439.9	7.59E+07	0.0	0.85	
L65II		171.0	439.9	5.01E+07	0.0	0.67	
L6E1I050		239.9	559.9	7.19E+07	0.0	1.02	
L6E2I050		239.9	559.9	7.27E+07	0.0	1.03	
LC-3		Asada, NUPEC (Japan) [33, 34]	304.1	491.6	8.25E+07	0.0	1.11
LC-4			304.1	491.6	7.78E+07	0.0	1.21

Table 14. Inputs and output BM Ratio for SC_fail single crack validation cases (cont)

Experiment Number	Program	Yield Strength (MPa)	Ultimate Strength (MPa)	Maximum Experimental Moment (N-mm)	Pipe Internal Pressure (MPa)	Output BM Ratio	
LC-5		304.1	491.6	7.93E+07	0.0	1.15	
LC-6		261.3	455.1	8.95E+08	0.0	1.02	
LC-7		261.3	455.1	8.58E+08	0.0	1.13	
MB-11		304.1	491.6	8.54E+07	0.0	1.05	
MB-12		222.0	477.1	7.94E+07	0.0	1.11	
MB-21		304.1	491.6	8.01E+07	0.0	1.13	
MB-22		222.0	477.1	6.92E+07	0.0	1.12	
MB-30		304.1	491.6	8.59E+07	0.0	1.05	
MB-32		304.1	491.6	8.38E+07	0.0	1.19	
MB-40		261.3	455.1	9.48E+08	0.0	1.07	
MB-42		185.5	428.2	9.00E+08	0.0	1.19	
DETN11		Faigy, EDF (France) [35]	182.7	437.8	5.66E+08	0.0	0.89
DETN12			177.2	433.0	1.04E+09	0.0	0.96
S-300-1	Deepwater Offshore Pipeline Group program [36]	511.6	560.5	6.28E+07	0.0	1.19	
S-300-2		511.6	560.5	6.15E+07	0.0	1.20	
S-300-3		511.6	560.5	6.36E+07	0.0	1.24	
S-300-4		511.6	560.5	5.90E+07	0.0	1.14	
S-301-1		511.6	560.5	5.19E+07	0.0	1.10	
S-301-2		511.6	560.5	5.43E+07	0.0	1.10	
1-R(a)	Wilkowski and Eiber, American Gas Association [37]	410.9	577.8	2.99E+09	0.0	0.78	
2-R(a)		410.9	577.8	3.17E+09	0.0	0.79	
2-R Repeat(a)		410.9	577.8	3.55E+09	0.0	0.88	
3-R(a)		410.9	577.8	3.99E+09	0.0	0.95	
Single Crack Four Point Bending Tests with Internal Pressure							
4131-2	The Degraded Piping Program [30]	138.6	449.5	3.41E+07	2.45E+04	1.32	
4131-4		239.2	527.4	1.60E+08	1.83E+04	1.03	
4141-2		138.6	449.5	4.11E+07	1.52E+04	0.88	
4141-4		180.0	458.5	5.02E+08	1.10E+04	0.93	
4141-6		180.0	458.5	4.45E+08	1.10E+04	0.84	
4142-1		138.6	449.5	9.32E+07	7.93E+03	1.28	
4142-2		138.6	449.5	6.33E+07	3.27E+04	1.00	
4142-3		138.6	449.5	5.36E+07	3.93E+04	0.94	
4142-4		180.0	458.5	9.92E+08	2.24E+04	1.07	
4143-2		173.1	501.2	3.86E+08	1.55E+04	0.91	
4143-1		231.0	610.2	6.72E+08	1.55E+04	0.80	
4143-3		173.1	501.2	4.10E+08	1.55E+04	1.16	
4141-8		237.2	610.2	5.94E+08	1.55E+04	0.92	
1.1-7		IPIRG-1 [38,39,40,41]	319.9	620.5	7.72E+07	1.55E+04	0.97
1.1-9	319.9		620.5	6.16E+07	1.55E+04	0.82	
4.3-2	IPIRG-1 [38,39,40,41]	244.1	575.0	7.20E+09	9.10E+03	1.02	
1.2.1.20	Short Cracks in Piping [27]	223.7	508.8	3.56E+08	1.55E+03	0.81	
1.2.3.15		231.0	544.0	2.19E+09	9.56E+03	0.74	
1.2.3.16		143.4	427.5	2.09E+09	1.01E+04	0.74	
1.2.3.17		234.1	541.6	2.58E+09	1.55E+04	0.69	
1-4	IPIRG-2 [42]	206.8	448.2	7.75E+08	1.55E+04	1.15	
1-6		180.0	458.5	6.97E+08	1.55E+04	0.87	
	Schulze [28]	335.1	490.2	1.06E+07	4.60E+03	1.36	

Table 14. Inputs and output BM Ratio for SC_fail single crack validation cases (cont)

Experiment Number	Program	Yield Strength (MPa)	Ultimate Strength (MPa)	Maximum Experimental Moment (N-mm)	Pipe Internal Pressure (MPa)	Output BM Ratio	
		335.1	490.2	9.20E+06	4.60E+03	1.20	
		335.1	490.2	8.80E+06	4.60E+03	1.21	
		335.1	490.2	8.50E+06	4.60E+03	1.17	
		335.1	490.2	9.40E+06	4.60E+03	1.29	
		335.1	490.2	9.10E+06	4.60E+03	1.29	
		335.1	490.2	8.10E+06	1.00E+04	1.17	
		335.1	490.2	8.20E+06	4.60E+03	1.16	
		335.1	490.2	8.60E+06	4.60E+03	1.22	
		335.1	490.2	8.70E+06	4.60E+03	1.23	
		335.1	490.2	7.50E+06	4.60E+03	1.17	
		335.1	490.2	8.00E+06	4.60E+03	1.24	
		335.1	490.2	6.20E+06	4.60E+03	1.12	
		335.1	490.2	6.70E+06	4.60E+03	1.37	
		335.1	490.2	7.80E+06	4.60E+03	2.10	
		335.1	490.2	5.30E+06	4.60E+03	1.78	
BVZ 160	Phenomenological Pipe and Vessel Burst Tests, MPA Stuttgart (Germany) [43,44]	470.2	619.1	1.31E+10	1.46E+04	0.96	
BVZ 110		470.2	619.1	7.05E+09	1.34E+04	0.66	
BVZ 120		470.2	619.1	1.107E+10	1.33E+04	0.88	
BVZ 130		470.2	619.1	1.13E+10	1.52E+04	0.90	
BVZ 150		470.2	619.1	9.30E+09	1.57E+04	0.80	
BVZ 140		470.2	619.1	8.30E+09	1.5168E+04	0.76	
BVS 110		415.1	632.9	8.59E+09	1.53E+04	0.67	
BVS 102		415.1	632.9	1.12E+10	1.51E+04	0.85	
BVS 070		415.1	632.9	6.60E+09	1.60E+04	0.55	
BVS 080		415.1	632.9	5.55E+09	1.48E+04	0.53	
3		Julisch, MPA Stuttgart (Germany) tests [29]	559.9	679.8	5.21E+08	8.00E+03	0.41
4			559.9	679.8	5.44E+08	8.00E+03	0.42
5			559.9	679.8	1.47E+08	8.00E+03	0.19
6			559.9	679.8	2.10E+07	8.00E+03	0.05
7	559.9		679.8	1.61E+09	8.00E+03	0.96	
8	559.9		679.8	9.25E+08	8.00E+03	0.66	
9	559.9		679.8	5.95E+08	8.00E+03	0.56	
10	559.9		679.8	5.67E+08	8.00E+03	0.55	
11	559.9		679.8	5.40E+08	8.00E+03	0.52	
12	559.9		679.8	5.44E+08	8.00E+03	0.71	
13	559.9		679.8	5.28E+08	8.00E+03	0.69	
14	559.9		679.8	5.50E+08	8.00E+03	0.89	
15	559.9		679.8	1.73E+09	8.00E+03	0.99	
16	559.9		679.8	1.52E+09	8.00E+03	0.93	
17	559.9		679.8	1.77E+09	8.00E+03	1.10	
18	559.9		679.8	1.91E+09	8.00E+03	1.12	
20	559.9		679.8	4.20E+08	8.00E+03	0.30	
21	559.9		679.8	1.40E+08	8.00E+03	0.14	
22	559.9		679.8	1.15E+09	8.00E+03	0.76	
23	559.9		679.8	7.55E+08	8.00E+03	0.62	
24	559.9	679.8	5.75E+08	8.00E+03	0.75		
25	559.9	679.8	1.40E+09	8.00E+03	0.88		
26	559.9	679.8	1.70E+09	8.00E+03	0.97		

Table 14. Inputs and output BM Ratio for SC_fail single crack validation cases (cont)

Experiment Number	Program	Yield Strength (MPa)	Ultimate Strength (MPa)	Maximum Experimental Moment (N-mm)	Pipe Internal Pressure (MPa)	Output BM Ratio
27	Sturm, Bernecker, MPA Stuttgart, BBC, Mannheim, and RW-TUV (Germany) tests [45,46]	559.9	679.8	1.57E+09	8.00E+03	1.05
4		548.1	701.2	6.15E+08	8.00E+03	0.79
5		548.1	701.2	6.42E+08	8.00E+03	0.81
8		279.9	608.1	4.10E+07	1.70E+04	0.95
9		279.9	608.1	3.60E+07	1.70E+04	0.86
10		279.9	608.1	8.00E+07	1.70E+04	1.10
PTH-01	Kurihara, Yagawa, JAERI (Japan) tests [47,48,49]	193.1	426.8	2.21E+07	6.86E+03	0.51
PTH-02		193.1	426.8	5.15E+07	6.86E+03	1.03
PTH-03		193.1	426.8	1.72E+07	6.86E+03	1.04
PTH-04		193.1	426.8	3.92E+07	6.86E+03	1.27
PTH-05		193.1	426.8	5.99E+07	6.86E+03	1.27
6001		193.1	426.8	3.47E+07	6.86E+03	1.43
6002		193.1	426.8	5.88E+07	6.86E+03	1.22
6003		193.1	426.8	5.53E+07	6.86E+03	1.15
Single Crack Inertially Loaded Tests + Internal Pressure						
1.1-4	IPIRG-1 [38,39,40,41]	319.9	620.5	7.56E+07	1.55E+04	0.83
1.1-5		138.6	449.5	5.47E+07	1.55E+04	1.21
1.1-6		319.9	620.5	4.86E+07	1.55E+04	0.96
1.1-8		319.9	620.5	7.90E+07	1.55E+04	1.15
Single Crack Pipe System Tests – Bending + Internal Pressure						
1.3-2	IPIRG-1 Pipe System Fracture Tests [41]	237.2	610.2	3.41E+08	1.55E+04	0.52
1.3-3		175.8	458.5	4.26E+08	1.55E+04	0.82
1.3-4		237.2	610.2	6.18E+08	1.55E+04	0.97
1.3-5		175.8	458.5	4.93E+08	1.55E+04	0.87
1.3-7		205.5	602.6	5.90E+08	1.55E+04	0.70
1-1	IPIRG-2 Tests [42]	175.8	458.5	5.98E+08	1.55E+04	0.94
1-2		237.2	610.2	4.76E+08	1.55E+04	0.70
1-5		175.8	458.5	7.76E+08	1.55E+04	0.84
BINP T 1	BINP Program tests [50]	175.8	458.5	4.70E+08	1.55E+04	0.76
BINP T 2		175.8	458.5	6.24E+08	1.55E+04	0.96
Average						0.987
Standard Deviation						0.268

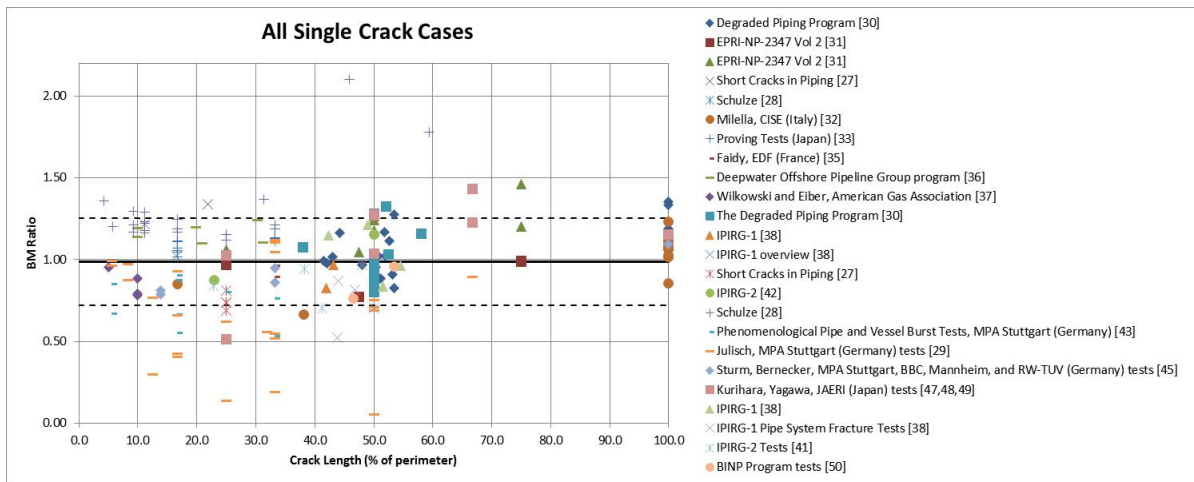


Figure 6. BM ratio versus crack length for all single crack cases

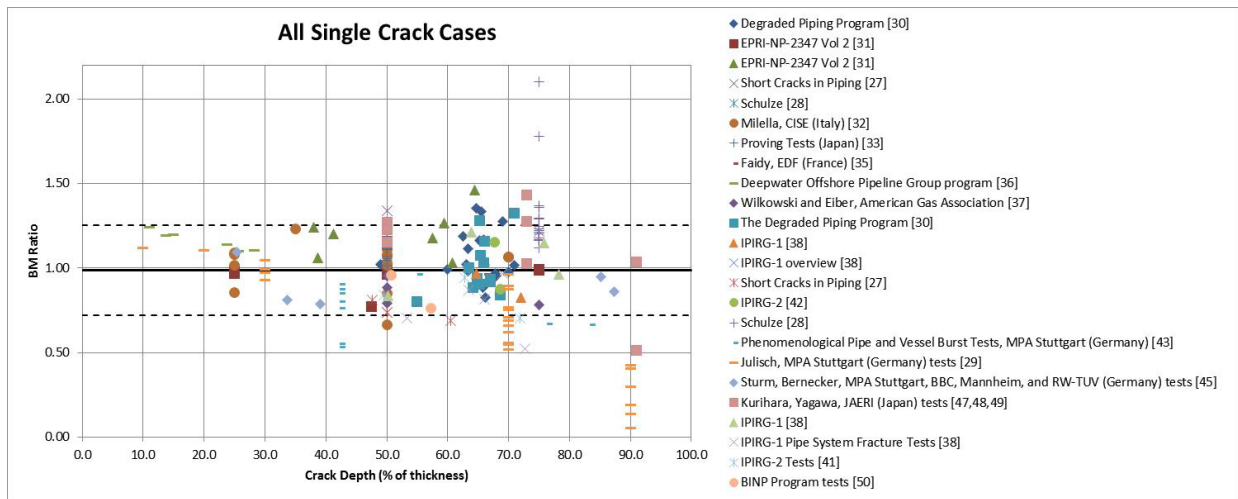


Figure 7. BM ratio versus crack depth for all single crack cases

3.6.1.2 Comparisons with Multiple Crack Surface Cracked Pipe Experiments

The SC_fail code developers did find one reference [51] with experimental results for failure of a pipe with multiple surface cracks. This set of three experiments had the following properties:

- Number of cracks per test: two cracks symmetrically distributed about the top dead center location of the pipe
- Outside diameter: 114.8 mm
- Pipe wall thickness: 8.6 mm
- Pipe material: Type 304 stainless steel
- Surface crack depth to wall thickness ratio (a/t): 0.74
- Crack length: $\pi/6$ radians

- Internal pressure: 15.51 MPa
- Axial force: 0 N.

The three experiments varied only in the angular distance (α) from the top dead center of the pipe to the two adjacent crack tips. The right hand column in Table 15 shows the ratio of the maximum bending moment from the multiple crack pipe experiments to the critical bending moment predicted by the SC_fail module. A value of 1.0 would indicate that there was perfect agreement between the SC_fail predictions and the experimental results. Deviations from this value of 1.0 represent uncertainty in either the analysis methodology or the input data. Values greater than 1.0 indicate that the SC_fail module is under predicting the critical bending moment (i.e. conservative in the sense that the module predicts failure at lower bending moments than observed in the experiments). Values less than 1.0 indicate that the SC_fail module is overpredicting the critical bending moment (i.e. non-conservative in the sense that the module predicts failure at higher bending moments than observed in the experiments). In all three cases, the critical bending moment predicted by the SC_fail module is less than the maximum bending moment from the pipe experiments, thus the SC_fail module behaves conservatively in the sense that it would predict failure prior to observed in the experiments. The average value for BM ratio was 1.04 with a standard deviation of 0.01 which easily satisfies the SRD requirement for validation of SCF-7. However, it is recognized that the existing experimental data set for multiple cracks is very small. Ideally, more multiple crack experiments would really be needed to fully validate the SC_fail multiple crack analysis.

Table 15. Comparison of old SC_fail module, new SC_fail module, and pipe experiments for multiple crack cases

α/π	BM Experiment (N-mm)	BM SC_fail Critical Module (N-mm)	BM Experiment / BM SC_fail Critical (<i>BM ratio</i>)
0.11111	3.20×10 ⁷	3.06×10 ⁷	1.05
0.22222	3.43×10 ⁷	3.28×10 ⁷	1.05
0.33333	3.63×10 ⁷	3.53×10 ⁷	1.03
Average			1.04
Standard Deviation			0.01

3.6.2 TWC_fail Module Validation

3.6.2.1 TWC_fail Module Validation through Comparisons with Experimental Data

The validation of the TWC_fail module is documented in detail in the MVR for the TWC_fail module [10]. This MVR documents the validation activities that characterize the predictive capability of the TWC_fail module over a prescribed range of applicability, relative to available full-scale pipe test experimental data. The module was validated by comparing the outputs of the module with existing full-scale experimental pipe fracture data.

The test specimens for these experiments were sections of nuclear grade piping of various sizes and materials. The experiments evaluated a number of different loading conditions and crack geometries.

- Pipe sizes: 2- to 42-inch nominal diameter, with wall thicknesses up to approximately 90 mm (3.5 inches)
- Materials: carbon steels (including representative weld processes), stainless steels (including representative weld processes), and dissimilar metal welds joining sections of carbon and stainless steel pipe
- Loading conditions: simple quasi-static four-point bending, combined pressure and four-point bending, dynamic, cyclic, and combined dynamic/cyclic pipe system experiments.
- Crack geometries: simple through-wall cracked pipe.

In total, there were approximately 140 pipe fracture experiments conducted at Battelle over the years. Included in this overall set of pipe fracture experiments, 57 evaluated circumferential through-wall cracked pipes subjected to a variety of loading conditions. Of these 57 circumferential through-wall cracked pipe experiments, 32 were chosen for validation of the TWC_fail module. These experiments were chosen from the overall data set because all of the necessary data for validation of the TWC_fail module were available for these 32 experiments. For some experiments, crack growth data were not available so that it was not possible to establish the crack length at maximum moment. For the validation of TWC_fail, this crack length at maximum moment was used as the current crack length to establish the ratio of the current crack angle to the critical crack angle (ratio_theta) which was used as the measure of the validity of the TWC_fail module.

Table 16 shows the validation matrix for the TWC_fail module.

The required inputs for the TWC_fail module include:

- Pipe outside radius, mm
- Pipe wall thickness, mm
- Half crack length at maximum moment, radians
- Yield strength, MPa
- Ultimate strength, MPa
- Ramberg-Osgood alpha parameter, unitless
- Ramberg-Osgood reference stress (σ_0), MPa
- Ramberg-Osgood reference strain, unitless
- Ramberg-Osgood strain hardening exponent (n), unitless
- J at crack initiation (J_i), N/mm
- J-R curve fitting parameter (C), $N/mm^{(m+1)}$
- J-R curve exponent (m), unitless
- Maximum moment from the experiment, N-mm
- Pipe pressure, MPa
- Axial force, N
- I_write parameter, unitless.

In many ways, the pipe experiments represented in the validation matrix for TWC_fail (see Table 16) reflect actual plant piping systems. The pipe sizes (diameters and wall thicknesses) represent

the full spectrum of pipe sizes one might expect to encounter in a nuclear power plant. The materials were actual nuclear grade pipe materials obtained from the excess pipe inventory of an existing commercial plant or a cancelled plant. (The one exception is that none of the through-wall cracked pipe experiments included in the validation matrix evaluated low toughness aged cast stainless steel pipe. The only aged cast stainless steel pipe experiments conducted by Battelle were for surface cracked pipe.) The loading conditions addressed the full spectrum of loading conditions that a cracked piping system in a plant may experience, from combined pressure and quasi-static, monotonic four-point bending, representative of normal operating conditions, to dynamic, cyclic bending such as may occur during a seismic event. For the lower toughness materials (carbon steels and weldments), the machined cracks that were tested were fatigue pre-cracked such that the notch acuity was representative of an actual in-service crack. For the higher toughness materials (stainless steel base metals), it was found that sharp machine notches could be used because there was so much crack tip blunting that occurred prior to crack initiation that notch acuity was of little concern [30].

However, saying this, there were still a number of differences between actual plant piping behavior and these pipe experiments that should be discussed:

- The pipe experiments were typically simple four-point bend experiments for which the ends of the test pipe were allowed to rotate during the course of the loading. As part of the First IPIRG program [41], it was found that by restricting the rotations at the ends of the crack section, the crack could be much longer before failing than if these rotations were not restricted, see Figure 8. In an actual plant piping system these rotations would be restrained.
- The through-wall cracks in the pipe tests were always aligned such that the center of the through-wall crack was aligned with the maximum bending stress location in the pipe. This would not always be the case in plant piping. A primary water stress corrosion crack (PWSCC) could initiate and grow at any location around the crack circumference. This location would not necessarily be aligned with the maximum bending stress location from a seismic event.
- The cracks in these pipe experiments tended to be idealized through-wall cracks where the angle to the crack tip on the inside pipe surface equaled the angle to the crack tip on the outside pipe surface. In an actual plant piping system, the crack shape may be more natural where the crack angle on the inside pipe surface is longer than the crack angle on the outside pipe surface.
- For two of the pressure and bend experiments (4131-1 and 4131-3), a high temperature rubber bladder was used to seal the pipe pressure on the inside pipe surface. As such, for these two experiments, there was no crack face pressure operating on the crack. While crack face pressure is not included in the TWC_fail model it is known to have an effect on the crack-opening displacement model, especially for larger cracks.
- Because the loading conditions for these pipe experiments tended to be simple four-point bending, there were no torsional or shear loadings imposed during these pipe experiments. Typical plant piping systems may be subject to both.

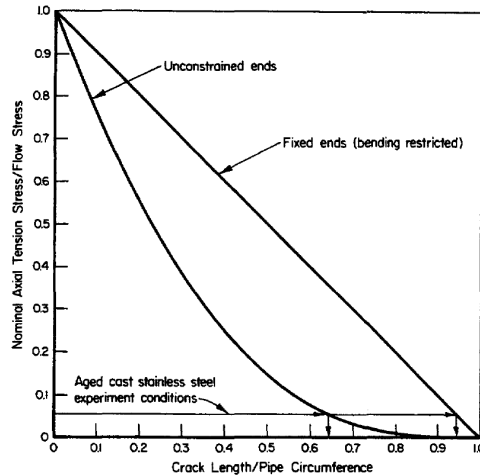


Figure 8. Net Section Collapse predictions, with and without considering induced bending, as a function of the ratio of the through-wall crack length to the pipe circumference

The results of the validation analysis for the TWC_fail module are provided in Table 17 (using J-M resistance curves) and Table 18 (using J-D resistance curves). For most of the experiments, multiple J-R curves were available for use in the analyses. The different J-R curves represented different specimen geometries, with 20 percent side grooves or without, and fatigue pre-cracked specimens or sharp machine notch specimens. Because it will probably not be possible to specify to the xLPR end user what J-R curve to use, or what formulation of J to use, Table 17 and Table 18 include the results for all of the different fracture toughness specimen geometries available for each of the materials tested in the pipe experiments. (Note, for some specimens, only J-M data were available for the analyses while for others, only J-D data were available, although both are rooted in exactly the same specimen load-displacement data. J-M uses a correction to the J-D curve that, typically, permits extrapolation of crack growth to closer to full wall thickness using sub-size specimens. The J-M corrections are nonlinear and must be applied to the raw load-displacement records so there is no way to convert from J-D to J-M and vice versa.) The far right hand column in Table 17 and the second column from the right in Table 18 shows the value of ratio_theta for each of the pipe experiments analyzed (ratio of the current crack angle to the critical crack angle where for this validation exercise the current crack angle is the crack angle at maximum moment from the pipe experiment). (Note, throughout this validation exercise the projected crack angle from the pipe experiments was used for those experiments where the crack grew out of the original circumferential plane of the crack.) A value of 1.0 for ratio_theta would indicate that there was perfect agreement between the TWC_fail prediction and the experimental results. Deviations from this value of 1.0 represent uncertainty in either the analysis methodology or the input data, including the uncertainty due to the choice of J-R curve used in the analysis. Comparing the results for the J-M analyses (Table 17) and the J-D analyses (Table 18), one can see that the use of J-M fracture toughness data resulted in better predictions with respect to the experimental data. The average value for ratio_theta when using the J-M fracture toughness data was 1.20 with a standard deviation of 0.35 compared with an average value for ratio_theta of 1.49 with a standard deviation of 0.64 when using the J-D fracture toughness data. When all of the J-M results are combined with all of the J-D results, the resultant average for ratio_theta was 1.34 (see bottom of Table 18) with a standard deviation of 0.53. If one does not specify which J-R curve to use, this represents the level of overall combined uncertainty of the analyses methodology and the input data.

Table 16. Validation matrix for TWC_fail module

Experiment Number	Program(1)	Material/ Crack Location	Loading Conditions	Outside Radius, mm	Wall Thickness, mm	Half Crack Length, (2) radians
4111-2	DP3-II	CS Base	4-Point Bend	355.60	23.62	1.1624
4111-3	DP3-II	SS Base	4-Point Bend	533.40	7.11	1.1624
4111-4	DP3-II	CS Base	4-Point Bend	533.40	15.88	1.1624
4111-5	DP3-II	SS Weld	4-Point Bend	359.79	30.20	1.1624
4131-5	DP3-II	SS Base	4-Point Bend	79.43	13.94	1.417
4131-7	DP3-II	CS Base	4-Point Bend	136.53	18.26	1.172
4141-1	DP3-II	SS Weld	4-Point Bend	84.14	14.27	1.1655
4141-3	DP3-II	SS Weld	4-Point Bend	206.76	26.19	1.1530
4141-5	DP3-II	SS Weld	4-Point Bend	83.88	14.10	1.2030
WJ-1	DP3-II	CS Weld	4-Point Bend	88.14	11.05	0.984
1.2-1	IPIRG-1	SS Base	4-Point Bend	84.49	13.89	1.1938
1.2-7	IPIRG-1	CS Base	4-Point Bend	83.82	13.97	1.1310
1.2-8	IPIRG-1	CS Base	4-Point Bend	83.72	13.69	1.1687
1.2-11	IPIRG-1	CS Base	4-Point Bend	83.55	13.11	1.311
1.2-12	IPIRG-1	CS Base	4-Point Bend	83.71	13.77	1.1718
4.2-1	IPIRG-2	CS Base	4-Point Bend	84.14	14.50	0.5236
1.1.1.21	Short Cracks	CS Base	4-Point Bend	355.60	22.68	0.1963
1.1.1.23	Short Cracks	SS Weld	4-Point Bend	355.60	30.23	0.1963
1.1.1.24	Short Cracks	CS Weld	4-Point Bend	306.07	31.34	0.2482
1.1.1.26	Short Cracks	SS Base	4-Point Bend	53.12	8.31	0.7665
4.3-1	IPIRG-2	CS Base	4-Point Bend	381.76	38.18	0.5215
EPRI-6T	EPRI	SS Base	4-Point Bend	30.16	6.02	0.7194
EPRI-8T	EPRI	SS Base	4-Point Bend	206.76	26.19	1.319
4131-1	DP3-II	SS Base	Pressure + Bend	83.22	13.41	1.1624
4131-3	DP3-II	CS Base	Pressure + Bend	137.07	18.69	1.1624
1-8	IPIRG-2	CS Base	Pressure + Bend	199.64	26.16	0.3770
1-9	IPIRG-2	CS Base	Pressure + Bend	84.46	11.18	0.886
DMW-6	DMW	DMW	4-Point Bend	108.45	21.25	0.6362
DMW-9	DMW	DMW	4-Point Bend	108.975	21.85	1.17
DMW-11	DMW	DMW	4-Point Bend	108.125	21.2	1.1838
DMW-13	DMW	DMW	4-Point Bend	108.8	21.2	1.1811
1.1.1.28	Short Cracks	DMW	4-Point Bend	463.55	85.85	1.1278

(1) DP3-II – Degraded Piping Program Phase II; IPIRG – International Piping Integrity Research Group program; DMW – Dissimilar Metal Weld Pipe Fracture program
 (2) Half crack length at maximum moment from the pipe experiment

The ratio-theta values shown in **red font** in Table 17 and Table 18 are those values of ratio_theta where the TWC_fail-predicted critical crack angle was more than a factor of 2 less than the current crack angle, i.e., the crack angle at maximum moment from the pipe experiment. As can be seen from Table 17, there are two experiments (1.1.1.24 and 1-8) for which the ratio_theta value was greater than 2.0 for at least one of the J_M-R curves used in the analyses. When using J-D, it can be seen in examining Table 18 that the number of “problematic” experiments increases to 5 (1.1.1.21, 1.1.1.23, and 1-9 in addition to 1.1.1.24 and 1-8). Focusing first on the results for the J-M analyses (Table 17), it can be seen that the choice of J-R curve can have a dramatic effect on the results. For Experiment 1.1.1.24, the value of ratio_theta is 2.47 when using J-R curve data from a 20% side-grooved specimen, while it is only 1.38 when using J-R curve data for a non-side grooved specimen. This improvement in the prediction when using the non-side grooved specimen can be easily explained when looking at the two J-R curves (20% side grooved versus non-side grooved), see Figure 9, for the material evaluated in this experiment (F49W). The J-R curves for the non-side grooved specimens (Fracture Toughness Specimens F49W-5 and F49W-6) are almost a factor of 2 higher than the J-R curves for the side grooved specimens (Fracture Toughness Specimens F49W-3 and F49W-4). For the other “problematic” experiment from Table 17 (Experiments 1-8) the failure mode was Net-Section-Collapse (NSC). One issue with the Net-Section-Collapse analyses is that it does not account for crack growth. This experiment exhibited significant crack growth (that was not properly accounted for) between crack initiation and maximum moment. The ratio of the crack angle at maximum moment to the crack angle at crack initiation for this experiment was 1.96. Consequently it should not be a surprise when the ratio_theta value for this experiment was so high.

The far right hand column in Table 18 shows the ratio of the crack size at maximum moment to the crack size at crack initiation for each of the experiments used in validating the TWC_fail module. In examining Table 18, it can be seen that the experiments which resulted in the higher values of ratio_theta tended to be those experiments which exhibited the most crack growth, i.e., those experiments for which the ratio of the crack size at maximum moment to the crack size at crack initiation was greatest. This trend is shown graphically in Figure 10 which shows the ratio_theta values for the pipe experiments used as part of this validation exercise as a function of the ratio of the crack size at maximum moment to the crack size at crack initiation. As can be seen in Figure 10, the greater the ratio of crack sizes (i.e., the more crack growth), the greater the ratio_theta value. This is a fundamental flaw with these through-wall crack stability analyses as they are currently configured. The Net-Section-Collapse analyses does not account for crack growth, while the LBB.ENG2 analyses method, which forms the basis for the EPFM ENG2 module in TWC_fail, significantly underpredicts the crack growth.

In an attempt to separate the uncertainty in the input data (including the choice of J-R curve) and the uncertainty in the methodology, η -factor analyses were conducted on selected pipe experiments [52]. It was felt that the resultant J-R curves from the η -factor analyses would best represent the actual J-R curves for the pipe experiments (and eliminate the uncertainty in the choice of J-R curves) such that the resultant ratio_theta values when using these η -factor derived J-R curves would better represent the uncertainty in the analysis methodology.

For the η -factor analyses, one must know the dimensions, geometry, and materials for the moment arm pipes. The available analysis model assumes that the moment arms are the same size (diameter and thickness) as the test specimen pipe. For some of the 32 experiments analyzed above, this was not the case. For example, the outer sections of the moment arm pipes for Experiment 1.1.1.21 were 30-inch nominal diameter with a wall thickness of 38.1 mm, while the test specimen was fabricated from 28-inch diameter pipe with a wall thickness of 22.68 mm. Other experiments had similar type mismatches between the moment arm pipes and

the test specimens, just not to this extent. In addition, for many of the experiments, the exact material properties or the dimensions of the moment arms are not documented. An additional complication in performing the η -factor analyses comes about when cracks grew out of plane, but only projected crack growth was reported (clearly, plastic energy is involved in all of the crack extension), see Figure 11. Accordingly, experiments such as 1.2-11, 1.2-12, and 4.2-1, where only projected crack growth was reported in the data record books for those experiments, had to be eliminated from consideration. Another limiting feature in conducting η -factor analyses of pipe experiments is that there seems to only be consensus on the equations for pure bending: There is much debate about the equations for combined pressure and bending. Finally, the η -factor analysis is based on experimental load-line displacement data for the pipe and crack only. As part of these analyses, the load-line displacement data has to be corrected for the test machine compliance. For some experiments, no record of the test machine compliance was provided, so those experiments could not be included as part of the η -factor analysis. Considering all of the factors mentioned above, of the 32 experiments considered as part of this validation effort, η -factor J-R curves could be developed for only 12 experiments. The results of these η -factor analyses for these 12 pipe experiments are shown in Table 19, along with the corresponding C(T) specimen and 3-point bend specimen J-R curve coefficients for comparison purposes.

When using the η -factor-derived J-R curves from the pipe tests with the TWC_fail module to predict values of ratio_theta for these 12 pipe experiments, it can be seen in Table 20 that the average value for ratio_theta is 1.14 with a standard deviation of 0.17. This, it is felt, represents the underlying uncertainty of the module, because: 1) it is assumed that the η -factor analysis accounts for any uncertainty in the choice of the J-R curve, and 2) there is very little uncertainty in the stress-strain data. Of note, when these same 12 experiments were analyzed using the available C(T) specimen data, the average value for ratio_theta was 1.09 with a standard deviation of 0.15, see Table 20.

Considering the distribution of the predictions, Figure 12 shows a plot of all of the θ/θ_{crit} data from Table 17. Variation in θ/θ_{crit} from using different kinds of fracture toughness specimen geometries are indicated by multiple symbols plotted at the same abscissa. Aside from the two outliers (1.1.1.24 and 1-8), all of the points lie within \pm one standard deviation of the mean. Additionally, Figure 12 suggests that it is unlikely that TWC_fail will yield a severely non-conservative prediction (θ/θ_{crit} much less than 1.0). Confidence interval testing with the data from Figure 12 suggests that the θ/θ_{crit} value is 1.34 with a 99-percent confidence that the true value is between 1.2 and 1.48.

Based on the above, as implemented in TWC_fail, predictions of through-wall crack instability, on average, are conservative, i.e., the average value for ratio_theta (ratio of current crack angle to critical crack angle) for the pipe experiments is greater than 1.0. That is, TWC_fail will predict that a crack being evaluated at some moment, pressure and axial load, will fail before such a failure is observed in an experiment. The implication for xLPR is that TWC rupture probabilities, from a crack stability perspective, are conservatively high. Part of this conservatism can be attributed to the fact that the LBB.ENG2 method (which forms the basis for the ENG2 solution in TWC_fail) tends to underpredict the amount of crack growth from the pipe experiments. On average, the LBB.ENG2 method, as implemented in the NRCPIPE computer code, under-predicted the amount of crack growth by a factor of almost 3. As discussed above, the experiments that resulted in the higher values of ratio_theta (more conservative) tended to be those experiments that exhibited the most crack growth, i.e., those experiments for which the ratio of the crack size at maximum moment to the crack size at crack initiation was greatest. This under-prediction of crack growth is a fundamental limitation with these stability analyses as

implemented for xLPR. This was an unexpected outcome based on previous experience with LBB.ENG2 and good predictions of maximum moment using that method.

Table 17. Results of TWC_fail validation analysis using J-M fracture toughness data

Expt. Number	J-D or J-M	Specimen Geometry	Failure Mode	ratio_theta
1.1.1.21	J-M	20% side groove; fatigue pre-crack	ENG2	1.15
1.1.1.21	J-M	20% side groove; sharp machine notch	ENG2	1.38
1.1.1.23	J-M	20% side groove; fatigue pre-crack	ENG2	1.37
1.1.1.23	J-M	0% side groove; fatigue pre-crack	ENG2	1.06
1.1.1.24	J-M	20% side groove; fatigue pre-crack	ENG2	2.47
1.1.1.24	J-M	0% side groove; fatigue pre-crack	NSC	1.38
1.1.1.26	J-M	0% side groove; fatigue pre-crack	No Failure	0.98
1.2-1	J-M	20% side groove; sharp machine notch	NSC	1.18
1.2-1	J-M	0% side groove; sharp machine notch	NSC	1.18
1.2-7	J-M	20% side groove; sharp machine notch	ENG2	1.04
1.2-7	J-M	0% side groove; sharp machine notch	ENG2	1.01
1.2-8	J-M	20% side groove; sharp machine notch	No Failure	0.94
1.2-8	J-M	0% side groove; sharp machine notch	No Failure	0.92
1.2-11	J-M	20% side groove; sharp machine notch	ENG2	1.07
1.2-11	J-M	0% side groove; sharp machine notch	ENG2	1.04
1.2-12	J-M	20% side groove; sharp machine notch	ENG2	1.06
1.2-12	J-M	0% side groove; sharp machine notch	ENG2	1.03
1-8	J-M	20% side groove; fatigue pre-crack	NSC	2.46
1-8	J-M	20% side groove; fatigue pre-crack (1)	NSC	2.46
1-9	J-M	20% side groove; fatigue pre-crack	ENG2	1.26
1-9	J-M	20% side groove; fatigue pre-crack (1)	ENG2	1.55
4.2-1	J-M	20% side groove; fatigue pre-crack	NSC	1.30
4.2-1	J-M	20% side groove; fatigue pre-crack (1)	NSC	1.30
4.3-1	J-M	20% side groove; fatigue pre-crack	NSC	1.54
4111-2	J-M	20% side groove; fatigue pre-crack	ENG2	1.07
4111-2	J-M	20% side groove; sharp machine notch	ENG2	1.13
4111-3	J-M	0% side groove; fatigue pre-crack	ENG2	1.07
4111-3	J-M	0% side groove; sharp machine notch	No Failure	0.85
4111-4	J-M	3-point bend; sharp machine notch	No Failure	0.97
4111-5	J-M	20% side groove; fatigue pre-crack	ENG2	1.01
4131-1	J-M	20% side groove; sharp machine notch	NSC	1.06
4131-1	J-M	0% side groove; sharp machine notch	NSC	1.06
4131-3	J-M	20% side groove; fatigue pre-crack	ENG2	1.20
4131-3	J-M	0% side groove; fatigue pre-crack	ENG2	1.08
4131-3	J-M	0% side groove; sharp machine notch	ENG2	1.12
4131-3	J-M	20% side groove; sharp machine notch	ENG2	1.27
4131-5	J-M	20% side groove; sharp machine notch	NSC	1.38
4131-5	J-M	0% side groove; sharp machine notch	NSC	1.38
4131-7	J-M	20% side groove; fatigue pre-crack	ENG2	1.07
4131-7	J-M	0% side groove; fatigue pre-crack	No Failure	0.95
4131-7	J-M	0% side groove; sharp machine notch	No Failure	0.99
4131-7	J-M	20% side groove; sharp machine notch	ENG2	1.14
1.1.1.28	J-M	20% side groove; fatigue pre-crack	No Failure	0.94
1.1.1.28	J-M	20% side groove; sharp machine notch	No Failure	0.94
4141-1	J-M	0% side groove; fatigue pre-crack	ENG2	1.26
4141-1	J-M	0% side groove; sharp machine notch	ENG2	1.25
4141-3	J-M	0% side groove; fatigue pre-crack	ENG2	1.09
4141-3	J-M	0% side groove; sharp machine notch	ENG2	1.08
4141-5	J-M	0% side groove; sharp machine notch	ENG2	1.09
EPRI-6T	J-M	3-point bend; sharp machine notch	NSC	1.02
EPRI-8T	J-M	3-point bend; sharp machine notch	ENG2	1.21
WJ-1	J-M	20% side groove; fatigue pre-crack	No Failure	0.93
WJ-1	J-M	0% side groove; fatigue pre-crack	No Failure	0.93
Average (using only J-M specimen data)				1.20
Standard Deviation (using only J-M specimen data)				0.35

(1) Dynamically loaded C(T) specimen; all other specimens loaded quasi-statically

Table 18. Results of TWC_fail validation analysis using J-D fracture toughness data

Expt. Number	J-D or J-M	Specimen Geometry	Failure Mode	ratio_theta	2c_max moment / 2c_initiation
1.1.1.21	J-D	20% side groove; fatigue pre-crack	ENG2	1.83	2.07
1.1.1.21	J-D	20% side groove; sharp machine notch	ENG2	2.41	2.07
1.1.1.23	J-D	20% side groove; fatigue pre-crack	ENG2	2.91	1.77
1.1.1.23	J-D	0% side groove; fatigue pre-crack	ENG2	2.17	1.77
1.1.1.24	J-D	20% side groove; fatigue pre-crack	ENG2	4.15	1.51
1.1.1.24	J-D	0% side groove; fatigue pre-crack	ENG2	1.81	1.51
1.1.1.26	J-D	0% side groove; fatigue pre-crack	No Failure	0.98	1.06
1.2-1	J-D	20% side groove; sharp machine notch	ENG2	1.27	1.11
1.2-1	J-D	0% side groove; sharp machine notch	ENG2	1.28	1.11
1-8	J-D	20% side groove; fatigue pre-crack	ENG2	2.71	1.96
1-8	J-D	20% side groove; fatigue pre-crack (1)	ENG2	3.02	1.96
1-9	J-D	20% side groove; fatigue pre-crack	ENG2	1.56	1.13
1-9	J-D	20% side groove; fatigue pre-crack (1)	ENG2	2.09	1.13
4.2-1	J-D	20% side groove; fatigue pre-crack	NSC	1.30	1.42
4.2-1	J-D	20% side groove; fatigue pre-crack (1)	ENG2	1.32	1.42
4.3-1	J-D	20% side groove; fatigue pre-crack	ENG2	1.79	1.47
4111-2	J-D	20% side groove; fatigue pre-crack	ENG2	1.22	1.12
4111-2	J-D	20% side groove; sharp machine notch	ENG2	1.38	1.12
4111-3	J-D	0% side groove; fatigue pre-crack	No Solution	N/A	1.06
4111-3	J-D	0% side groove; sharp machine notch	ENG2	1.20	1.06
4111-4	J-D	3-point bend; sharp machine notch	ENG2	1.05	1.08
4131-1	J-D	20% side groove; sharp machine notch	ENG2	1.14	1.09
4131-1	J-D	0% side groove; sharp machine notch	ENG2	1.12	1.09
4131-3	J-D	20% side groove; fatigue pre-crack	ENG2	1.32	1.14
4131-3	J-D	0% side groove; fatigue pre-crack	ENG2	1.20	1.14
4131-3	J-D	0% side groove; sharp machine notch	ENG2	1.25	1.14
4131-3	J-D	20% side groove; sharp machine notch	ENG2	1.55	1.14
4131-5	J-D	20% side groove; sharp machine notch	ENG2	1.50	1.16
4131-5	J-D	0% side groove; sharp machine notch	ENG2	1.52	1.16
4131-7	J-D	20% side groove; fatigue pre-crack	ENG2	1.19	1.08
4131-7	J-D	0% side groove; fatigue pre-crack	ENG2	1.07	1.08
4131-7	J-D	0% side groove; sharp machine notch	ENG2	1.11	1.08
4131-7	J-D	20% side groove; sharp machine notch	ENG2	1.52	1.08
1.1.1.28	J-D	20% side groove; fatigue pre-crack	No Failure	0.99	1.08
1.1.1.28	J-D	20% side groove; sharp machine notch	ENG2	1.01	1.08
4141-1	J-D	0% side groove; fatigue pre-crack	ENG2	1.73	1.06
4141-1	J-D	0% side groove; sharp machine notch	ENG2	1.57	1.06
4141-3	J-D	0% side groove; fatigue pre-crack	ENG2	1.23	1.09
4141-3	J-D	0% side groove; sharp machine notch	ENG2	1.19	1.09
4141-5	J-D	0% side groove; sharp machine notch	ENG2	1.19	1.06
EPRI-6T	J-D	3-point bend; sharp machine notch	NSC	1.02	1.02
EPRI-8T	J-D	3-point bend; sharp machine notch	ENG2	1.32	1.14
WJ-1	J-D	20% side groove; fatigue pre-crack	No Failure	0.96	1.03
WJ-1	J-D	0% side groove; fatigue pre-crack	No Failure	0.93	1.03
DMW-6	J-D	20% side groove, fatigue pre-crack	ENG2	1.06	1.18
DMW-9	J-D	20% side groove, fatigue pre-crack	No Failure	0.97	1.06
DMW-11	J-D	20% side groove, fatigue pre-crack	ENG2	1.01	1.07
DMW-13	J-D	20% side groove, fatigue pre-crack	No Failure	0.98	1.09
Average (using only J-D specimen data)				1.49	
Standard Deviation (using only J-D specimen data)				0.64	
Average (using both J-M and J-D specimen data)				1.34	
Standard Deviation (using both J-M and J-D specimen data)				0.53	

(1). Dynamically loaded C(T) specimen; all other specimens loaded quasi-statically

Table 19. Comparison of η -factor extrapolated J-R curve coefficients and CT or 3-point bend specimen extrapolated J-R curve coefficients

Experiment Number	η -factor extrapolated J-R curve coefficients			CT (or 3-point bend) specimen extrapolated J-R curve coefficients			
	J_i , N/mm	C,	m	Specimen Geometry	J_i , N/mm	C,	m
4111-2	489.6	67.0	0.679	20% side groove; fatigue pre-crack - JM	217.2	149.4	0.756
				20% side groove; sharp machine notch - JM	206.5	163.8	0.651
				20% side groove; fatigue pre-crack - JD	217.2	156.0	0.530
				20% side groove; sharp machine notch - JD	206.5	188.8	0.328
4111-3	1,434.6	14.5	1.337	0% side groove; fatigue pre-crack - JM	547	466.5	0.611
				0% side groove; sharp machine notch - JM	682	191.4	0.937
				0% side groove; fatigue pre-crack - JD	547	469.1	0.320
				0% side groove; sharp machine notch - JD	682	217.5	0.577
4111-4	1,005.8	205.7	0.743	3-point bend; sharp machine notch - JM	399	372.7	0.753
				3-point bend; sharp machine notch - JD	399	411.0	0.608
4131-7	196.0	85.4	0.736	20% side groove; fatigue pre-crack - JM	158	149.8	0.675
				0% side groove; fatigue pre-crack - JM	155	204.3	0.832
				0% side groove; sharp machine notch - JM	298	160.1	0.809
				20% side groove; sharp machine notch - JM	196	100.8	0.605
				20% side groove; fatigue pre-crack - JD	158	157.6	0.438
				0% side groove; fatigue pre-crack - JD	155	250.1	0.530
				0% side groove; sharp machine notch - JD	298	197.5	0.455
				20% side groove; sharp machine notch - JD	196	113.6	0.198
WJ-1	408.3	160.5	0.498	20% side groove; fatigue pre-crack - JM	165	228.7	0.770
				0% side groove; fatigue pre-crack - JM	105	239.6	0.887
				20% side groove; fatigue pre-crack - JD	165	198.7	0.592
				0% side groove; fatigue pre-crack - JD	105	241.4	0.609
1.2-1	881.7	168.5	0.769	20% side groove; sharp machine notch - JM	1,090	364.8	0.849
				0% side groove; sharp machine notch - JM	1,420	570.9	0.732
				20% side groove; sharp machine notch - JD	1,090	233.1	0.695
				0% side groove; sharp machine notch - JD	1,420	394.0	0.354
1.2-7	188.2	47.7	0.788	20% side groove; sharp machine notch - JM	103	109.8	0.811
				0% side groove; sharp machine notch - JM	119	121.0	0.867
1.2-8	102.9	50.2	0.658	20% side groove; sharp machine notch - JM	103	109.8	0.811
				0% side groove; sharp machine notch - JM	119	121.0	0.867
EPRI-8T	3,351.6	83.1	0.960	3-point bend; sharp machine notch - JM	2,294	1,422	0.684
				3-point bend; sharp machine notch - JD	2,294	1,261	0.572
DMW9	560.0	66.5	0.960	20% side groove, fatigue pre-crack - JD	512.3	358.7	0.628
DMW11	1,031.1	59.2	0.953	20% side groove, fatigue pre-crack - JD	847.6	379.9	0.782
DMW13	951.1	71.4	0.867	20% side groove, fatigue pre-crack - JD	847.6	379.9	0.782

Table 20. Comparison of results of TWC_fail analyses between when using η -factor derived J-R curves and CT or 3-point bend specimen J-R curves

Experiment Number	η -factor based ratio_theta	η -factor Failure Mode	CT Specimen Geometry – J Formulation (JM or JD)	CT Specimen Based ratio_theta
4111-2	1.23	ENG2	20% side groove; fatigue pre-crack - JM	0.99
			20% side groove; sharp machine notch - JM	1.13
			20% side groove; fatigue pre-crack - JD	1.22
			20% side groove; sharp machine notch - JD	1.38
4111-3	0.85	No Failure	0% side groove; fatigue pre-crack - JM	1.07
			0% side groove; sharp machine notch - JM	0.85
			0% side groove; sharp machine notch - JD	1.20
4111-4	1.04	ENG2	3-point bend; sharp machine notch - JM	0.97
			3-point bend; sharp machine notch - JD	1.05
4131-7	1.13	ENG2	20% side groove; fatigue pre-crack - JM	1.07
			0% side groove; fatigue pre-crack - JM	0.95
			0% side groove; sharp machine notch - JM	0.99
			20% side groove; sharp machine notch - JM	1.14
			20% side groove; fatigue pre-crack - JD	1.19
			0% side groove; fatigue pre-crack - JD	1.07
			0% side groove; sharp machine notch - JD	1.11
			20% side groove; sharp machine notch - JD	1.52
WJ-1	1.03	ENG2	20% side groove; fatigue pre-crack - JM	0.93
			0% side groove; fatigue pre-crack - JM	0.93
			20% side groove; fatigue pre-crack - JD	0.96
			0% side groove; fatigue pre-crack - JD	0.93
1.2-1	1.31	ENG2	20% side groove; sharp machine notch - JM	1.18
			0% side groove; sharp machine notch - JM	1.18
			20% side groove; sharp machine notch - JD	1.27
			0% side groove; sharp machine notch - JD	1.28
1.2-7	1.15	ENG2	20% side groove; sharp machine notch - JM	1.04
			0% side groove; sharp machine notch - JM	1.01
1.2-8	1.06	ENG2	20% side groove; sharp machine notch - JM	0.94
			0% side groove; sharp machine notch - JM	0.92
EPRI-8T	1.53	ENG2	3-point bend; sharp machine notch - JM	1.21
			3-point bend; sharp machine notch - JD	1.32
DMW9	1.04	ENG2	20% side groove, fatigue pre-crack - JD	0.97
DMW11	1.18	ENG2	20% side groove, fatigue pre-crack - JD	1.01
DMW13	1.13	ENG2	20% side groove, fatigue pre-crack - JD	0.98
Average	1.14			1.09
Standard Deviation	0.17			0.15

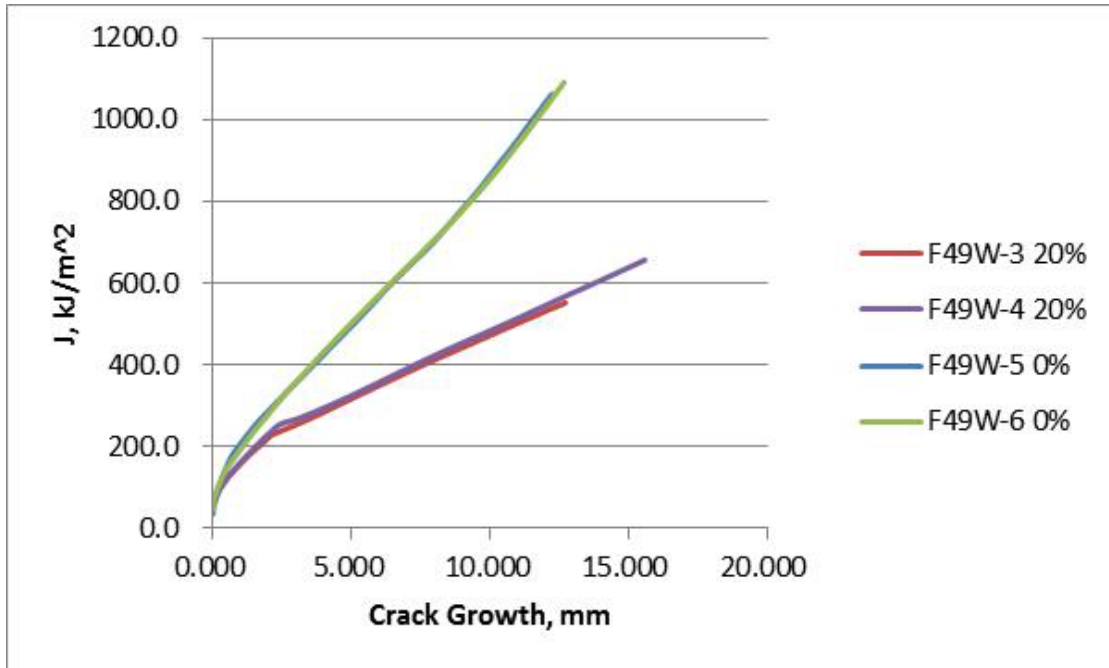


Figure 9. Comparison of J-R curves for weld F49W between 0% and 20% side-grooves (F49W is weld material evaluated in Experiment 1.1.1.24)

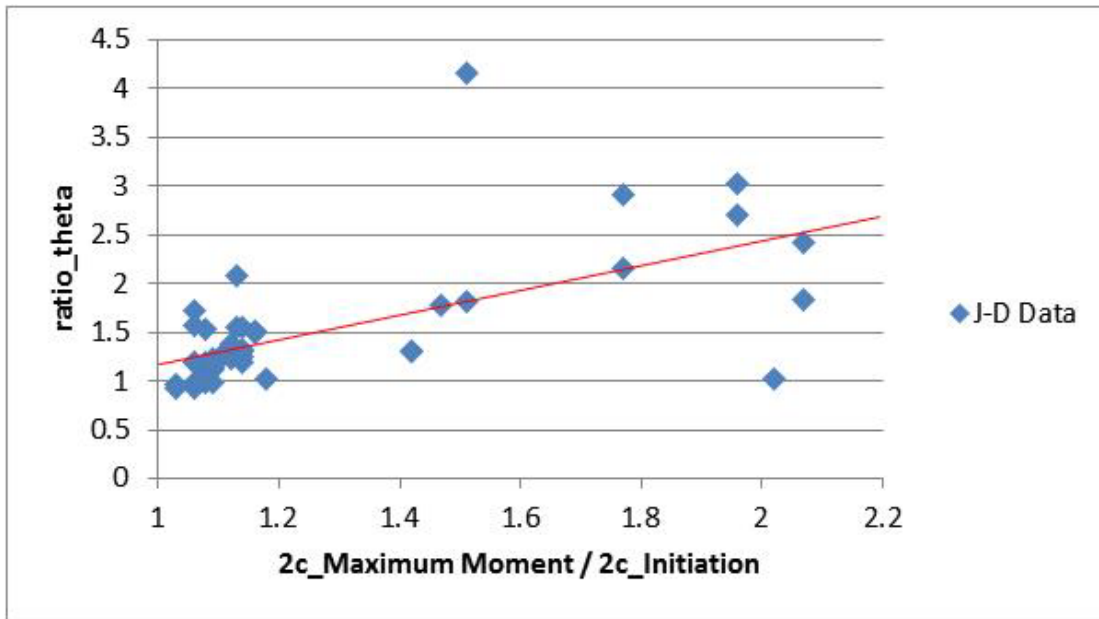


Figure 10. Plot of the ratio_theta values for the pipe experiments considered in this validation exercise as a function of the ratio of the crack size at maximum moment to the crack size at crack initiation

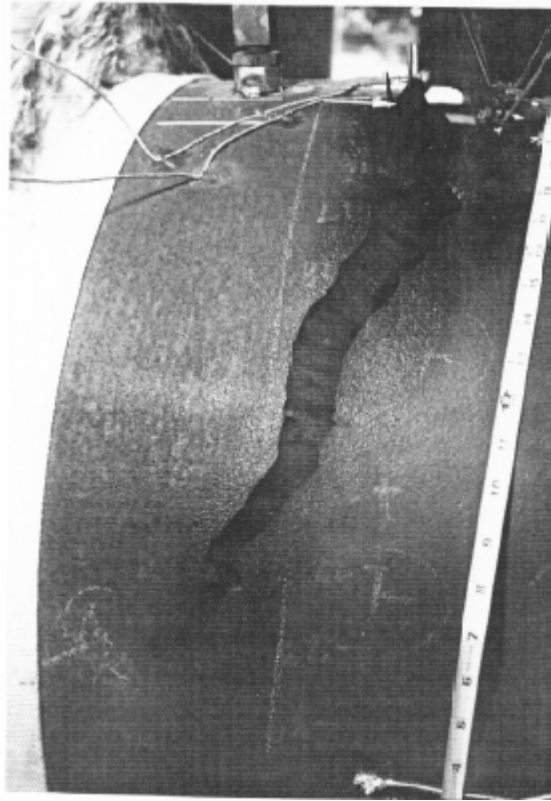


Figure 11. Post-test photograph of Experiment 1.1.1.21 showing out of plane crack growth

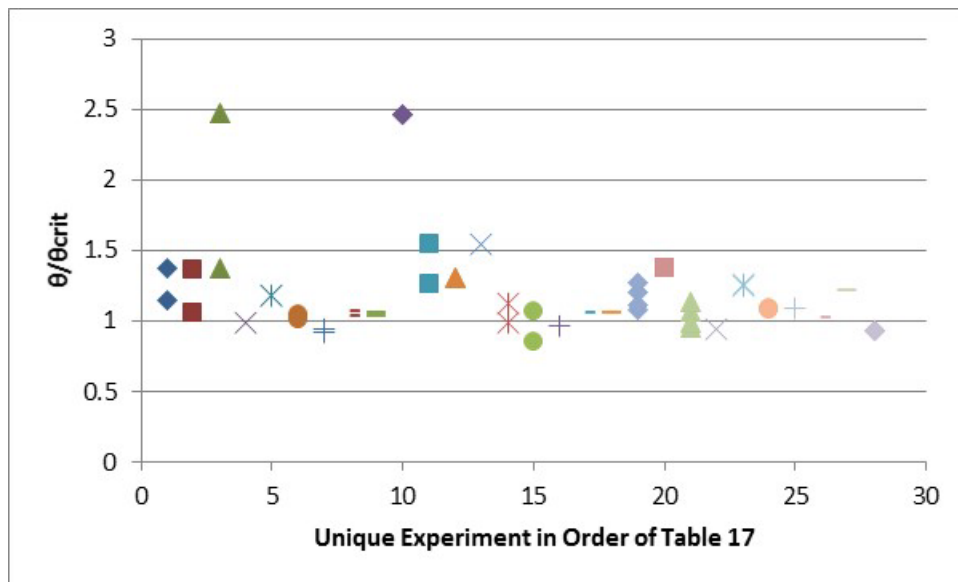


Figure 12. Distribution of θ/θ_{crit} results from Table 17 using J-M fracture toughness data

3.6.3 Axial Crack Stability (AxCS) Module Validation

3.6.3.1 Axial SC

A total of seventeen axial SC pipe experiments [53,54] shown in Table 21 were chosen for use in validating the Axial_SC_fail module. The ratio of the experimental pressure to the pressure predicted using the Ductile Fracture Handbook [20] method was obtained by running the Axial_SC_fail module, with the computation of an effective half-crack length for a semi-elliptical SC turned off because the axial surface cracks used in these experiments were constant depth surface cracks. For most of the cases shown in Table 21 (13 out of 17), the Axial_SC_fail module was able to conservatively predict failure ($P_{Expt}/P_{Crit} > 1$). The average value of ratio of the experimental pressure to the predicted critical pressure (P_{Expt}/P_{Crit}) was 1.070 with a standard deviation of 0.190.

Table 21. Input and output from validation limit load solutions in Axial_SC_fail module

1pt	Material / Crack Location	Outer Diameter, OD, mm	Wall Thickness, t, mm	Initial Half Crack Length, c, mm	Crack Depth, a, mm	Pressure Expt. P_{Expt} , MPa	Yield Strength σ_Y , MPa	Ultimate Strength σ_U , MPa	Ratio P_{Expt}/P_{Crit}
AEC20	A106B	609.600	17.323	66.675	8.890	13.514	259.243	543.996	0.813
AEC19	A106B	609.600	41.123	147.320	26.670	29.647	231.664	567.439	1.057
AEC18	A106B	609.600	17.780	136.525	9.017	11.170	239.938	552.960	0.788
AEC8	A106B	609.600	43.688	311.150	32.258	19.305	217.874	508.833	1.134
AEC4	A106B	609.600	43.256	360.680	33.020	17.237	235.111	561.923	1.057
AEC9	A106B	609.600	41.910	311.150	36.830	9.377	240.627	570.196	1.063
AEC25	TP316	609.600	38.100	76.200	22.860	27.924	155.132	426.096	1.076
AEC26	TP316	609.600	38.100	147.320	17.780	24.683	155.132	426.096	0.984
AEC24	TP316	609.600	38.100	147.320	22.860	22.201	158.579	430.922	1.066
BVZ070	20MnMoNi55	796.900	47.498	350.012	38.202	22.436	440.099	615.902	1.399
BVZ022	20MnMoNi55	799.008	47.498	391.008	38.303	21.870	416.299	599.499	1.477
BVZ030	20MnMoNi55	799.490	47.295	750.011	36.195	19.491	429.502	613.502	1.203
BVZ080	20MnMoNi55	794.791	46.812	750.011	36.195	20.581	513.901	641.302	1.193
BVZ060	20MnMoNi55	797.103	47.092	750.011	35.992	17.961	423.497	627.002	1.098
BVS020	22NiMoCr37	793.090	47.193	354.508	37.313	14.810	363.202	621.100	0.935
BVS042	22NiMoCr37	793.090	47.092	354.508	38.100	16.672	423.497	618.701	1.087
BVS030	22NiMoCr37	796.493	47.193	550.012	35.001	12.976	359.603	597.500	0.762
Mean									1.070
Standard Deviation									0.190

3.6.3.2 Axial TWC

Seventeen tests conducted by Eiber, et al. [53] for the Atomic Energy Commission (AEC) were used in validation of the limit load/NSC solutions in the Axial_TWC_fail module, see Table 22. In addition, three axial TWC pipe experiments conducted by Engineering Mechanics Corporation of Columbus (Emc²) for Pipeline Research Council International (PRCI) [55] were also used in validating the Axial_TWC_fail module, see Table 22. Finally, six tests conducted by Tokyo Gas on X65 and X80 line pipe material were also included in this validation matrix [56].

Table 22. Input and output from validation of limit load solutions within Axial_TWC_fail module

Exp Number	Material	OD, mm	Wt, t, mm	Initial Half-Crack Length, c, mm	Pressure Experiment , P _{Expt} , MPa	σ _Y , MPa	σ _U , MPa	Ratio C _{Expt} /C _{Crit}
PRCI 156-1	X70	914.400	15.875	132.969	9.625	536.481	652.520	0.896
PRCI 164-1	X80	914.400	11.786	109.703	9.080	575.712	681.891	1.115
PRCI 164-2	X80	914.400	11.786	83.820	11.687	575.712	681.891	1.312
TG B1	X65	609.600	16.002	124.968	10.687	448.159	602.602	0.800
TG B2	X65	609.600	16.002	150.114	9.032	448.159	602.602	0.774
TG B3	X65	609.600	16.002	199.898	6.895	448.159	602.602	0.730
TG E1	X80	762.000	17.501	175.006	10.480	551.581	783.244	0.818
TG E2	X80	762.000	17.501	225.247	8.136	551.581	783.244	0.761
TG E3	X80	762.000	17.501	270.002	6.619	551.581	783.244	0.709
AEC-1	A106B	609.600	42.520	234.950	22.063	227.527	519.865	0.997
AEC-2	A106B	609.600	40.462	234.950	19.030	226.148	517.107	0.910
AEC-3	A106B	609.600	44.069	311.150	15.720	227.527	520.554	0.801
AEC-5	A106B	609.600	41.656	234.950	17.995	210.980	517.107	0.824
AEC-6	A106B	609.600	43.561	147.320	28.131	235.111	561.923	0.755
AEC-7	A106B	609.600	41.529	234.950	18.616	210.980	517.107	0.866
AEC-10	A106B	609.600	41.656	234.950	19.374	224.769	537.102	0.855
AEC-11	A106B	609.600	17.907	130.175	10.135	251.659	515.038	0.955
AEC-12	A106B	609.600	18.034	66.675	14.307	251.659	515.038	0.793
AEC-13	A106B	609.600	17.780	184.150	7.377	251.659	515.038	0.907
AEC-14b	TP316	609.600	38.938	311.150	10.756	164.785	417.822	0.850
AEC-15b	A106B	609.600	41.656	234.950	21.650	224.769	537.102	0.986
AEC-16b	A106B	609.600	17.780	31.750	19.133	239.248	492.975	0.871
AEC-17	A106B	609.600	41.910	76.200	37.301	231.664	567.439	0.641
AEC-21	A106B	323.850	18.034	31.750	33.715	295.096	510.212	0.687
AEC-22	A106B	323.850	17.958	66.675	21.339	295.096	510.212	0.709
AEC-23	A106B	323.850	17.780	130.175	13.445	295.096	510.212	0.777
Mean								0.850
Standard Deviation								0.142

The ratios of the experimental half-crack lengths (C_{Expt}) to the critical half-crack lengths (C_{Crit}) predicted using the limit load (NSC) solution obtained by running the *Axial_TWC_fail* module for these axial TWC experiments are shown in far right hand column of Table 22. For most of the cases shown in Table 22 (24 of 26 cases), the C_{Expt}/C_{Crit} ratio was less than 1.0, i.e., non-conservative results. Because the limit load solutions do not take into account the effect of the ductile tearing or toughness of the material, they tend to be non-conservative. The average value

of ratio of the experimental crack length to the predicted critical crack length ($C_{\text{expt}}/C_{\text{crit}}$) was 0.850 with a standard deviation of 0.142.

In a similar vein to the solutions obtained using the NSC method, EPFM solutions were obtained for twelve of the AEC tests shown in Table 23. Because the Ramberg-Osgood parameters were not available for the X65, X70, and X80 materials (first 9 tests listed in Table 22), the EPFM solutions were not attempted for these cases. However, for twelve of the AEC tests (eleven A106B tests and one TP316 test), Ramberg-Osgood parameters and J-R curve data were obtained using the material strength properties (yield and ultimate stress) and Charpy fracture toughness data along with equations from the literature [57,58] to estimate the material properties needed to validate the EPFM solution. Table 23 shows the pipe dimensions and the stresses obtained from the AEC tests [53]. Because the AEC tests predate the Ramberg-Osgood type elastic-plastic material property characterization used in EPFM analysis, the following (Eqn. 54) and (Eqn. 55) from the literature [57,58] provide the estimation of the Ramberg-Osgood parameters.

$$\frac{\frac{\sigma_u}{\sigma_y} \exp\left(\frac{1}{n}\right)}{\left(1.002 + \frac{\sigma_y}{E}\right)} = \left(\frac{\frac{1}{n}}{\ln\left(1.002 + \frac{\sigma_y}{E}\right)}\right)^{\frac{1}{n}} \quad (\text{Eqn. 54})$$

$$\frac{\sigma_o}{\sigma_u} (1.002 + \varepsilon_o) = (2.718 n \ln(1.002 + \varepsilon_o))^{\frac{1}{n}} \quad (\text{Eqn. 55})$$

It was found from checking a few cases from NUREG-6337 [57] that an average of the hardening exponent estimated from the EPRI and Framatome equations provides the closest comparison to the Ramberg-Osgood parameters obtained from the curve fits to stress-strain data. Hence, the parameter, α was also estimated using the EPRI and Framatome equations, (Eqn. 56) and (Eqn. 57), respectively, and an average value was used for the value of α shown in Table 23.

$$\alpha = \frac{\left[\frac{\ln(1.002 + \varepsilon_o)^{\frac{1}{n}}}{(1.002 + \varepsilon_o)}\right]^n}{\varepsilon_o} \quad (\text{Eqn. 56})$$

$$\alpha = \frac{[(1/\varepsilon_o)\ln(1.002 + \varepsilon_o) - 1.002 - \varepsilon_o]}{(1.002 + \varepsilon_o)^n} \quad (\text{Eqn. 57})$$

Because J-R curves are not available for the older AEC test materials, the following Equation (28), obtained from NG-18 report to PRCI [59], was used to estimate the JIC values for each of the pipes listed in Table 23. The Charpy V-notch impact test upper shelf energy (USE) values were used in (Eqn. 58) to arrive at the JIC values.

$$J_i = 9.6 \times 10^{-5} \text{ CVN } \sigma_f \quad (\text{Eqn. 58})$$

The following expression, (Eqn. 59), for the tearing modulus (Tmat) was used to obtain the constants C and m in the $J = J_i + C(\alpha a)^m$ J-R curve equation.

$$T_{mat} = \frac{125 CVN}{\sigma_f} \quad (\text{Eqn. 59})$$

Assuming an average value of the tearing modulus [60], as given in (Eqn. 60), (Eqn. 61) and (Eqn. 62) were used in the estimation of the J-R curve constant, C, by assuming m=1.

$$T_{mat} = \frac{E}{\sigma_f^2} \frac{dJ}{da} \quad (\text{Eqn. 60})$$

$$\frac{dJ}{da} = C m (\Delta a)^{m-1} = C \quad (\text{Eqn. 61})$$

$$\frac{T_{mat} \sigma_f^2}{E} = C, \quad m = 1 \quad (\text{Eqn. 62})$$

Table 23. Pipe dimensions and material properties from twelve AEC tests used in EPFM analysis [53]

Test Number	Radius	Thickness	Axial c	σ_y	σ_u	α	σ_o	ϵ_o	n	J_i	C	m	Pressure
	mm	mm	mm	MPa	MPa	-	MPa	mm/mm	-	N/mm	N/mm ^(m+1)	-	MPa
AEC1	304.8	42.520	234.950	227.527	519.865	2.283	227.527	0.001100	4.090	60.596	15.018	1	22.063
AEC2	304.8	40.462	234.950	226.148	517.107	2.294	226.148	0.001093	4.088	60.261	14.935	1	19.030
AEC6	304.8	43.561	147.320	235.111	561.923	2.226	235.111	0.001137	3.917	65.593	16.256	1	28.131
AEC7	304.8	41.529	234.950	210.980	517.107	2.246	210.980	0.001020	3.864	59.919	14.850	1	18.616
AEC11	304.8	17.907	130.175	251.659	515.038	2.107	251.659	0.001217	4.530	44.868	11.120	1	10.135
AEC12	304.8	18.034	66.675	251.659	515.038	2.107	251.659	0.001217	4.530	44.868	11.120	1	14.307
AEC13	304.8	17.780	184.150	251.659	515.038	2.107	251.659	0.001217	4.530	44.868	11.120	1	7.377
AEC15b	304.8	41.656	234.950	224.769	537.102	2.306	224.769	0.001087	3.932	65.486	16.230	1	21.650
AEC17	304.8	41.910	76.200	231.664	567.439	2.253	231.664	0.001120	3.838	59.917	14.850	1	37.301
AEC21	161.925	18.034	31.750	295.096	510.212	1.861	295.096	0.001427	5.470	32.400	8.030	1	33.715
AEC22	161.925	17.958	66.675	295.096	510.212	1.861	295.096	0.001427	5.470	32.400	8.030	1	21.339
AEC23	161.925	17.780	130.175	295.096	510.212	1.861	295.096	0.001427	5.470	32.400	8.030	1	13.445

Table 24 shows the ratios of experimental crack lengths to the predicted critical crack lengths obtained from the both the limit load and EPFM axial through-wall crack analyses for these 12 experiments. As shown, the results between the limit load and EPFM solutions are within 10% for most (10 out of 12) cases where the difference between the two remaining cases (AEC-21 and AEC-22) is only about 15%. For these 12 experiments for which it was possible to estimate the EPFM critical half crack length, the average value of the experimental half crack length to the predicted half critical crack length was 0.875 with a standard deviation of 0.111. Consequently, the axial TWC EPFM solution tends to be non-conservative, just like the axial TWC limit load solution. As noted previously, the smaller of the two predicted critical crack sizes from the limit load and EPFM solutions is used as the critical crack size for the Axial_TWC_fail module. As such, the larger of the two ratios of c_{Exp}/c_{Crit} would be used to assess the validity of the Axial_TWC_fail module. As can be seen in the far right hand column of Table 24, the average value of Axial_TWC_ratio when using the smaller value of c_{Crit} from the limit load and EPFM analyses to define the critical crack length, is 0.879 with a standard deviation of 0.112.

Table 24. Comparison of Axial_TWC_ratio obtained from limit load and EPFM analysis

Expt. Number	C _{Expt} /C _{Crit}		Failure Mechanism (1)	Axial_TWC_ratio (1)
	Limit Load	EPFM		
AEC-1	0.997	0.995	Limit Load	0.997
AEC-2	0.910	0.892	Limit Load	0.910
AEC-6	0.756	0.754	Limit Load	0.756
AEC-7	0.866	0.851	Limit Load	0.866
AEC-11	0.955	1.045	EPFM	1.045
AEC-12	0.793	0.870	EPFM	0.870
AEC-13	0.908	0.986	EPFM	0.986
AEC-15b	0.986	0.976	Limit Load	0.986
AEC-17	0.641	0.665	EPFM	0.665
AEC-21	0.687	0.792	EPFM	0.792
AEC-22	0.709	0.811	EPFM	0.811
AEC-23	0.777	0.861	EPFM	0.861
Average	0.832	0.875		0.879
Standard Deviation	0.121	0.111		0.112

(1). Smaller of the two critical crack sizes (larger c/c_{crit} ratios) from limit load and EPFM analyses used as output from Axial_TWC_fail module

3.7 Limitations with the Crack Stability Modules

Crack stability modules have been developed for both circumferentially-oriented and axially-oriented surface cracks and through-wall cracks in pipes. While these modules represent the current state-of-the-art in the technology, there remain a few limitations with each that may warrant additional consideration in the future.

For the circumferentially-oriented surface crack module (SC_fail), the existing module only includes a limit-load solution based on the Net-Section-Collapse method for a constant depth surface crack. Provisions for the inclusion of solutions for parabolic or elliptical crack shapes have been considered, but have not been implemented into the xLPR framework at this time. Furthermore, Net-Section-Collapse (NSC) limit load solutions do not perform well for short, deep surface cracks because the assumption that the cross section becomes fully plastic cannot be realized before the crack breaks through the pipe wall, even for fully ductile, high toughness materials, such as stainless steels. In addition, no elastic plastic fracture mechanics (EPFM) solution has been implemented into the existing version of SC_fail. While prior studies using the dimensionless plastic zone parameter (DPZP) analysis [61], see (Eqn. 63), have shown that limit load solutions work well for most surface cracked pipe analysis, with the possible exception of the short, deep surface crack case, there may be additional cases of larger diameter, lower toughness pipes for which the DPZP is less than 0.1 where an EPFM solution may be more appropriate, see Figure 13. One issue with the inclusion of an EPFM surface crack solution is that the C(T) specimen geometry, typically used to define the material's fracture toughness, does not represent the proper constraint of a surface crack in a pipe, see Figure 14. As a result, a C(T) specimen

tends to under-predict the material's fracture toughness for a surface-cracked pipe EPFM analysis.

$$DPZP = \frac{2EJ_i}{\pi^2 D_m \sigma_f^2} \quad (\text{Eqn. 63})$$

where,

- E = elastic modulus
- J_i = initiation toughness
- D_m = mean pipe diameter
- σ_f = flow stress.

Another limitation with the SC_fail module is that there is a very limited database of pipe fracture experiments that can be used to validate the multiple surface crack aspects of the module. There is an extensive database (169) of experiments that can be used to validate the single surface crack analysis method, but there are only 3 experiments that can be used to validate the multiple surface crack analysis.

For the circumferentially-oriented through-wall crack module (TWC_fail), the existing module includes both a NSC limit load solution [17,18] as well as an EPFM solution based on the LBB.ENG2 method [19]. The methodology uses the smaller of the two crack sizes (i.e., smaller of the NSC or ENG2 predicted crack sizes) as the critical crack size. As can be seen in reviewing Table 17 and Table 18, the ENG2 method tends to govern (i.e., result in the smaller predicted critical crack size) more often than not. One issue identified with the ENG2 method is the choice of J-R curve to use in the analysis. To illustrate, close examination of Table 17 and Table 18 reveals that for Experiment 1.1.1.21, the ratio of the crack angle at maximum moment from the pipe experiment to the critical crack angle varied from 1.15 to 1.83 (a 60 percent difference), based strictly on the choice of the formulation of the J-R curve used in the analysis, i.e., J-M or J-D. The same 20% side-grooved fatigue pre-cracked specimen (Specimen F26-19) was used in both analyses. Only the choice of J-M or J-D varied.

Furthermore, in examining Table 18, it can be seen that the experiments which resulted in the higher values of the ratio_theta parameter tended to be those experiments which exhibited the most crack growth, i.e., those experiments for which the ratio of the crack size at maximum moment to the crack size at crack initiation was greatest. This trend is shown graphically in Figure 10 which shows the ratio_theta values for the pipe experiments used as part of this validation exercise as a function of the ratio of the crack size at maximum moment to the crack size at crack initiation. As can be seen in Figure 10, the greater the ratio of crack sizes (i.e., the more crack growth), the greater the ratio_theta value. This is a fundamental flaw with these through-wall crack stability analyses as they are currently configured. The Net-Section-Collapse analysis does not account for crack growth and the LBB.ENG2 analyses method, which forms the basis for the EPFM ENG2 module in TWC_fail, significantly under-predicts the crack growth. Put another way, analyses performed using NSC consider only a fixed flaw size, whereas crack growth is an inherent part of J-tearing analyses such as LBB.ENG2.

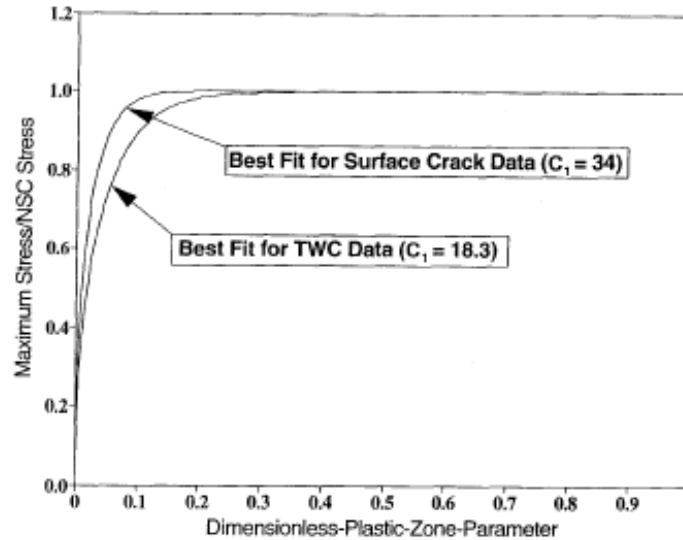


Figure 13. Plot of the ratio of the failure stress to Net-Section-Collapse stress as a function of the Dimensionless Plastic Zone Parameter (DPZP)

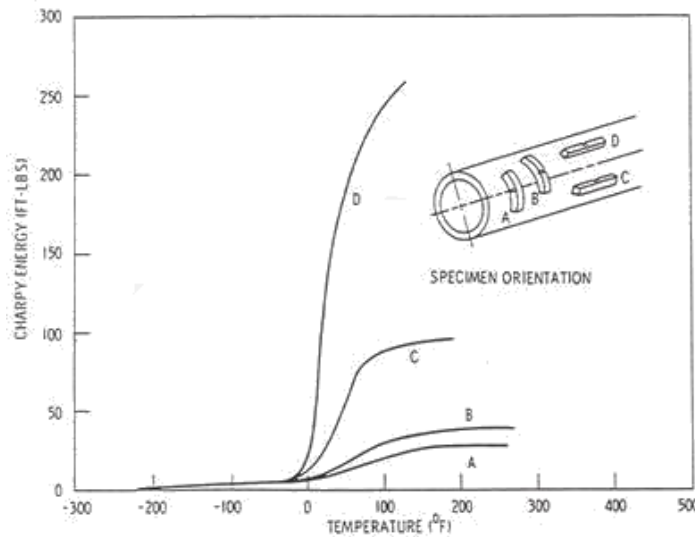


Figure 14. Effect of specimen orientation on fracture toughness in terms of Charpy Energy

For the axial crack stability modules, the most significant limitations are: 1) The experimental data sets for comparison are small, 2) The through-wall crack analysis validation of the EPFM methodology relies upon correlations rather than actual measured material property inputs. The small sample size can only be overcome by more testing. Unfortunately, axial crack burst testing in heavy walled pipe is not all that common: The vast majority of interest lies in thin-wall pipe applications (oil and gas). The impact of having to use correlations to generate the required material properties for the EPFM validation can only be assessed by performing sensitivity studies on the chosen parameters. In general, axial cracks are not expected to dominate failure probabilities for nuclear piping, so these limitations are not deemed critical.

In all of the stability models and the validation experiments, the crack is planar with two distinctly parallel crack faces. PWSCC, on the other hand, has no single distinct crack. Rather, it has many smaller branching and interconnected cracks with ligaments of metal connecting the crack faces in places. Accordingly, the current stability models can only be considered an approximation of PWSCC crack from a geometry perspective. Furthermore, no pipe fracture experiments have ever been performed on pipes with PWSCC flaws, so there is no way to quantify the conservatism of the present stability models.

4. RECOMMENDATIONS FOR VERSION 3.0 MODIFICATIONS

One of the problems with the limit load solutions for circumferentially-oriented surface cracks in pipes, even with very ductile materials such as stainless steels, is that they tend to be non-conservative for short, deep surface cracks. This is the result of the fact that the net section for such cracks cannot achieve full plasticity conditions prior to the crack breaking through the pipe wall thickness and becoming a through-wall crack. An elastic-plastic fracture mechanics method is necessary for these small cracks. Kurihara [47] first observed this when he performed tests on short surface cracked pipe subjected to bending. Kurihara also proposed an empirical correction to NSC equations. The reduction in NSC is dramatic for short angle cracks and, unfortunately, is not conservative. It is noted that the SC.ENG2 method, which uses an equivalent thickness based on the limit load solutions of Kurihara, compares best with finite element solutions of the J-integral indicating that the correction is reasonable. It is recommended that in the future, consideration be given to include the Kurihara modification to the method, perhaps for Version 3. Furthermore, the current SC_fail module only considers constant depth surface cracks. The inclusion of additional crack profiles may also be warranted in the future.

If the decision is made to proceed with the development of an EPFM solution for circumferentially-oriented surface cracks in pipes, then a means of properly characterizing the material's fracture resistance, in light of the obvious constraint differences between surface cracked pipe and C(T) specimens must be made. A number of possible corrections to the C(T) specimen data have been made in the past to correct for this difference in constraint, but to date, nothing has been proposed that is universally accepted by the technical community.

As far as the solution for circumferentially-oriented through-wall cracks (TWC_fail) is concerned, the existing methodology is probably robust enough for these types of probabilistic assessments. Short of explicitly specifying what formulation of J-R curve the user must use in order to reduce the level of uncertainty, little can probably be gained from future enhancements to the TWC_fail module. The one possible enhancement would be to improve these methods so that they better capture the crack growth. The Net-Section-Collapse method does not account for crack growth while the LBB.ENG2 method significantly under-predicts the amount of crack growth.

While there are limitations with the existing axial crack stability analyses methods, e.g., validation of the EPFM solution was somewhat crude due to the lack of the necessary material properties, further investment in this technical area would be hard to justify, in light of existing research budgets, due to the unlikely occurrence of an axial crack rupture in a nuclear plant piping system due to the relatively short nature of these types of cracks.

In light of the apparent mismatch between the idealized crack geometry of the present stability models and actual PWSCC flaws, the very basis of the stability models might be questioned. Can pipes with PWSCC reach net-section stress conditions? Is J the correct parameter to characterize applied and material toughness for PWSCC cracks? Answers to these questions may point to the need for different kinds of stability models.

5. LESSONS LEARNED

The circumferentially oriented surface crack stability module (SC_fail) is currently configured to address constant depth surface cracks using a Net-Section-Collapse limit load solution. Coding for both elliptical and parabolic crack shapes have been included in the model, but are currently not implemented within the xLPR framework. Eventually these alternative crack shapes, as well as new and improved EPFM surface cracked pipe solutions, may be included. Consequently, the inputs for SC_fail have been designed to accommodate these upgrades so no revision to the calling routine will be required when these features are added. The validation of the SC_fail module for both the single and multiple crack cases met the applicable requirement in the SC_fail SRD [1], SCF-7, which states that the agreement between the maximum moment values from a series of surface cracked pipe experiments and the corresponding critical bending moment predicted by SC_fail should be within 10%, on average. For the single crack case, the average value for the bending moment ratio (maximum experimental moment-to-SC_fail predicted critical moment) was 0.987. For the limited multiple crack database (3 experiments), the average value of the bending moment ratio was 1.04. Thus, the mean value for both the single crack and multiple crack cases were easily within the 10-percent threshold specified in SCF-7. Saying that, however, the database of multiple surface-cracked pipe experiments is quite limited (i.e., three experiments). Thought should be given to expanding this database if possible.

The circumferentially oriented through-wall crack stability module (TWC_fail) is currently configured to consider both an idealized Net-Section-Collapse (NSC) limit load solution [17, 18] as well as an EPFM solution based on the LBB.ENG2 method [19]. The solution that yields the smaller crack size is used for the pass/fail assessment. Eventually other solutions may be included in TWC_fail. As a result, the inputs have been designed to accommodate these potential future upgrades. It was found that the EPFM solution (ENG2) was highly dependent on the choice of J-R curve used. Better predictions were realized when using modified J (J-M) than deformation theory J (J-D), but still, the level of uncertainty when only using J-M formulated J-R curves still exceeded the requirements specified in the TWC_fail SRD [2], TWCF-7, which states that the agreement between the through-wall crack sizes for a series of through-wall cracked pipe experiments and the predicted critical crack size should be within 10% on average. When only using J-M, the average value of the ratio of the maximum experimental moment crack size to the TWC_fail predicted critical crack size was 1.20, which is outside the 10% requirement as specified by the TWC_fail SRD [2]. Part of this uncertainty is associated with the fact that the ENG2 method under-predicts the crack growth. Prior studies showed that the LBB.ENG2 method, which formed the basis for the ENG2 method in TWC_fail, did a good job of predicting the maximum moments from the experiments [62], but no attempts were made previously to ascertain how good LBB.ENG2 did at predicting the crack growth. As part of the MVR development process for TWC_fail, an assessment of how well ENG2 did at predicting crack growth was made and the results were less than encouraging. The LBB.ENG2 method in the NRCPIPE code, on average under-predicted the experimental crack growth at maximum moment by almost a factor of 3. If through-wall crack stability is found to be a major driver for the overall uncertainty associated with xLPR, then it may be prudent to address this limitation with TWC_fail. It is interesting to note that the SC_fail module did a much better job of predicting the experimental results than did the TWC_fail module. This is undoubtedly due to the fact that the surface crack experiments experienced very little crack growth between crack initiation and maximum moment, whereas the through-wall crack experiments typically experienced quite a bit of crack growth.

Due to the fact that the uncertainty associated with the TWC_fail module was found to be highly dependent on the choice of J-R curve used in the analysis, an attempt was made to separate the model uncertainty from the inputs uncertainty by developing pipe experiment specific J-R curves

using the η -factor approach [52] for use in the TWC_fail model. It was felt that the use of these pipe experiment-specific η -factor J-R curves in the analyses would eliminate the question of which J-R curve was best for analyzing these pipe experiments. In doing so, the average value of the ratio of the experimental crack size at maximum moment to the TWC_fail predicted crack size was 1.14 (see Table 20), which is better than when using a J-M based J-R curve from a C-T specimen, but still outside the range specified by the requirement in the TWC_fail SRD [2].

The axial crack stability module includes stability models for both internal axial surface cracks (Axial_SC_fail) and axial through-wall cracks (Axial_TWC_fail). The axial surface crack model is based on a plastic collapse analysis as documented in the Ductile Fracture Handbook [20]. The axial through-wall crack model uses both a limit load analysis and an EPFM analysis based on the work of Kim, et al. [21]. For the axially oriented surface crack pipe experiments, the average ratio of the experimental pressure to the predicted pressure was 1.070, which is easily within the 10% validation criteria specified in the SRD for Axial_SC_fail [11]. For the axially oriented through-wall crack pipe experiments, the average ratio of the experimental crack size to the critical crack size was 0.879 (see right hand column in Table 24), which is just outside the limits of the criteria specified in the SRD. However, for the axial through-wall crack case, the experimental data set used for validation was somewhat limited.

6. ASSUMPTIONS AND IMPLICATIONS

The major assumptions and the implications of those assumptions made during the SC_fail, TWC_fail, and AxCS development processes are presented in Table 25.

Table 25. List of assumptions and implications of those assumptions made during the SC_fail, TWC_fail and AxCS development processes

Assumption	Implications
<p>All stability modules assume a planar crack or set of planar cracks.</p>	<p>Because planar cracks are assumed, the crack are an idealized representation. Actual PWSCC cracks are not planar and do not have a simple leak path for through-wall cracks. Thus, for a given leak rate, a PWSCC crack system would be more diffuse than a planar crack system. PWSCC cracks are characterized by a distributed, connected network of cracks in 3D rather than a single, idealized 2D planar crack. A model for the stability of diffuse and connected (i.e. distributed damage model or flow through porous media) set of cracks is very different from the ideal crack case used in xLPR. This assumption overpredicts the occurrence of ruptures.</p>
<p>SC_fail analysis is based on a constant depth surface crack geometry.</p>	<p>Because the depth of the constant depth surface crack is equal to the maximum depth of the surface crack under question and the length of the constant depth surface crack is equal to the length of the surface crack under question, the assumption of a constant depth surface crack will result in a conservative under-prediction of the critical bending moment.</p>
<p>It is assumed that Net-Section-Collapse (NSC) limit load solution included in SC_fail is applicable to all surface cracks.</p>	<p>It is known that NSC does not perform well for short, deep surface cracks because the assumption that the cross section becomes fully plastic cannot be realized before the crack breaks through the pipe wall, even for fully ductile, high toughness materials, such as stainless steels. The remedy is to include a surface crack EPFM solution in future versions of xLPR.</p>
<p>It is assumed that an idealized TWC geometry adequately captures behavior for the TWC_fail Net-Section-Collapse analysis.</p>	<p>TWC cracks rarely grow with crack tips oriented radially. Rather, the crack angle on the OD and ID are different (so-called natural crack growth). To eliminate this assumption, a natural crack growth routine may be needed in the next version of TWC_fail. Currently, it is believed that this may be non-conservative with respect to crack stability.</p>
<p>It is assume that axial loads in SC_fail and TWC_fail analyses can be treated as an effective pressure term.</p>	<p>This is a reasonable means of accounting for axial loads and means that fundamental changes to codes were not required. No implications for conservativeness.</p>

Assumption	Implications
<p>SC_fail and TWC_fail assume no torsional or shear loads.</p>	<p>Plant piping systems will experience both, but they are typically not a dominant load contributor. This assumption leads to an underestimate with respect to the applied J which is considered non-conservative with respect to crack stability. However, this is considered a second-order effect. This is dealt with in the current version of xLPR in the Framework by recasting the moments into an effective moment.</p>
<p>The TWC_fail module assumes crack face closure effects.</p>	<p>Reasonable assumption as crack faces will tend to carry compressive load due to the fact that they are typically very tight in service, i.e., little unloaded crack opening displacement.</p>
<p>For the Axial_TWC_fail EPFM analysis, elastic influence functions (F) are based on R_m/t ratio and normalized crack size ($\lambda = c/(R_m t)^{0.5}$). Plastic influence functions (h_1) are based on R_m/t ratio, normalized crack (λ) size, and strain hardening exponent (n). Design space for parametric parameters are:</p> <ul style="list-style-type: none"> • $0.05 \leq \lambda \leq 3$ • $5 \leq R_m/t \leq 20$ • $1 \leq n \leq 7$ <p>It is assumed that the crack or pipe geometry or material properties are within these ranges.</p>	<p>Design space should cover most possible combinations of pipe/crack geometries and pipe materials used in primary systems in nuclear power plants. Some primary side piping systems may have R_m/t ratios less than 5 and some secondary side piping systems may be fabricated from larger diameter, thinner wall pipe for which the R_m/t ratio is greater than 20. Some practical applications require $n > 7$ (i.e., 11-14), but this is judged to be a minor influence on the results because the stress-strain curves begin to flatten off once “n” reaches a value of 7 or more. If cases are outside the stated bounds, then the code uses influence functions at the limits of the particular range.</p>
<p>Axial_TWC_fail EPFM model assumes linear interpolation of influence functions. Discrete values used in FEA for determining influence functions were:</p> <ul style="list-style-type: none"> • R_m/t: 5 and 20 • λ: 0.05, 1, 2, and 3 • n: 1, 3, and 7 	<p>Curvatures of the functions are judged to be modest, such that, linear interpolation is justified. Note: The analysis uses Reference 21 which included a sparse solution set.</p>

Assumption	Implications
<p>A Ramberg-Osgood material representation for an isotropic, homogeneous material was assumed during the development process of both the TWC_fail and Axial_TWC_fail EPFM analyses. As such, the resultant material inputs required by both models are the necessary Ramberg-Osgood parameters, i.e., yield or reference stress, reference strain, strain hardening exponent (n), and alpha (α)</p>	<p>To make the EPFM solutions tractable, a simple constitutive model must be adopted in spite of the fact that some materials do not fit the Ramberg-Osgood model precisely. Presently, there is no way to assess the impact of such “misfits” on conservatism without significant changes to user inputs and module code (point-by-point stress-strain curve inputs would be required).</p> <p>In addition to the basic constitutive model consideration, the choice of tensile data to use in the analyses can have a significant effect on the predictions. It is known that there may be significant differences in the stress-strain curves between quasi-statically loaded tensile specimens and dynamically loaded tensile specimens for the same material. As such, when analyzing dynamically loaded pipe experiments with quasi-static stress-strain data, an additional level of uncertainty is introduced. It is felt that it is not possible to specify to the end user of the code which stress-strain curve to use because they may not have dynamic data available.</p> <p>For TWC_fail, cracks in welds should be analyzed assuming the base metal tensile properties and weld metal fracture toughness properties. For cracks in dissimilar metal welds, the mixture percentage approach should be used to establish the appropriate stress-strain properties.</p> <p>The fit of the Ramberg-Osgood parameters to the tensile data is recommended to follow “best engineering judgement”, such that the range of stress-strain data considered should be between 0.1 percent strain and the strain corresponding 80 percent of the ultimate strength using engineering stress-engineering strain curves. Users do not, necessarily, have to abide by this recommendation.</p>
<p>Validation of Axial_TWC_fail EPFM analysis method required assuming Ramberg-Osgood parameters and J-R curve coefficients derived using available tensile and Charpy data using correlations available in the literature.</p>	<p>Uncertainty (means and standard deviations) reported for the Axial_TWC_fail EPFM analysis should be viewed with caution.</p>
<p>It is assume that axial cracks in welds cannot be analyzed using the current AxCS module.</p>	<p>The theory for AxCS is derived assuming that cracks are in a homogenous material. Therefore, the current AxCS module should be used with caution when analyzing axial cracks in welds. It is highly unlikely that an axial crack will be a limiting case for crack stability, so the effect on overall probabilities of rupture should not be significant..</p>

Assumption	Implications
<p>The elastic portion of the Axial_TWC_fail EPFM analysis has assumed that a plastic zone size correction on the crack size is appropriate.</p>	<p>Comparisons with and without the plastic zone size correction were conducted. Test cases showed that the use of the plastic zone size provides better correlations.</p>
<p>TWC_fail analysis assumes that the ends of the pipe are free to rotate. Effects of restraint of pressure induced bending and system stiffness were not included.</p>	<p>Experimental data has shown that a through-wall crack may grow much greater in length before failure than predicted based on analysis methods developed for the case where the ends of the pipe are free to rotate.</p> <p>This is conservative with respect to crack stability, but may be non-conservative with respect to leak rate.</p>
<p>It is assumed that idealized crack shapes can be used to approximate real crack geometries.</p>	<p>Both of the surface crack stability modules assume that surface cracks are constant depth and both through-wall crack modules assume that the crack tips are along a radius from the center of the pipe.</p> <p>Natural crack shapes may be much different, with longer cracks on the ID surface than OD surface. Furthermore, the idealized crack shapes do not seem to be a particularly good model of PWSCC cracks.</p> <p>Considering the different crack OD and ID length issue, the idealized shape assumption may or may not be conservative. Potentially, one could have a very short length on the OD and a 360-degree long and deep crack on the ID. The idealized crack would, very likely, estimate greater stability than the crack actually has.</p> <p>Considering an actual PWSCC crack, it looks like distributed porosity and this bears only vague resemblance to an idealized crack. Very likely, the actual PWSCC crack would have greater stability than the idealized representation.</p>
<p>It is assumed that prior load history effects are completely erased for EPFM. That is, all J-R curves start from zero crack extension for every time-step during a realization.</p>	<p>The program does not account for previously used deformation energy if there are two consecutive ductile tearing episodes during the analysis. The implication is that you enter the J-R curve at the wrong location, or that the wrong J-R curve is being used. With only PWSCC and fatigue loading, all of the previous energy consumed is “erased” so there is no impact on the stability predictions. If, on the other hand, a seismic load causes ductile tearing, a second temporally consecutive seismic loading would reset the initiation J to the original value as opposed to some higher one.</p> <p>Multiple consecutive ductile tearing episodes may not be very likely, so the consequences, with respect to conservatism, may not be large.</p>

7. SUMMARY

A number of new modules for assessing the stability of cracks in nuclear power plant piping systems have been developed as part of the xLPR Version 2.0 development process. These modules assess the stability of both axially-oriented and circumferentially-oriented surface cracks (SC) and through-wall cracks (TWC) in pipes.

The SC_fail module assesses the stability of multiple circumferentially-oriented surface cracks (SC) in a pipe subjected to combined tension and bending loading. This module is valid for cases when one or more cracks are present in the pipe. Based on input pipe/crack geometries, pipe material properties, and loads, the ultimate moment-carrying capacity of multiple surface cracks, as well as an individual surface crack, are compared with the current (applied) loading. Presently, a constant surface crack depth profile is considered. Eventually, a local collapse surface crack solution and/or an elastic-plastic fracture mechanics (EPFM) surface crack solution may be included in xLPR. Accordingly, the inputs for SC_fail have been designed to accommodate these updates, so no revision to the calling routine will be required when these features are added.

The TWC_fail module assesses the stability of a circumferentially-oriented through-wall crack (TWC) in a pipe subjected to combined tension and bending loading. Based on input pipe/crack geometries, pipe material properties, and loads, the critical crack size of the through-wall crack (θ_{crit}) is compared with the current crack size. A flag is returned that indicates the result of this comparison: Predicted failure, yes or no, as well as the ratio of the current crack angle (θ) to the critical crack angle (θ_{crit}).

The TWC_fail module uses a main subroutine TWC_fail, for doing the through-wall crack assessment. Presently, two TWC critical crack size (θ_{crit}) prediction methodologies are implemented:

- Idealized through-wall crack NSC analysis method, and
- LBB.ENG2 elastic-plastic fracture mechanics (EPFM) through-wall crack J-estimation scheme.

In the current version of TWC_fail, both the idealized crack NSC and LBB.ENG2 elastic-plastic through-wall crack predictions are made. Upon return to the calling program, the solution that yields the smallest critical crack size is used for the pass/fail assessment and for calculating the ratio of the current crack size to the critical crack size.

Eventually, other through-wall crack solutions might be included in xLPR. Accordingly, the inputs for TWC_fail have been designed to accommodate these updates, so limited revisions to the calling routine will be required when these features are added.

The axial surface crack and axial through-wall crack stability modules are stand-alone modules called from within the xLPR Framework. The Axial_SC_fail module employs a plastic collapse analysis to assess the stability of an internal axial surface crack, while the Axial_TWC_fail module employs both limit load and elastic-plastic fracture mechanics (EPFM) analyses to assess the stability of an idealized axial TWC in a single pipe material. (Note while the analysis of an axial crack in welds with two separate materials, namely a base-metal and a weld, is beyond the scope of the present design, such cracks in welds have been known to exist in service, e.g., the VC Summer crack.) Both of these modules use input variables for the pipe and axial crack dimensions and the pipe material properties obtained from the xLPR Framework.

The Axial_SC_fail subroutine performs the stability calculation for an axial surface crack using a plastic collapse method. Ax_SC_fail returns a flag indicating whether or not the flaw has failed and the ratio of the input pressure to the critical pressure.

The Axial_TWC_fail subroutine performs the main stability calculation for an axial TWC using both limit load and EPFM methods. The subroutine calculates the critical axial through-wall crack length using both limit load and EPFM methods and compares the smaller of these two values to the current axial through-wall crack length. If the current crack length is greater than the critical crack length (i.e., the smaller of the two values obtained from the limit load and EPFM solutions), then the TWC fails. If not, then the TWC remains stable

The verification of the SC_fail, TWC_fail, and AxCS models is documented in detail in the Software Test Results Reports (STRR) for each of these models. The testing activities described in the STRRs are intended to verify that the requirements specified in the applicable Software Requirements Documents (SRD) are met. To date most of these requirements have been shown to have been met. However, some of the requirements in these SRDs are applicable to the xLPR Framework and thus, verification of those requirements can only be accomplished when these modules are integrated into the Framework.

Validation of these models was accomplished by comparing the predictions from the various models with available experimental data from full-scale pipe experiments. In validating the SC_fail module, there were a total of 169 full-scale, single surface cracked pipe experiments to which to compare the results from SC_fail to. For these 169 experiments, the average value of the bending moment ratio (experimental bending moment to predicted bending moment) was 0.987 with a standard deviation of 0.268. This level of agreement between the experiments and the predictions easily met the requirement for validation as specified in the SRD for this module. While the database of single surface crack experiments was quite extensive, the database of multiple surface crack experiments was quite limited. In total, only 3 multiple surface crack experiments were found in the literature. For these 3 experiments the average value for BM ratio was 1.04 with a standard deviation of 0.01 which easily satisfies the SRD requirement for validation.

In validating the TWC_fail module a total of 32 through-wall cracked pipe experiments were included in the validation matrix. These experiments considered a wide range of pipe sizes (2 to 42-inch nominal diameter), crack sizes (0.35 to 1.4 radian half crack angle), materials (carbon steel and stainless steels and their associated weldments plus dissimilar metal welds), and loading conditions (simple four-point bending, combined pressure and four-point bending, and dynamic, cyclic pipe system experiments with internal pipe pressure). The results of this validation exercise were found to be highly dependent on the choice of J-R curve used, i.e., side-grooved specimen or not, fatigue pre-cracked or not), and the formulation for J (deformation J (J-D) or modified J (J-M)). It was found as part of this validation that the TWC_fail module resulted in a better prediction of the critical crack size using J-M than J-D. However, it was thought that it would not be possible to specify to the end user what formulation of J to use or what geometry of fracture toughness specimen to use (side-grooved or not and fatigue pre-cracked or not), so an assessment of the validity of the TWC_fail module was made considering data from all possible combinations of fracture toughness specimen geometries, using both J-D and J-M formations for J. The resultant average value of the ratio of the current crack angle (crack angle at maximum load from the pipe experiment) to the critical crack angle (smaller of the two crack angles from the NSC and ENG2 analysis methods) was 1.34 with a standard deviation of 0.53. This level of uncertainty was deemed to exceed the validity requirement in the SRD. As a result, additional analyses were undertaken in an attempt to isolate the cause of this uncertainty.

In assessing the results from the TWC_fail validation exercise discussed above, it was concluded that the overall uncertainty observed was the result of two separate but equally important contributions. One, it was thought that there is a level of uncertainty due solely to the model (model uncertainty), and two, it was thought that there is a level of uncertainty due to the inputs (input uncertainty). With respect to the input uncertainty, one leading contributor is the uncertainty due to the choice of J-R curve to use in the analysis. In an attempt to separate the model uncertainty from the input uncertainty due to the choice of J-R curve, η -factor analyses were conducted in order to establish a J-R curve directly from the pipe experimental load-displacement data. It was then thought that if one used these η -factor derived J-R curves from the pipe experiments in the TWC_fail analyses, one could get an idea of the uncertainty due solely to the model, i.e., model uncertainty. In order to conduct these η -factor analyses, additional data were needed from the pipe experiments, e.g., details on the moment arm pipes and the compliance of the test frame used. For a number of the 32 experiments considered in the original validation efforts for TWC_fail, these data were unavailable. As a result, the validation matrix for these η -factor analyses only included 12 experiments. For these 12 experiments, the average value of the ratio of the current crack angle (crack angle at maximum moment from the pipe experiment) to the critical crack angle was 1.14 with a corresponding standard deviation of 0.17. It was felt that this level of agreement better represented the overall uncertainty of the model (model uncertainty) separate from the input uncertainty.

A total of 17 axial SC pipe experiments were chosen for validation of the Axial_SC_fail module. The ratio of the experimental pressure to the pressure predicted using the ductile fracture handbook plastic collapse method was obtained by running the Axial_SC_fail module. Overall, the average value of $P_{\text{Expt}}/P_{\text{Pred}}$ for these 17 experiments is 1.07 with a standard deviation of 0.190, which indicates that the Axial_SC_fail model does a very job of predicting the experimental results. Furthermore, on average, the Axial_SC_fail module was conservative since the average value of $P_{\text{Expt}}/P_{\text{Pred}}$ was greater than 1.0

A total of 26 axial TWC pipe experiments were used for validating the Axial_TWC_fail module. The ratio of the experimental pressure to the critical pressure was obtained by running the Axial_TWC_fail module. For these 26 experiments the average ratio of the experimental crack size to the critical crack size ($C_{\text{Expt}}/C_{\text{crit}}$) for the limit load analysis was 0.850 with a standard deviation of 0.142 which means that the limit load analysis in the Axial_TWC_fail module is slightly non-conservative. Of these 26 experiments only 12 could be analyzed using the EPFM TWC analysis method. For these 12 experiments, the average ratio of the experimental crack size to the critical crack size for the EPFM analysis was 0.875 with a standard deviation of 0.111 which means that the EPFM analysis in the Axial_TWC_fail module is also slightly non-conservative.

Considering all factors, two overarching questions stand out as needing some resolution: 1) Do planar crack models, such as used in all of the stability modules, adequately capture the behavior of PWSCC with its distributed, branching and discontinuous morphology?, and 2) Are the planar crack stability models conservative or non-conservative when applied to PWSCC flaws? At this point, there are no data to enable answering either question because there has never been a pipe fracture test done with a PWSCC flaw. Heuristically, it might be argued that planar crack stability models should provide an upper bound on stability behavior (more ruptures predicted) because the metal ligaments in the PWSCC crack will make the pipe “stronger” than an unconnected planar surface. On the other hand, it is also possible that the PWSCC pipe will be so “porous” that it is held together only by some small ligaments and, therefore, has almost no resistance to bending loads. Both arguments seem plausible and, until some test data are generated to show even just trends, the adequacy of the present models, or the need for a completely different kind of model formulation, can only be speculated.

8. REFERENCES

1. xLPR-SRD-SC_Fail, xLPR Software Requirements Description for Circumferential Surface Crack Stability, Version 1.1, November 2014.
2. xLPR-SRD-TWC_fail, xLPR Software Requirements Description for TWC_fail Module, Version 4.0, January 2015.
3. xLPR-SDD-SC_Fail, xLPR Software Design Description for Circumferential Surface Crack Stability, Version 1.1, November 2014.
4. xLPR-SDD-TWC_fail, xLPR Software Design Description for Circumferential Through-Wall Crack Stability Module, Version 4.0, February 2015.
5. SC_fail STP, xLPR Software Test Plan for the Circumferential Surface Crack Stability, Version 1, January 2015.
6. xLPR-STP-TWC_fail, xLPR Software Test Plan for the TWC_fail Module, Version 2.0, October 2014.
7. xLPR-STRR-SC_fail, xLPR Software Test Results Report for Circumferential Surface Crack Stability, Version 1.0, February 2015.
8. xLPR-STRR-TWC_fail, xLPR Software Test Results Report (STRR) for Circumferential Through-Wall Crack Stability Module (TWC_fail), Version 1.0, November 2014.
9. xLPR Modular Validation Report for Circumferential Surface Crack Stability (SC_fail) Module, Version 1.0, July 2015.
10. xLPR-MVR-TWC_fail, xLPR Module Validation Report for Circumferential Through-Wall Crack Stability (TWC_fail) Module, Version 1.0, January 2015.
11. xLPR-SRD-AxCS, xLPR Software Requirements Description for Axial Crack Stability Module, Version 3.0, February 2015.
12. xLPR-SDD-AxCS, xLPR Software Design Description for Axial Crack Stability Module, Version 2.0, July 2014.
13. xLPR-STP-AxCS, xLPR Software Test Plan for Axial Crack Stability Modules, Version 1.0 July 2014.
14. xLPR-STRR-AxCS, xLPR Software Test Results Report (STRR) for Axial Crack Stability Module (AxCS), Version 1.0, May 2015.
15. xLPR Modular Validation Report for Axial Surface Crack and Axial Through-Wall Crack Stability (Axial_SC_fail and Axial_TWC_fail) Modules, Version 1.0, July 2015.
16. Dingreville, R., Eckert-Gallup, A., Sallaberry, C., "Uncertainty Analysis for the Net-Section-Collapse Failure Criterion of Circumferentially Cracked Cylinders for Multiple Arbitrary-shaped Circumferential Cracks", International Journal of Pressure Vessels and Piping, 123-124 (2014) pp. 30-45.
17. Rahman, S.; " Net-Section-Collapse Analysis of Circumferentially Cracked Cylinders - Part II: Idealized Cracks and Closed-Form Equations", Engineering Fracture Mechanics, Vol. 61, 1998, pp. 213-230.
18. Rahman, S. and Wilkowski, G.; "Net-Section-Collapse Analysis of Circumferentially Cracked Cylinders - Part I: Arbitrary-Shaped Cracks and Generalized Equations", Engineering Fracture Mechanics, Vol. 61, 1998, pp. 191-211.

19. Brust, F.W., and Gilles, P.; "Approximate Methods for Fracture Analysis of Tubular Members Subjected to Combined Tensile and Bending Loads", *Journal of Offshore Mechanics and Arctic Engineering*, Vol. 116, Nov 1994, pp. 221-227.
20. Zahoor, A., *Ductile Fracture Handbook*, EPRI Report NP-6301-D, V3, 1989.
21. Kim, Y.J., Huh, N.S., Park, Y.J., Kim, Y.J., "Elastic Plastic J and COD Estimates for Axial Through-wall Cracked Pipes", *Intl J Pressure Vessels and Piping*, 79, 2002, pp. 451-464.
22. Li, Y., et al.; "Prediction of Collapse Stress for Pipes with Arbitrarily Multiple Surface Flaws", *Journal of Pressure Vessel Technology*, Vol 132, 2010, 061204.
23. xLPR Software Configuration Management Plan, xLPR-SCMP V4.
24. xLPR Software Quality Assurance Plan, xLPR-SQAP-V5.
25. Williams, P.T., *Recommended Programming Practices and Standards for Developing xLPR Modules Using Fortran*, ORNL/TM-2013/64, Oak Ridge National Laboratory, Oak Ridge, TN, August 2013.
26. Beyond Compare 3, Scooter Software, <http://www.scootersoftware.com>
27. Wilkowski, G.M., et al., "Short Cracks in Piping and Piping Welds~ Seventh Program Report, March 1993- December 1994", NUREG/CR-4599, Vol. 4, No. 1, April 1995.
28. Schulze, et al., "Fracture Mechanics Analysis on the Initiation and Propagation of Circumferential and Longitudinal Cracks in Straight Pipe and Pipe Bends", *Nuclear Engineering and Design*, Vol. 58 (1980), pp. 19-31.
29. Julisch, P., et al., "Exclusion of Rupture for Welded Piping Systems of Power Stations by Component Tests and Failure Approaches", SMIRT-12 Paper GF09/2, August 1993.
30. Wilkowski, G.M., et al., "Degraded Piping Program - Phase II, Summary of Technical Results and Their Significance to Leak-Before-Break and In-Service Flaw Acceptance Criteria, March 1984- January 1989", NUREG/CR-4082, Vol. 8, March 1989.
31. Kanninen, M., et al., "Instability Predictions for Circumferentially Cracked Type-304 Stainless Steel Pipes Under Dynamic Loading", EPRI NP-2347, Volume 2, April 1982.
32. Milella, P., "Outline of Nuclear Piping Research Conducted in Italy", *Nuclear Engineering and Design*, Vol. 98, 1987, pp. 219-229.
33. "Proving Test on the Integrity of Carbon Steel Piping in LWRs", A translation of excerpt from Summary Report of Proving Tests on the Reliability of Nuclear Power Plant," Nuclear Power Engineering Test Center, Tokyo, Japan, 1989.
34. Asada, Y., "Verification Test Program on Integrity of Carbon Steel Piping in LWR Plants"
35. Faidy, C., et al., "Leak Before Break in French Nuclear Power Plants", *International Journal of Pressure Vessels and Piping*, Vol. 43 (1-3) (1990), pp. 151-163.
36. Wilkowski, G.M., et al., "Task 7. Girth Weld Defect Tolerance", Final Report to Deepwater Offshore Pipeline Group, May 1980.
37. Wilkowski, G.M. and Eiber, R.J., "Determination of the Maximum Size of Girth Weld Repair on Offshore Pipelines", Final Report on Project PR-3-100 to Welding Supervisory Committee of the American Gas Association, April 1979.
38. Wilkowski, G.M., and et al., "International Piping Integrity Research Group (IPIRG) Program", NUREG/CR-6233, Vol. 4, June 1997.

39. Scott, P.M., et al., "Stability of Cracked Pipe Under Inertial Stresses – Subtask 1.1 Final Report", NUREG/CR-6233, Vol. 1, August 1994.
40. Schmidt, R.A., et al., "The International Piping Integrity Research Group (IPIRG) Program - An Overview", SMiRT 11 Proceedings Paper G23/1, August 1991.
41. Scott, P.M., et al., "The IPIRG-1 Pipe System Fracture Tests: Experimental Results", PVP Vol. 280, pp. 135-151, June 1994.
42. Hopper, A., et al., "The Second International Piping Integrity Research Group (IPIRG-2) Program - Final Report, October 1991- April 1996", NUREG/CR-6452, March 1997.
43. Sturm, D., et al., "Phenomenological Pipe and Vessel Burst Tests", Final Report, Nov. 1989.
44. Azodi, D., et al., "Fracture Mechanics Evaluations of Precracked Cylindrical Vessels Subjected to Limit Load Conditions", SMiRT-12 Paper G04/2, August 1993.
45. Sturm, D., et al., "The Behavior of Dynamically Loaded Pipes with Circumferential Flaws Under Internal Pressure and External Bending Loads", Nuclear Engineering and Design, Vol. 96, pp. 99-113, 1986.
46. Bernecker, G., et al., "Proof of the Fracture Resistance of the Pipes in the THTR 300 Plant Using High Temperature Burst Tests with X20CrMoV 12 1 Components", Nuclear Engineering and Design, Vol. 84, pp. 97-107, 1985.
47. Kurihara, et al., "Estimation of the Ductile Unstable Fracture of Pipe with a Circumferential Surface Crack Subjected to Bending", Nuclear Engineering and Design, Vol. 106, pp. 265-273, 1988.
48. Yagawa, et al., "Research Activities on Fracture Mechanics for Nuclear Piping in Japan", Nuclear Engineering and Design, Vol. 98, 1987, pp.231-241.
49. "Technical Report on the Piping Reliability Proving Tests at the Japan Atomic Energy Research Institute", Report JAERI-M 93-076, March 1993.
50. Scott, P., et al., "The Battelle Integrity of Nuclear Piping (BINP) Program Final Report", NUREG/CR-6837, June 2005.
51. Hasegawa, K., Saito K., Iwamatsu, F., Miyazaki, K., "Prediction of Fully Plastic Failure Stresses for Pipes with Multiple Circumferential Flaws", In: Proceedings of the ASME Pressure Vessels and Piping Conference, Vol. 1; 2007, p. 415-419.
52. Kanninen, M.F., et al., "The Development of a Plan for the Assessment of Degraded Nuclear Piping by Experimentation and Tearing Instability Fracture Mechanics Analysis", NUREG/CR-3142, Vols. 1 and 2, June 1983.
53. Eiber, R.J., Maxey, W.A., Duffy, A.R. and Atterbury, T.J., "Investigation of the Initiation and Extent of Ductile Pipe Rupture", AEC tests, Battelle Columbus Laboratories Report, BMI-1866, 1969.
54. Reynolds, M.B., "Reactor Primary Coolant System Rupture Study, Task C, Fracture Mechanics, Quarterly Progress Report 16", GEAP-10024, AEC R&D Report, General Electric Company, January-March, 1969.
55. Shim, D.-J., Wilkowski, G., Uddin, M., Hioe, Y., Kalyanam, S., Tosi, B., and Mincer, P., "Develop Fracture Initiation Criteria for High-Strength Steel Line Pipe - Phase II, PRCI Report", Catalog No. PR-276-094509-R01, Pipeline Research Council International, Inc., 2014.

56. Kawaguchi, S., Hagiwara, N., Ohata, M., Toyoda, M., "Modified Equation to Predict Leak/Rupture Criteria for Axially Through-Wall Notched X80 and X100 Linepipes Having Higher Charpy Energy", Proc. of Intl. Pipeline Conf., 2004, IPC04-0322.
57. Rahman, S., Olson, R., Rosenfield, A., Wilkowski, G., "Summary of Results from the IPIRG-2 Round-Robin Analyses", NUREG/CR-6337, February 1996.
58. Schwalbe, K. H., Hayes, B., Baustian, K., "Validation of the Fracture Mechanics Test Method EGF P1-87D (ESIS P1-90/ESIS P1-92)", Fatigue and Fracture of Eng. Matls. and Struct., Vol. 16, No. 11, 1993, pp. 1231-1284.
59. Leis, B.N., Brust, F.W., "Ductile Fracture Properties of Selected Line-Pipe Steels", NG-18 Report No. 183, Pipeline Research Council International, Inc., 1990.
60. Kumar, V., German, M.D., "Elastic-Plastic Fracture Analysis of Through-Wall and Surface Flaws in Cylinders", EPRI Report, NP-5596, 1988.
61. Wilkowski, G.M., and Scott, P.M., "A Statistically Based Circumferentially Cracked Pipe Fracture Mechanics Analysis for Design or Code Implementation", Nuclear Engineering and Design, Vol. 111, 1989, pp. 173-187.
62. Brust, F., et al., "Assessment of Short Through-Wall Circumferential Cracks in Pipes – Experiments and Analysis – March 1990 – December 1994", NUREG/CR-6235, April 1995.